INFORMATION TO USERS

This manuscript has been reproduced from the microfilm master. UMI films the text directly from the original or copy submitted. Thus, some thesis and dissertation copies are in typewriter face, while others may be from any type of computer printer.

The quality of this reproduction is dependent upon the quality of the copy submitted. Broken or indistinct print, colored or poor quality illustrations and photographs, print bleedthrough, substandard margins, and improper alignment can adversely affect reproduction.

In the unlikely event that the author did not send UMI a complete manuscript and there are missing pages, these will be noted. Also, if unauthorized copyright material had to be removed, a note will indicate the deletion.

Oversize materials (e.g., maps, drawings, charts) are reproduced by sectioning the original, beginning at the upper left-hand corner and continuing from left to right in equal sections with small overlaps.

Photographs included in the original manuscript have been reproduced xerographically in this copy. Higher quality 6" x 9" black and white photographic prints are available for any photographs or illustrations appearing in this copy for an additional charge. Contact UMI directly to order.

University of Alberta

Capillary Coatings for Protein Separations in Capillary Electrophoresis

by

Nicole Elizabeth Baryla ©

A thesis submitted to the Faculty of Graduate Studies and Research in partial fulfillment

of the requirements for the degree of Doctor of Philosophy.

Department of Chemistry

Edmonton, Alberta

Spring 2002

The author has granted a non-exclusive licence allowing the National Library of Canada to reproduce, loan, distribute or sell copies of this thesis in microform, paper or electronic formats.

L'auteur a accordé une licence non exclusive permettant à la Bibliothèque nationale du Canada de reproduire, prêter, distribuer ou vendre des copies de cette thèse sous la forme de microfiche/film, de reproduction sur papier ou sur format électronique.

The author retains ownership of the copyright in this thesis. Neither the thesis nor substantial extracts from it may be printed or otherwise reproduced without the author's permission.

L'auteur conserve la propriété du droit d'auteur qui protège cette thèse. Ni la thèse ni des extraits substantiels de celle-ci ne doivent être imprimés ou autrement reproduits sans son autorisation.

0-612-68541-1

Canadä

University of Alberta

Library Release Form

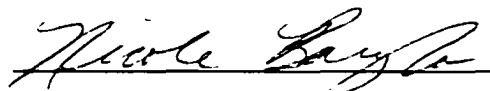**Name of Author:** Nicole Elizabeth Baryla

Title of Thesis: Capillary Coatings for Protein Separations in Capillary Electrophoresis

Degree: Doctor of Philosophy

Year this Degree Granted: 2002

Permission is hereby granted to the University of Alberta Library to reproduce single copies of this thesis and to lend or sell such copies for private, scholarly or scientific research purposes only.

The author reserves all other publication and other rights in association with the copyright in the thesis, and except as herein before provided, neither the thesis nor any substantial portion thereof may be printed or otherwise reproduced in any material form whatever without the author's prior written permission.
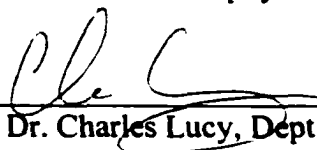
567 Borebank St.
Winnipeg, Manitoba
R3N 1E8
CANADA

Date

University of Alberta

Faculty of Graduate Studies and Research

The undersigned certify that they have read, and recommend to the Faculty of Graduate Studies and Research for acceptance, a thesis entitled "Capillary Coatings for Protein Separations in Capillary Electrophoresis" submitted by Nicole Elizabeth Baryla in partial fulfillment of the requirements for the degree of Doctor of Philosophy.

_____
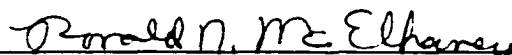Supervisor, Dr. Charles Lucy, Dept. of Chemistry

_____
Dr. Ole Hindsgaul, Dept. of Chemistry

_____
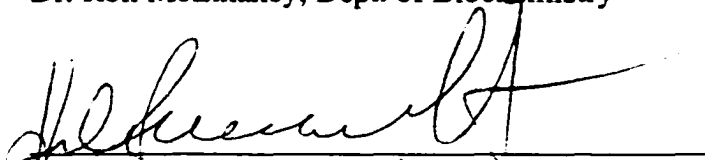Dr. X. Chris Le, Dept. of Public Health Sciences

_____
Dr. Mark McDermott, Dept. of Chemistry

_____
Dr. Ron McElhaney, Dept. of Biochemistry

_____
External Examiner, Dr. Hélène Perreault,
Dept. of Chemistry, University of Manitoba

_____
Date

ABSTRACT

Capillary electrophoresis (CE) is a separation technique based on the differential migration of ions in an electric field. In CE, control of the electroosmotic flow (EOF) and wall chemistry are critical for many separations. The separation of proteins is particularly challenging due to their strong adsorption to the capillary wall. Herein, the use of surfactant-based capillary wall coatings are investigated for improved protein separations as well as EOF control.

The single-chained zwitterionic surfactant coco (amidopropyl) ammoniumdimethylsulfobetaine (CAS U) formed a wall coating that prevented protein adsorption while maintaining a strong EOF so that both cationic and anionic proteins could be simultaneously separated. Efficiencies up to 1.5 million plates/m and recoveries greater than 91% were observed. However, single-chained surfactants must be present in the buffer to maintain the coating. Alternatively, the cationic double-chained surfactant didodecyldimethylammonium (DDAB) forms a highly stable coating at the capillary wall such that excess surfactant can be removed from the capillary.

Organization of surfactant aggregates on the silica surface was probed using atomic force microscopy (AFM). Single-chained surfactants such as cetyltrimethylammonium (CTAB) and CAS U form spherical aggregates while double-chained surfactants such as DDAB form flat bilayers on silica. The increased coverage afforded by the bilayer minimizes protein adsorption.

To achieve a stable coating and the ability to separate both cationic and anionic proteins, a double-chained zwitterionic surfactant 1,2-dilauroyl-*sn*-phosphatidylcholine (DLPC) was investigated. DLPC forms a semi-permanent coating at the capillary wall,

allowing excess surfactant to be removed from the capillary prior to separation. A DLPC-coated capillary yielded high efficiencies (> 1 million plates/m) and good protein recovery (up to 93%) for both cationic and anionic proteins.

The ability to vary the EOF within the capillary using a CAS U coating was used for achieving pH independent large-volume sample stacking of positive or negative analytes. This online sample concentration technique improved detection limits up to 85 fold, while retaining the ability to use buffer pH to optimize the separation.

Finally, coatings comprised of mixtures of DDAB and DLPC were used to control the EOF. Tuning the EOF in this manner allowed optimization of the separation of inorganic anions and proteins.

ACKNOWLEDGEMENTS

I would like to thank Dr. Charles Lucy for his continual support and guidance throughout my graduate degree program. Past and present group members are also gratefully acknowledged for their help over the years. Specifically, I would like to thank Jeremy Melanson for his friendship and many helpful ideas and discussions. Thanks also to Jennifer Cunliffe whose personality and competence in the lab made my 8-month role as a supervisor enjoyable. Furthermore, numerous members of the department provided great support. In particular I would like to thank Dr. Mark McDermott for the use of his AFM equipment. Also, Truong Ta's patience and help with AFM imaging will not be forgotten.

TABLE OF CONTENTS

CHAPTER ONE. Introduction

CHAPTER TWO. Simultaneous Separation of Cationic and Anionic Proteins Using Zwitterionic Surfactants in Capillary Electrophoresis

CHAPTER THREE. pH Independent Large-Volume Sample Stacking of Positive or Negative Analytes in Capillary Electrophoresis

CHAPTER FOUR. Characterization of Surfactant Coatings in Capillary Electrophoresis by Atomic Force Microscopy

CHAPTER FIVE. Phospholipid Bilayer Coatings for the Separation of Proteins in Capillary Electrophoresis

LIST OF TABLES

LIST OF FIGURES

.

LIST OF SYMBOLS AND ABBREVIATIONS

Symbol	Parameter
ε	dielectric constant
ε	molar extinction coefficient
η	viscosity of medium
μ_a	apparent mobility
$\bar{\mu}_a$	mean apparent mobility
μ_e	electrophoretic mobility
μ_{eof}	electroosmotic mobility
$\Delta\mu$	mobility difference
v	mobilization velocity
σ^2_{diff}	variance due to longitudinal diffusion
ζ	zeta potential
a_h	cross-sectional area of head-group
A	absorbance
b	optical path length
c	molar sample concentration
D	diffusion coefficient
F_N	normal force
k	cantilever spring constant
l_c	length of hydrocarbon chain moiety
L_d	capillary length from inlet to detector
L_t	total capillary length

N	efficiency
P	packing parameter
q	net charge on ion
r	radius of ion
R	resolution
S	sensitivity
t_{delay}	time delay of pressure application
t_{inj}	injection time
t_m	migration time
t_{px}	migration time for peak x
t_{volt}	time voltage applied
V	applied voltage
$V_{breakaway}$	breakaway voltage
V_c	volume of hydrocarbon chain moiety
$V_{setpoint}$	setpoint voltage
$w_{1/2}$	peak width at half height
AFM	atomic force microscopy
CAS U	coco (amidopropyl) ammoniumdimethylsulfobetaine
CE	capillary electrophoresis
CEC	capillary electrochromatography
CHES	2-(N-cyclohexylamino)ethanesulfonic acid
CMC	critical micelle concentration
CTAB	cetyltrimethylammonium bromide

CVC	critical vesicle concentration
CZE	capillary zone electrophoresis
DDAB	didodecyldimethylammonium bromide
DDPC	1,2-didecanoyl-*sn*-phosphatidylcholine
DLPC	1,2-dilauroyl-*sn*-phosphatidylcholine
DMPC	1,2-dimyristoyl-*sn*-phosphatidylcholine
DOPA	DL-3,4-dihydroxyphenylalanine
DOPAC	3,4-dihydroxyphenylacetic acid
DTAB	dodecyltrimethylammonium bromide
EDTA	ethylenediaminetetraacetic acid
EIC	electrostatic ion chromatography
EOF	electroosmotic flow
EPA	Environmental Protection Agency
ESI-MS	electrospray ionization mass spectrometry
LIF	laser-induced fluorescence
LVSS	large-volume sample stacking
MALDI-MS	matrix-assisted laser desorption ionization mass spectrometry
MEKC	micellar electrokinetic chromatography
MLV	multilamellar vesicles
PAGE	polyacrylamide gel electrophoresis
pI	isoelectric point
RSD	relative standard deviation
SDS	sodium dodecyl sulfate

SPB	supported phospholipid bilayer
SPM	scanning probe microscopy
STM	scanning tunneling microscopy
SUV	small unilamellar vesicles
TTAB	tetradecytrimethylammonium bromide
UV	ultraviolet

CHAPTER ONE. Introduction

As we embark upon the post-genomic era, there is little debate surrounding the importance of studying the proteins that the genome expresses. Proteomics involves the separation, identification, and characterization of proteins present in biological samples. By comparison of diseased and control samples, it is possible to identify "disease-specific proteins". These are potential targets for drug development. In fact, many of the best-selling drugs either act by targeting proteins or are proteins themselves. As there are millions of proteins to characterize, fast separations are required to obtain the greatest information in the shortest period of time. Research in proteomics is well underway, but many anticipate that this task will be more challenging than the human genome project. Due to the success of capillary electrophoresis (CE) with the genome project [1], applying CE to the study of proteins seems like a natural progression. However, protein analysis by CE has been limited by the strong adsorption of proteins onto the negatively charged capillary wall. Thus the wall must be modified to prevent protein adsorption. Developing coatings for CE and understanding how these coatings act at the molecular level are the main objectives of my thesis research.

1.1   Principles of capillary electrophoresis (CE)

1.1.1   Historical background and development of capillary electrophoresis

Electrophoretic analysis of biological molecules was first demonstrated in 1937 by Tiselius, who showed the separation of the serum proteins, albumin, and α-, β-, and γ-globulins [2]. Electrophoresis refers to the separation of solutes based on their differential migration in an electric field. The velocity of the solute is proportional to the applied

voltage. Thus high voltage is theoretically desirable for fast and efficient separations. In practice (and as seen by Tiselius), the use of high electric fields is limited due to the generation of Joule heating. Consequently, electrophoresis has traditionally been performed in anti-convective media (*e.g.* polyacrylamide gel) with low applied voltages [3]. Today, polyacrylamide gel electrophoresis (PAGE) has become a standard technique in biochemistry laboratories for separating macromolecules such as proteins, peptides and nucleic acids.

Although slab gel electrophoresis is one of the most commonly used separation techniques, it suffers from long analysis times and low efficiencies due to the use of viscous gel media and low applied voltage. Alternatively, the use of narrow bore tubes or capillaries was proposed. Since capillaries themselves provide good heat dissipation, gels are not needed to perform that function. Hjertén first demonstrated capillary electrophoresis (CE) with 3-mm tubes in 1967 [4]. As the technology advanced, capillaries with smaller inner diameters were used in electrophoretic separations to achieve higher resolutions and efficiencies [5-7]. Currently, CE is mostly performed in 10 to 100 μm inner diameter (375 μm outer diameter) fused silica capillaries. The capillary is protected by a polyimide outer coating, which makes the capillary flexible and easy to handle. The high surface-to-volume ratio of the narrow capillaries allows for very efficient dissipation of Joule heat. Further, the use of capillaries in electrophoresis allows separation of a wide variety of analytes ranging from small inorganic ions to biological macromolecules.

1.1.2 CE instrumentation

A schematic diagram of a capillary electrophoresis instrument is shown in Figure 1-1. Typical capillary lengths range from 20 to 100 cm, and capillary inner diameters are
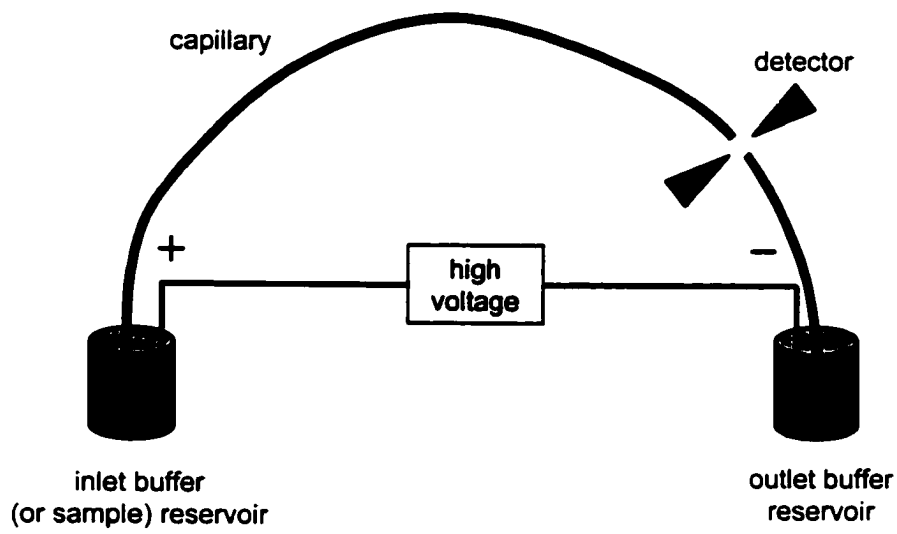
Figure 1-1. Schematic of a capillary electrophoresis instrument.

10 to 100 μm. Each end of the capillary is immersed in a buffer reservoir, which are connected to the high voltage power supply (5 000-30 000 V) via platinum electrodes.

To perform a CE separation, the capillary is filled with a buffer by applying an external pressure to the inlet reservoir. Then the inlet reservoir is replaced with a sample reservoir, from which a small plug of sample is pushed into the capillary by either applying a small pressure or voltage. Typical injection volumes are 1-10 nL. Next the inlet reservoir is put back in place, and separation begins upon the application of an electric field. Typical applied voltages are 100 to 500 V/cm. Ions in the sample migrate with an electrophoretic mobility determined by their charge and mass. Photometric detection is usually performed on-capillary near the outlet reservoir. Removing a section of the polyimide coating creates a window for optical detection. Data is collected and stored by a computer.

1.1.3 Electrophoretic mobility

Separation by electrophoresis is governed by the differences in the electrophoretic mobility of the solutes. The electrophoretic mobility is determined by the electric force that the ion experiences, balanced by its frictional drag through the medium. Electrophoretic mobility (μ_e) can be expressed as

$$\mu_e = \frac{q}{6\pi\eta r}$$ (Eqn. 1-1)

where q is the net charge of the ion, η is the viscosity of the medium, and r is the radius of the ion. Thus, electrophoretic separation occurs for solutes with different charge-to-size ratios.

1.1.4 Electroosmotic flow

In addition to the electromigration of analyte ions, an electroosmotic flow (EOF) also occurs upon application of the electric field in CE. The theory of EOF in fused silica capillaries has been described in great detail elsewhere [8], so will only be described briefly here. The inner walls of fused silica capillaries possess a negative charge due to the presence of acidic silanol groups ($pK_a \sim 5.3$ [9]). To maintain electroneutrality, cations present in the buffer build up near the capillary wall, forming an electrical double layer. Upon the application of an electric field across the capillary, the cations in the diffuse portion of the double layer migrate toward the cathode. These hydrated cations induce a bulk flow of solution within the capillary that exhibits a flat flow profile. The magnitude of the EOF (μ_{eof}) is described by the Smoluchowski equation:

$$\mu_{eof} = -\frac{\varepsilon\zeta}{\eta} \qquad \text{(Eqn. 1-2)}$$

where ε and η are the dielectric constant and viscosity of the solvent, and ζ is the zeta potential. The zeta potential is the potential slightly off the silica surface at the plane of shear, and is a function of the deprotonation of the silanols, ion adsorption onto the surface, and the ionic strength of the buffer.

The surface charge present on the capillary wall will dictate the direction of migration of the EOF. If the capillary wall has been coated with a cationic species, the EOF will be directed towards the anode (EOF reversal). If a neutral coating is applied to the capillary wall, the mobility of the EOF will be essentially zero and there will be no bulk flow within the capillary (EOF suppression). These situations will be encountered throughout Chapters Two to Six of this thesis.

1.1.5 Capillary zone electrophoresis

In capillary zone electrophoresis (CZE), analytes experience their intrinsic electrophoretic mobility (μ_e), as well as the electroosmotic flow mobility (μ_{eof}). The resultant apparent mobility (μ_a) is calculated according to:

$$\mu_a = \mu_e + \mu_{eof} \qquad \text{(Eqn. 1-3)}$$

The apparent mobility (μ_a) is measured from the time an analyte migrates from the capillary inlet to the detector (t_m), as shown by:

$$\mu_a = \frac{L_d L_t}{t_m V} \qquad \text{(Eqn. 1-4)}$$

where L_d is the capillary length from the inlet to the detector, V is the applied voltage, and L_t is the total length of the capillary. The electroosmotic flow mobility (μ_{eof}) can be determined experimentally and calculated according to Eqn. 1-4 by measuring the mobility of a neutral analyte such as mesityl oxide or benzyl alcohol.

Most analytes separated by CZE possess an electrophoretic mobility that is less than the mobility of the electroosmotic flow, allowing for the simultaneous separation of both positively and negatively charged analytes, as shown in Figure 1-2. Here, positive analytes migrate in the same direction as the EOF (co-EOF condition) while negative analytes migrate in the opposite direction to the EOF (counter-EOF condition). As long as the negative analytes possess an electrophoretic mobility that is less than that of the EOF ($\mu_e < \mu_{eof}$), the anions will be swept towards the detector (positioned at the cathodic end of the capillary). Figure 1-2 shows a diagram of a CZE separation occurring within the capillary (Figure 1-2A) accompanied by its corresponding electropherogram (Figure 1-2B). The order of the peaks displayed by a typical electropherogram would be cation
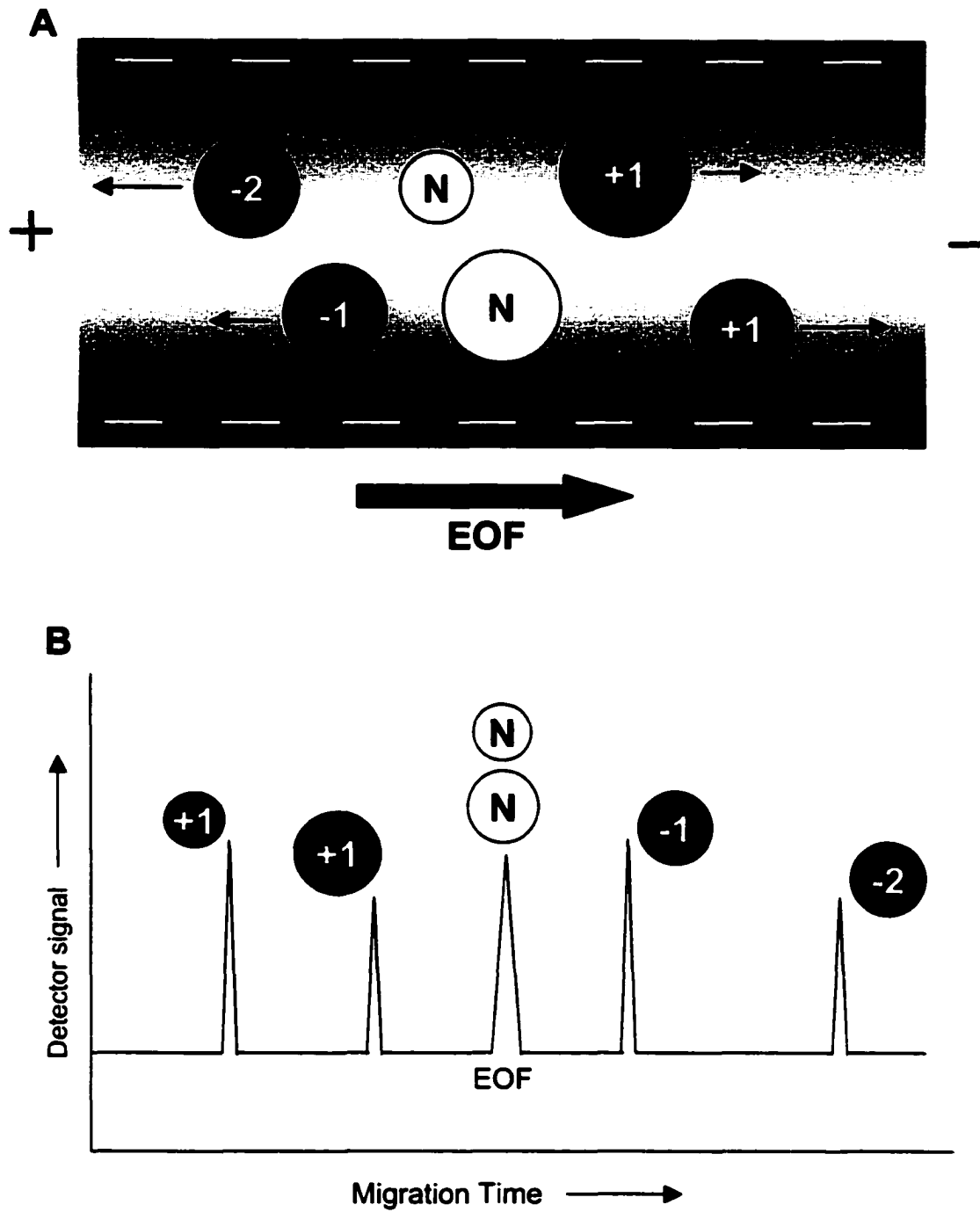
Figure 1-2. Diagram showing A) migration direction of cations, anions, and neutrals in CZE and B) the corresponding electropherogram.

peaks, EOF peak (neutrals), and finally anion peaks. Note that when ions are the same

size, the ion of highest charge migrates faster than the ion of lower charge. Also, when

ions are of equal charge, the smaller ion migrates faster than the larger ion (Eqn. 1-1).

1.1.5.1 Longitudinal diffusion

Peaks in CZE are characterized by their width, as well as their migration time

(t_m). Peak width is a result of band broadening of the sample zone as the sample travels

down the capillary, and is undesirable as it compromises the ability of CZE to separate

compounds. In theory, the dominant source of band broadening in CZE is longitudinal

diffusion. Longitudinal diffusion refers to the axial diffusive spreading of the analyte

from the analyte zone into the bulk solution as it travels down the capillary. The variance

contributed by longitudinal diffusion is given by

$$\sigma^2_{diff} = 2\,D\,t_m \qquad\qquad \text{(Eqn. 1-5)}$$

where D is the diffusion coefficient of the analyte and t_m is the migration time. Hence,

longitudinal diffusion is proportional to the time the analyte spends in the capillary, and

longitudinal diffusion is more severe for analytes with large diffusion coefficients.

Therefore, for minimized longitudinal diffusion, it is desirable to use large applied

voltages in CZE (Eqn. 1-4) in order to speed up the analytes so they spend less time

migrating through the capillary.

1.1.5.2 Solute-wall interactions

Interactions between analytes and the silica capillary wall are primarily caused by

the electrostatic attractions between the anionic silanols and cationic solutes, and to a

lesser extent by hydrophobic interactions. Thus, solute adsorption onto the capillary wall

is most serious for cationic macromolecules such as proteins and large peptides [8].

The variance due to adsorption is strongly dependent on the magnitude of the capacity factor. Even capacity factors of less than 0.001 are detrimental to peak shape [10]. Peak tailing or even irreversible adsorption can occur depending on the degree of adsorption. Preventing adsorption to the capillary wall is the major focus of this thesis. Current methods available to minimize the solute-wall interaction are discussed in Section 1.2.

1.1.5.3 Efficiency and resolution

The efficiency (N) can be used as a measure of peak broadening or dispersion in a separation. Neglecting all other sources of band broadening, the maximum theoretical efficiency due only to longitudinal diffusion is given by:

$$N_{max} = \frac{L_d^2}{2Dt_m}$$

(Eqn. 1-6)

where L_d is the capillary length from the inlet to the detector. The efficiency can also be experimentally determined from the migration time (t_m) and peak width at half height ($w_{1/2}$) according to:

$$N = 5.54 \times \left(\frac{t_m}{w_{1/2}} \right)^2$$

(Eqn. 1-7)

Because the theoretical efficiency (Eqn. 1-6) accounts only for longitudinal diffusion, in practice the measured efficiency (Eqn. 1-7) is usually lower than the theoretical value.

Nevertheless, CZE can achieve highly efficient separations (N>100 000 plates). Thus the resolving power of this technique is also enhanced. The resolution (R) of two components achievable in CZE is expressed by:

$$R = \frac{1}{4} \sqrt{N} \frac{\Delta\mu}{\overline{\mu}_a}$$

(Eqn. 1-8)

where N is the efficiency, $\Delta\mu$ is the mobility difference between the two analytes and $\bar{\mu}_a$ is the mean apparent mobility of the analytes. Method development in CZE often focuses on maximizing the mobility difference ($\Delta\mu$). However, experimental parameters such as pH affect the electroosmotic flow (and thus $\bar{\mu}_a$) as well as the mobility difference. Chapter Three of this thesis focuses on methodologies that allow independent control of the mobility difference (via pH) and the electroosmotic flow (via surfactant additives).

1.1.6 Detection

Many techniques have been reported for detection in CE since its inception [11]. Optical techniques such as absorbance and fluorescence have seen widespread use while electrochemical techniques have also been applied successfully to detection in CE. Electrospray ionization mass spectrometry (ESI-MS) has also been successfully implemented in CE.

On-column UV absorbance detection is by far the most common method of detection in CE today since many compounds of interest absorb light in the UV region (at least to some extent) without needing chemical derivatization. UV absorbance detection is the method used throughout my thesis research. A fundamental limitation of absorbance detection is that the overall signal is a difference between two large signals. This problem is magnified since a very small amount of absorbing sample is initially injected into the capillary. Moreover, the path length in the capillary is very short. According to Beer's law, absorbance (A) is given by

$$A = \varepsilon bc \qquad \text{(Eqn. 1-9)}$$

where ε is the molar extinction coefficient of the sample, b is the optical path length, and

c is the molar sample concentration. Therefore the optical path length directly impacts

the sensitivity that can be achieved with absorbance detection.

1.1.6.1 Stacking

As explained in the previous section, detection sensitivity is a problem when on-

column UV detection is used. Stacking is an on-line sample concentration technique

often used in CE [12, 13]. This concept is shown in Figure 1-3. In sample stacking, a plug

of low conductivity sample solution is introduced hydrodynamically into a capillary filled

with a higher conductivity separation buffer (Figure 1-3, step I). When a high voltage is

applied across the capillary, the sample ions experience a higher field strength than the

buffer ions due to the difference in conductivity between the zones. This causes the

sample ions to migrate quickly to the sample-buffer interface (Figure 1-3, step II). Here

the ions experience a lower field strength and slow down, causing a narrow zone of

analytes to be formed at this boundary (Figure 1-3, step III). The separation then

proceeds according to normal electrophoresis. Chapter Three of this thesis will examine

a novel variation of this conventional stacking technique for improved detection limits.

1.2   Capillary coating techniques

Although CE provides rapid, high-resolution separations of many analytes, there

are situations in CE that demand altering the chemistry at the capillary wall to improve

(and even allow) a separation. For example, protein analysis by CE has been limited

because proteins adhere strongly to the negatively charged capillary wall. Mazzeo and

Krull identified the four characteristics that an ideal coating should exhibit [8] for the

I

low conductivity
sample

high conductivity buffer

II

+

−

III

+

−
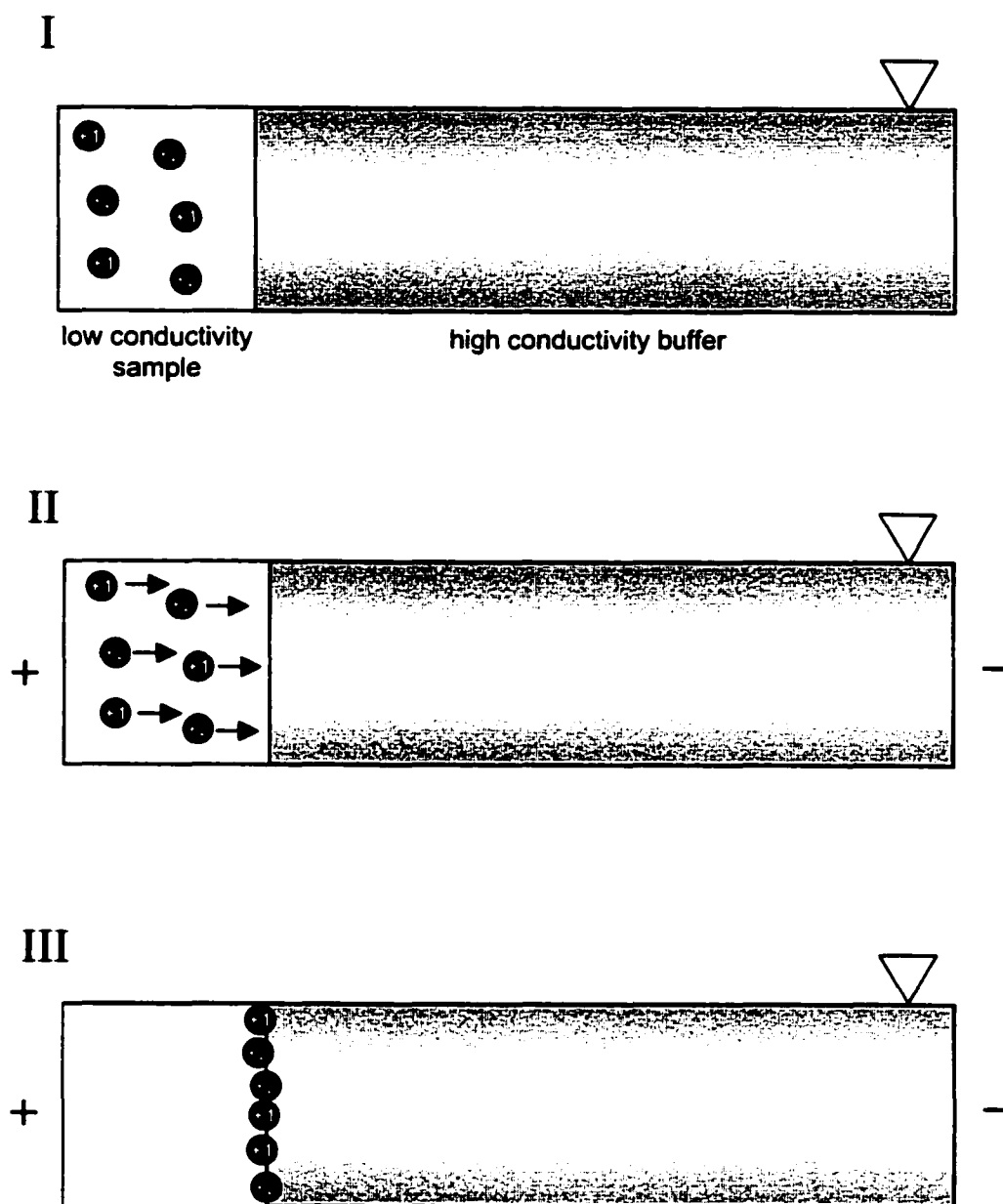
Figure 1-3. Mechanism of stacking in CE. Step I) sample plug is injected, Step II) high voltage is applied and ions accelerate to sample-buffer boundary, Step III) ions stack at boundary and are separated according to normal CZE conditions. See text (section 1.1.6.1) for more details.

separation of proteins: (1) separation efficiency (in theory this should approach 1-2 million plates/m); (2) protein recovery (this should approach 100%); (3) reproducibility of migration time from run to run and day to day; and (4) retention of the EOF so that cationic and anionic proteins can be separated in the same run. To these we would add that the coating procedure should also ideally be: (5) easy to apply; (6) inexpensive; and (7) applicable over a wide range of buffer conditions.

Also, analysis of small anions has been a challenge since the EOF generated within the capillary is not strong enough to sweep these high-mobility anions to the detector. Thus, capillary coatings are also used in CE for control of the EOF.

1.2.1 Permanent capillary coatings

Covalently modified capillaries generally employ polymers such as polyethyleneimine or polyacrylamide to permanently shield the bulk solution from the silanol groups on the capillary wall [14-18]. Such permanent coatings are used for both EOF suppression and prevention of protein adsorption. Despite the success of these capillaries, derivatization procedures can be lengthy, their lifetime may be short, they can be unstable outside a limited pH range, and reproducibility from capillary to capillary may be poor. For example polyethyleneimine has been covalently attached to the capillary wall [15]. The derivatization procedure took longer than 2 hours to perform and the separations were only reproducible for 5 days. The stability of this coating was improved by cross-linking the polyethyleneimine to the wall [14, 15]; however the derivatization procedure took over 12 hours. Kleindienst attached derivatized polystyrene particles to the wall to create a stable, reproducible coating [17]. However, the coating was only useful at pH 3. Furthermore, the cost associated with permanently

derivatized capillaries can be substantial (>$300 for commercially available permanently coated capillaries) and may not be practical for high-throughput analyses.

1.2.2 Regenerated polymeric capillary coatings

To overcome some of the problems associated with derivatized capillaries, cationic polymers such as Polybrene have been used for non-covalent capillary coatings [19-21]. These polymers adsorb strongly onto the capillary surface due to the strong electrostatic attraction between these polycations and the anionic silanols. After the capillary is coated, the excess polymer is flushed from the capillary. Capillaries can be coated, regenerated, and then recoated, making them more cost-effective than permanently derivatized coatings. However, coating procedures can be time consuming (up to 2 hours [20]) and reproducibility can be poor. For instance, in a recent study of four such polymers, the EOF decreased by as much as 10% over 25 runs performed after the initial coating procedure [21]. Thus recoating of the capillary must be performed frequently to achieve adequate reproducibility. Another method recently reported involved several layers dynamically coated onto the capillary. Graul and Schlenoff [22] applied 6.5 layers of alternating positively and negatively charged polyelectrolyte polymer to the capillary wall. They achieved an efficiency maximum of 700 000 plates/m for their protein separations but it took over an hour to apply the coating. Other approaches required even longer rinse times. For instance, Wang and Dubin's [23] noncovalent polycation coating took 16 h to apply. Given the time associated with such coating procedures, this can make such non-covalent polymer coatings unattractive.

1.2.3 Dynamic capillary coatings

An alternative to both covalent and non-covalent adsorptive coatings in capillary

electrophoresis is the use of dynamic capillary coatings. Dynamic coatings can be

thought of as an equilibrium process in which a buffer additive has a strong affinity for

the capillary surface. Traditionally, cationic surfactants such as

tetradecyltrimethylammonium bromide (TTAB) or cetyltrimethylammonium bromide

(CTAB) have been added to the separation buffer to form dynamic wall coatings in CE [24-

26]. Surfactants such as TTAB and CTAB consist of a single hydrophobic tail and a

quaternary amine head group. Above a specific concentration, these surfactants

aggregate and adsorb reversibly onto the negatively charged wall, reversing the surface

charge and thus the EOF [26]. When a surfactant is present in a solution at a concentration

greater than the critical micelle concentration (CMC), free surfactant will aggregate to

form micelles as shown in Figure 1-4A. The driving force for aggregation is the

unfavourable interaction between the hydrocarbon chains and water. The hydrophobic

tails of the surfactants associate in the core of the micelle to maximize their interaction

with one another and minimize their interaction with water. Increasing the length of the

hydrophobic tail increases the hydrophobic attraction and thus decreases the CMC [27].

The second factor that governs micelle formation is repulsion between the hydrophilic,

cationic headgroups. That is, the hydrophobic tails of the surfactants cause them to want

to aggregate, while the electrostatic repulsion between the headgroups inhibits this

aggregation. The structure of the aggregate at the capillary wall has been a subject of

considerable debate and will be addressed in Chapter Four of this thesis. Previously the

A

CMC

surfactant
monomers

micelles

B

bilayer

micelle layer
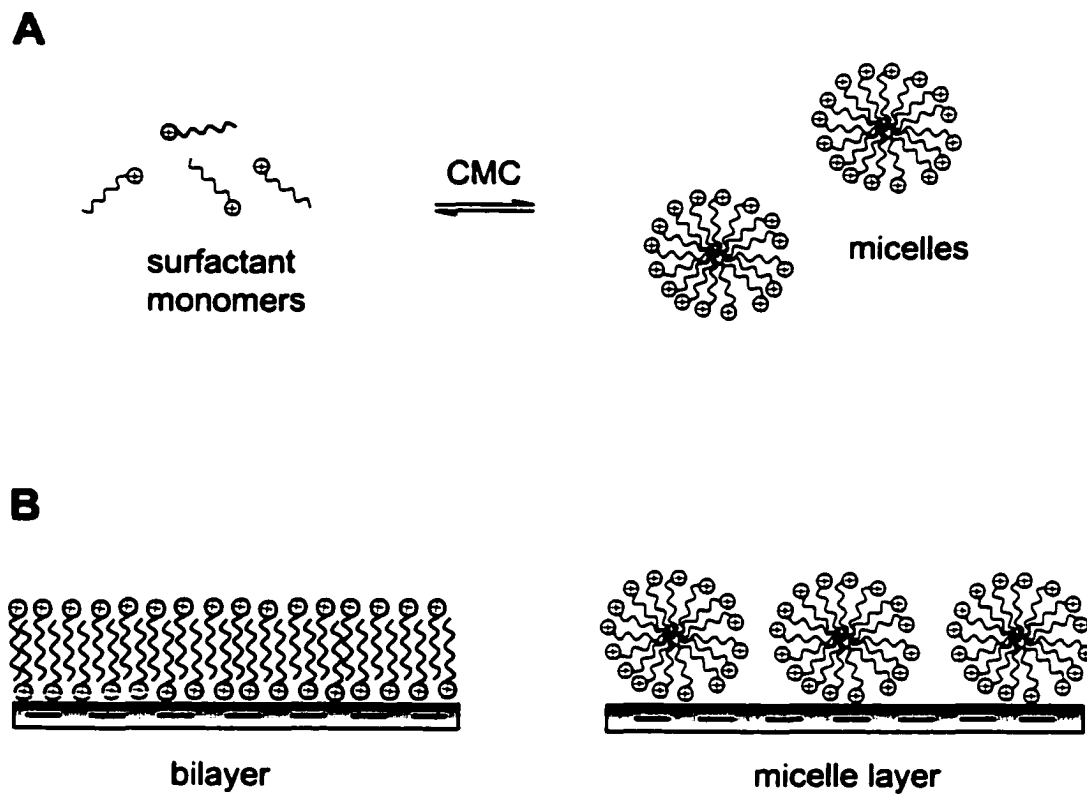
Figure 1-4. Diagram showing (A) the formation of micelle aggregates from free surfactant monomers and (B) previous depictions of surfactant aggregate structure at the capillary wall.

aggregate structure has been depicted as either a micelle layer or more commonly as a bilayer as shown in Figure 1-4B.

Generally, 0.5 mM CTAB is added to the background electrolyte to reverse the EOF [24, 25]. At this concentration micelles will be present in the buffer. These micelles can interact with particular analytes and thus hinder separations [28]. Free surfactant molecules will also be present in the buffer at a concentration equal to the CMC. Thus, analytes can undergo ion-pairing with free surfactants which can also adversely affect separations. Free surfactants in the buffer can also make CE incompatible with detection schemes such as mass spectrometry due to the resultant large background signals [29].

Traditionally, dynamic coatings have been employed exclusively for EOF reversal in the separation of small anions. However dynamic coatings have also been used for the separation of proteins. Cifuentes *et al.* demonstrated the separation of basic proteins with CTAB, but required high concentrations of the surfactant (10 mM) and sub-ambient temperatures (10°C) [30]. Furthermore, while convenient, many dynamic coatings do not yield high efficiencies. Gong and Ho [31] only achieved 50 000 plates/m for lysozyme with their dynamic surfactant coating.

1.3   Thesis overview

Developing simple coatings for capillary electrophoresis and gaining an understanding of how these coatings behave at the molecular level are the main objectives of my thesis research. In Chapter Two I present a capillary coating technique using a zwitterionic surfactant for the simultaneous separation of basic and acidic proteins. As a tangent to this work I used the ability to control the EOF using the

zwitterionic surfactant for a novel stacking technique for on-line preconcentration in CE.

This research is presented in Chapter Three. Chapter Four describes the use of a double-chained surfactant as a wall coating in CE and is compared to wall coatings provided by traditionally used single-chained surfactants. Atomic force microscopy (AFM) imaging is used to elucidate the coating morphology at the capillary wall of both the single-chained and double-chained surfactants. Using the knowledge gained from the research presented in Chapters Two and Four, phospholipids were explored as wall coatings for CE separations of proteins. The results of this research are presented in Chapter Five. Finally, Chapter Six presents a simple method of tuning the EOF using a mixture of double-chained surfactants for improved separations of proteins as well as inorganic anions.

1.4 References

(1)   Zubritsky, E. *Anal. Chem.* **2002,** *74,* 23A.

(2)   Tiselius, A. *Trans. Faraday Soc.* **1937,** *33,* 524.

(3)   Raymond, S.; Weintraub, L. *Science* **1959,** *130,* 711.

(4)   Hjerten, S. *Chromatogr. Rev.* **1967,** *9,* 122.

(5)   Vertanen, R. *Acta Polytechnica Scand.* **1974,** *123,* 1.

(6)   Mikkers, F. E. P.; Everaerts, F. M.; Verheggen, T. P. E. M. *J. Chromatogr.* **1979,** *169,* 11.

(7)   Jorgenson, J. W.; Lukacs, K. D. *Anal. Chem.* **1981,** *53,* 1298.

(8)   In *Handbook of Capillary Electrophoresis,* Landers, J. P. ed. ; CRC Press: Boca Raton, FL, 1994.

(9)   Schwer, C.; Kenndler, E. *Anal. Chem.* **1991,** *63,* 1801.

(10)   McManigill, D.; Swedberg, S. A. *Tech. in Protein Chem.*; Academic Press: San Diego, 1989.

(11)   Ewing, A. G.; Wallingford, R. A.; Olefirowicz, T. M. *Anal. Chem.* **1989,** *61,* 292A.

(12)   Burgi, D. S.; Chien, R.-L. *J. Microcolumn Sep.* **1991,** *3,* 199.

(13)   Burgi, D. S.; Chien, R.-L. *Anal. Chem.* **1991,** *63,* 2042.

(14)   Towns, J. K.; Regnier, F. E. *J. Chromatogr.* **1990,** *516,* 69.

(15)   Figeys, D.; Aebersold, R. *J. Chromatogr. B* **1997,** *695,* 163.

(16)   Huang, X. Y.; Doneski, L. J.; Wirth, M. J. *Anal. Chem.* **1998,** *70,* 4023.

(17)   Kleindienst, G.; Huber, C. G.; Gjerde, D. T.; Yengoyan, L.; Bonn, G. K. *Electrophoresis* **1998,** *19,* 262.

(18) Shao, X. W.; Shen, Y. F.; O'Neill, K.; Lee, M. L. *J. Microcolumn Sep.* **1999**, *11*, 325.

(19) Yao, Y. J.; Khoo, K. S.; Chung, M. C. M.; Li, S. F. Y. *J. Chromatogr. A* **1994**, *680*, 431.

(20) Erim, F. B.; Cifuentes, A.; Poppe, H.; Kraak, J. C. *J. Chromatogr. A* **1995**, *708*, 356.

(21) Cordova, E.; Gao, J.; Whitesides, G. M. *Anal. Chem.* **1997**, *69*, 1370.

(22) Graul, T. W.; Schlenoff, J. B. *Anal. Chem.* **1999**, *71*, 4007.

(23) Wang, Y.; Dubin, P. L. *Anal. Chem.* **1999**, *71*, 3463.

(24) Jones, W. R.; Jandik, P. *J. Chromatogr.* **1991**, *546*, 445.

(25) Jones, W. R.; Jandik, P. *J. Chromatogr.* **1992**, *608*, 385.

(26) Lucy, C. A.; Underhill, R. S. *Anal. Chem.* **1996**, *68*, 300.

(27) Israelachvili, J. *Intermolecular and Surface Forces*; Academic Press: San Diego, CA, 1992.

(28) Zemann, A.; Volgger, D. *Anal. Chem.* **1997**, *69*, 3243.

(29) Varghese, J.; Cole, R. B. *J. Chromatogr. A* **1993**, *652*, 369.

(30) Cifuentes, A.; Rodriguez, M. A.; Garcia-Montelengo, F. J. *J. Chromatogr. A* **1996**, *742*, 257.

(31) Gong, B. Y.; Ho, J. W. *Electrophoresis* **1997**, *18*, 732.

CHAPTER TWO. Simultaneous Separation of Cationic and Anionic Proteins Using Zwitterionic Surfactants in Capillary Electrophoresis[*]

2.1 Introduction

In capillary electrophoresis, control of the electroosmotic flow (EOF) and wall chemistry is critical for many separations. The separation of proteins is particularly challenging due to their strong adsorption to the capillary wall [1,2]. This adsorption results in a loss of efficiency, low protein recovery, and poor reproducibility in migration times. There have been a number of approaches developed to suppress the EOF and/or prevent wall adsorption so as to obtain improved separations [3]. These are discussed in detail in section 1.2.

Since some methods of modification of the inner capillary wall are laborious and time-consuming [4-10], dynamic coatings are desirable due to their low cost and simplicity of application. For example, in 1997 Yeung and Lucy [11] demonstrated that low concentrations of the zwitterionic surfactant Rewoteric CAS U (Figure 2-1) yields extremely high efficiencies for cationic proteins (>750,000 plates/m) such as lysozyme and α-chymotrypsinogen A. A strongly suppressed cathodic EOF (< 1.25×10^{-4} cm^2/Vs) was also observed. The EOF was suppressed over the pH range from 3 to 12, and high efficiency separations of cationic proteins were demonstrated from pH 4 to 7. Thus the zwitterionic surfactant CAS U demonstrated almost all of the criteria proposed by Mazzeo and Krull [12] for an ideal wall coating (Section 1.2). The only deficiency of the

---

$$R-\overset{\overset{\displaystyle O}{\|}}{C}-NH-CH_2-CH_2-CH_2-\overset{\overset{\displaystyle CH_3}{|}}{\underset{\underset{\displaystyle CH_3}{|}}{N^+}}-CH_2-\overset{\overset{\displaystyle OH}{|}}{CH}-CH_2-\overset{\overset{\displaystyle O}{\|}}{\underset{\underset{\displaystyle O}{\|}}{S}}-O^-$$

$$R = C_8H_{17} \text{ to } C_{18}H_{37}$$
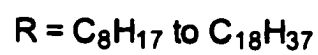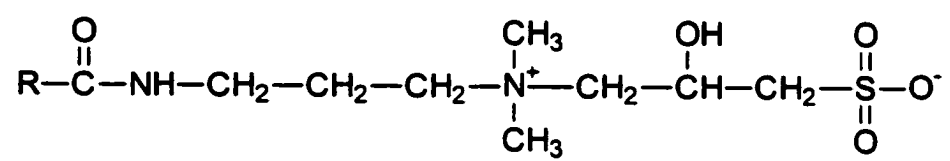
Figure 2-1. Structure of CAS U.

CAS U coating was that the suppressed EOF did not allow for the simultaneous separation of both cationic and anionic proteins.

To date, the only work to demonstrate simultaneous separations of cationic and anionic proteins using a dynamic coating was that of Hult *et al*.[13]. They used mixtures of cationic and anionic fluorosurfactant to dynamically coat the capillary wall. However, based on their electropherograms, it is estimated that the efficiencies were less than 200 000 plates/m. Also this coating was only demonstrated at pH 7. The anionic fluorosurfactant they used contained a carboxylate group, which could give rise to pH dependence. Separation selectivity was achieved by altering the cationic and anionic fluorosurfactant ratio in the buffer rather than changing pH or ionic strength.

In this chapter I discuss a means of recovering the EOF using a zwitterionic surfactant additive system, while simultaneously maintaining high efficiencies for both cationic and anionic proteins. New experimental evidence illustrates that chaotropic anions preferentially bind to the micelle layer formed on the capillary wall by CAS U. The addition of increasingly chaotropic anions in the buffer substantially increases the cathodic EOF to values nearing 3×10^{-4} cm^2/Vs. The higher EOF enables the simultaneous separation of both cationic and anionic proteins. Protein separations of less than 15 minutes with efficiencies as high as 1.5 million plates/m are achieved in this manner. This coating is generated on the capillary wall with a simple 2 min rinse with the buffer containing surfactant.

2.2 Experimental

2.2.1 Apparatus

A Beckman P/ACE 2100 System (Fullerton, CA, USA) with a UV absorbance

detector was used for all experiments. Untreated silica capillaries

(PolymicroTechnologies, Phoenix, AZ, USA) with an inner diameter of 50 μm (EOF

measurements) or 75 μm (protein separations), outer diameter of 365 μm, and total length

of 47 cm (40 cm to detector) were used unless otherwise indicated. Data acquisition (10

Hz) and control was performed using P/ACE Station Software for Windows 95

(Beckman) on a Pentium 120 MHz microcomputer.

2.2.2 Chemicals

All solutions were prepared in Nanopure ultra-pure water (Barnstead, Chicago,

IL, USA). Buffers were prepared from reagent grade orthophosphoric acid (BDH,

Darmstadt, Germany) and adjusted to the desired pH with potassium hydroxide (BDH).

The zwitterionic surfactant coco (amidopropyl) ammoniumdimethylsulfobetaine

$(RCONH(CH_2)_2N^+(CH_3)_2CH_2CH(OH)CH_2SO_3^-$, $R = C_8H_{17}$-$C_{18}H_{37})$ (Rewoteric AM CAS

U; Goldschmidt Chemical, Oakville, ON, Canada) was used as received.

For studies of the effect of the buffer anion on the EOF, the potassium salts of

iodide, bromide, perchlorate, chloride, and sulfate (Fisher, Fair Lawn, NJ, USA) were

used. A solution of 5mM mesityl oxide (Aldrich, Milwaukee, WI, USA) in water was

used as a neutral marker for the EOF measurements.

A mixture of 0.15 mg/ml of lysozyme (chicken egg white), ribonuclease A

(bovine pancreas), α-chymotrypsinogen A (bovine pancreas), and myoglobin (horse

skeletal muscle) (Sigma, St. Louis, MO, USA) was prepared in water and used for protein separations.

2.2.3 EOF measurements

New capillaries (50 μm; 47 cm total length) were pretreated by rinsing at high pressure (20 psi) with 0.1 M KOH for 10 min. Prior to each run, the capillary was rinsed at high pressure with 0.1 M KOH for 2 min, H_2O for 2 min, and buffer for 3 min. The buffer was 10 mM phosphate and 2 mM CAS U, and adjusted to pH 4.6 with KOH. Different potassium salts were added to the buffer to study their effect on the EOF.

The suppressed electroosmotic mobility ($< 3.0 \times 10^{-4}$ cm^2/Vs) was measured using the three-injection method introduced by Williams and Vigh [14]. This method is depicted in Figure 2-2. In this method, two bands of mesityl oxide, separated by buffer, are introduced onto the capillary using a low-pressure hydrodynamic injection (Figure 2-2, steps 1 to 3). A constant voltage is applied for a short period of time, t_{volt}. This voltage causes the two sample bands to move within the capillary as a result of the induced EOF (Figure 2-2, step 4). A third band of mesityl oxide is injected, and low pressure is used to push all three sample bands past the detector (Figure 2-2, step 5). The net result is that three peaks are observed. The difference between the first migration time gap (between peaks 1 and 2) and the second migration time gap (between peaks 2 and 3) is caused by the induced electroosmotic movement (see electropherogram in Figure 2-2). Hence the electroosmotic mobility is determined using [14]:

$$\mu = \frac{\left[t_{p3} - (t_{p2} - t_{p1}) - t_{p2} \right] v}{t_{volt}} \div \frac{V}{L_t} \qquad \text{(Eqn. 2-1)}$$
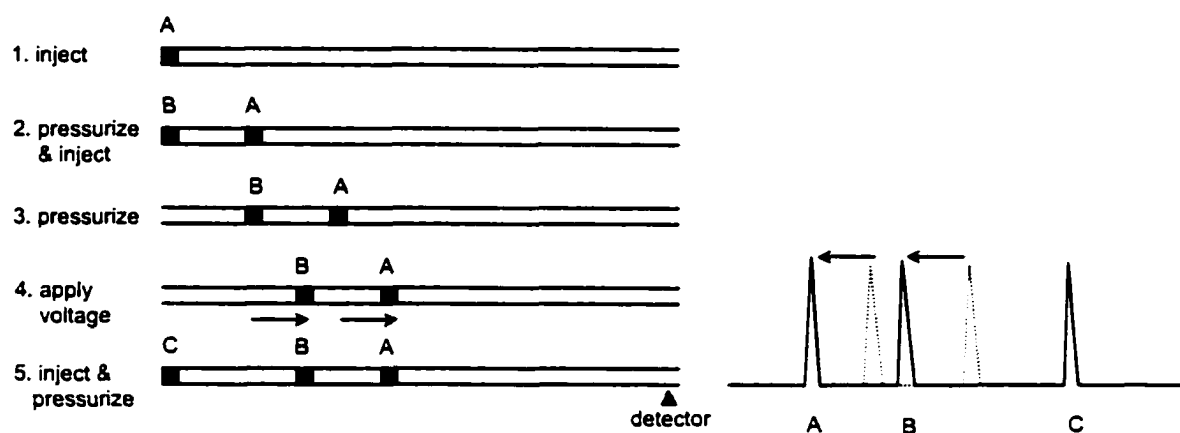
Figure 2-2. EOF Measurement by sequential injection. Shadowed bands and peaks represent the imaginary position if zero EOF is present (see section 2.2.3 for details).

where t_{p1}, t_{p2}, and t_{p3} are the migration times for peaks 1, 2 and 3 and t_{volt} is the length of time that the voltage is applied. The low pressure mobilization velocity, v, is expressed by [14]:

$$v = \frac{L_d}{t_{p3} + t_{inj}/2 - t_{delay}}$$

(Eqn. 2-2)

where t_{inj} is the injection time and t_{delay} is the time delay of pressure application from the beginning of data collection. In our case, t_{inj} (1 s) and t_{delay} (< 1 s) were found to be insignificant compared to t_{p3} (>10 min, with uncertainty of 3-6 s) and so were approximated as zero.

Herein, the first 1 mM mesityl oxide marker was injected using low pressure (0.5 psi) for 1 s. This band was pushed through the capillary for 2 min using low pressure. A second mesityl oxide marker was then introduced by an identical low pressure injection. A constant voltage of 15 kV was applied for 3 min causing the 2 markers to move within the capillary as a result of the EOF. A third mesityl oxide marker was then injected and all the bands were eluted by applying low pressure for 12 min. Detection was at 254 nm.

2.2.4 Protein separations

A new capillary (75 μm; 47 cm total length) was used for the protein separations. The capillary was pretreated as described in Section 2.2.3 with 0.1 M KOH for 10 min. Before each run the capillary was conditioned at high pressure (20 psi) with 0.1 M KOH for 1 min, H_2O for 1 min, and buffer for 2 min.

For studies of the effect of concentration of perchlorate on the protein separations, an electrophoretic buffer of 10 mM phosphate adjusted to pH 7.2 was used. Two mM of CAS U was added to this buffer along with varying concentrations of $KClO_4$. A mixture of 0.15 mg/ml of the cationic proteins in water was injected using low pressure (0.5 psi)

for 3.0 s. The applied voltage was 15 kV, detector rise time was 1.0 s, and detection was at 214 nm. Three replicates of each different buffer were run and efficiencies were calculated by the P/ACE Station Software using the peak width at half height method.

For studies of the effect of the concentration of CAS U on the protein separations, a 10 mM phosphate buffer was prepared containing 5 mM $KClO_4$. From 0.25 to 2.0 mM CAS U was added to the buffer. The separations and efficiency calculations were performed as above.

The optimized conditions used for the separation of cationic and anionic proteins were: 10 mM phosphate buffer adjusted to pH 7.2 with KOH; 5 mM $KClO_4$; and 1.0 mM CAS U. The separation of a mixture of 0.15 mg/ml each of lysozyme, ribonuclease A, α-chymotrypsinogen A, and myoglobin was performed in triplicate as above, using a 0.1 s rise time. Efficiencies were calculated as before.

The effect of pH on the protein separations was studied by preparing a series of buffers containing 10 mM phosphate, 5 mM $KClO_4$, and 1 mM CAS U adjusted to pH 4 to 9.5 with potassium hydroxide and performing the separation as before.

Migration time reproducibility was determined by performing 15 replicate injections on 3 successive days using the optimal conditions.

2.2.5 Protein recovery study

Protein recoveries were determined using the procedure of Towns and Regnier [15] modified for a one-detector CE [11]. In Towns and Regnier's method [15], two detectors were placed online at two different positions along the capillary, 20 and 70 cm from the capillary inlet. Protein recovery was determined by subtracting the peak areas observed at each detector for the proteins. If protein adsorption occurs, the area obtained from the

second detector would be smaller than that from the first. Unfortunately, our commercial instrument prohibits the use of two detectors. Thus the experimental procedure was modified in the following manner as previously described [11]. In this procedure, 4 replicate injections were performed using the optimal buffer conditions described in Section 2.2.4 on a 47-cm (40 cm to detector) capillary. The capillary was then shortened to 27 cm (20 cm to detector) and the injections were repeated. The applied voltage, rinse times, and injection time were reduced accordingly for the short capillary. Benzylamine was used as an internal standard to correct for injection volume variation. The percent recoveries of the proteins were determined by comparing the peak area between the long and short capillaries.

2.3 Results and Discussion

2.3.1 Effect of buffer anions on the EOF

In previous work using the zwitterionic surfactant CAS U, the suppressed EOF was alternately observed to be cathodic [11] or anodic [16, 17], depending on the buffer conditions. In both cases, the EOF was highly reproducible, but it was unclear what was causing the differences in observed EOF.

One observation made from the previous work was that the EOF was reversed under low ionic strength conditions and normal (albeit suppressed) under higher ionic strength conditions (I=50 mM with NaCl). It was therefore decided to monitor the effect of NaCl concentration on the observed EOF. The results of this study are shown in Figure 2-3A. For sake of comparison, in the absence of CAS U, the EOF would be about 5×10^{-4} cm^2/Vs under these buffer conditions. Thus, the addition of 2 mM CAS U
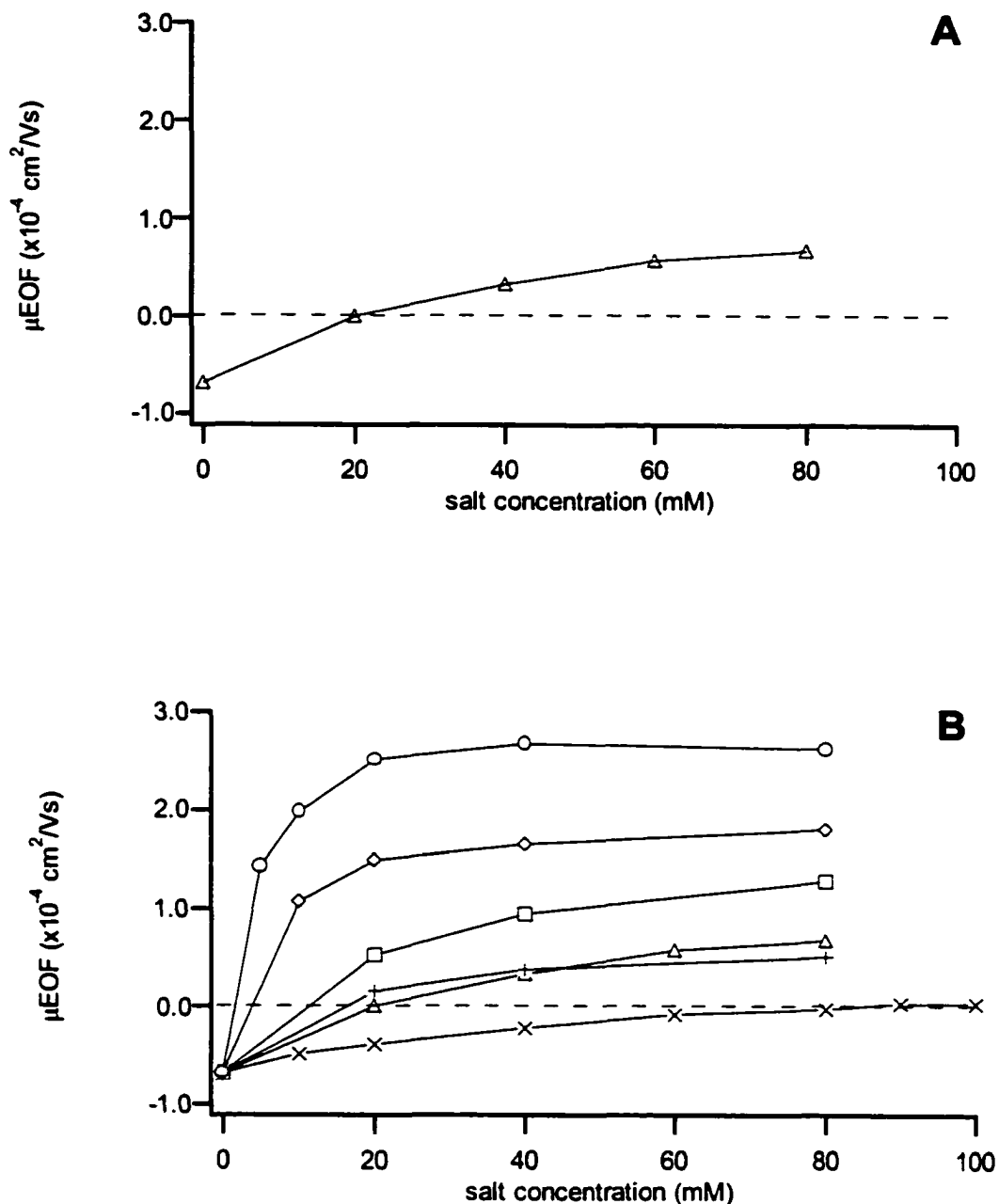
Figure 2-3. (A) Effect of chloride on the EOF in the presence of the zwitterionic surfactant CAS U. (B) Effect of several anions on the EOF in the presence of the zwitterionic surfactant CAS U. Anions: O ClO_4^-; ◊ I^-; □ Br^-; Δ Cl^-; + SO_4^{-2}; X phosphate. Experimental conditions: capillary length, 47 cm (40 cm to detector), 75 μm ID; buffer, 10 mM phosphate, 2 mM CAS U, varying amounts of potassium salts, pH 4.6. Lines through points act only as a guide to the eye.

resulted in a strongly suppressed EOF. The zwitterionic surfactant CAS U is postulated to adsorb onto the capillary wall to form a micelle layer, as depicted in Figure 1-4 B. This coating shields the silanols from the bulk solution, and thus suppresses the EOF.

At low NaCl concentrations, the EOF was low and reversed. As the NaCl concentration increased, the EOF switched to the normal direction and increased in magnitude, before finally leveling out at about 0.7×10^{-4} cm^2/Vs. This behavior was extremely perplexing as the magnitude of the EOF was actually increasing with ionic strength!

Altering buffer cations (Li^+, Na^+, K^+) had no effect on the EOF. The EOF varied less than 2.5% upon changing the buffer cation. There was also minimal difference in the EOF upon changing the buffer cation from monovalent to divalent (Mg^{+2}, Ca^{+2}). In this case the change in EOF was less than 10%. In contrast, the EOF observed in the presence of CAS U strongly depends on the buffer anion, as shown in Figure 2-3B. In 10 mM phosphate buffer containing 2 mM CAS U, a near zero (slightly reversed) EOF is observed. This is depicted as 0 mM added salt in Figure 2-3B. Addition of anions to the buffer causes the EOF to become cathodic and increase in magnitude. Figure 2-3B illustrates that the EOF increases as potassium salts of various anions are added, and then levels out at higher anion concentrations. The EOF shift increases in the order: $SO_4^{-2} <$ $Cl^- < Br^- < I^- < ClO_4^-$. This is the same order that has been observed in electrostatic ion chromatography (EIC). In electrostatic ion chromatography, a zwitterionic exchange site is used to separate anions. Separation in EIC is based on two simultaneous effects [18]. First, the outer sulfonate group on the zwitterionic phase contributes a negative charge that repels analyte anions. The magnitude of this negative charge is a function of how

strongly buffer cations interact with the sulfonate groups and how strongly buffer anions interact with the inner quaternary amine groups. Thus, the outer negative charge constitutes a barrier over which analyte anions must pass in order to interact with the quaternary amine groups. Second, the interaction and hence retention of analyte anions with the quaternary amine groups is based on the increasing chaotropic behaviour of the anions [18]. Chaotropic behaviour refers to an increase in entropy resulting from the disruption of the water molecules around these ions in solution. Highly chaotropic anions (ClO_4^-, I^-) interact more strongly with the inner quaternary amine groups than less chaotropic anions (Cl^-, SO_4^{-2}). Cations can be separated using EIC in the same manner as the anions by using a zwitterionic surfactant with the positive charge as the terminal group [19]. As stated above, the buffer cation (Li^+, Na^+, K^+, Mg^{+2}, Ca^{+2}) had minimal effect on the EOF with CAS U, which has a negative charge as the terminal group.

Also as stated above, the zwitterionic surfactant CAS U is postulated to adsorb onto the capillary wall to form a micelle layer. The precise morphology of this coating will be discussed in Section 4.5.2. Regardless of its morphology, the surfactant coating shields the silanols from the bulk solution and thus suppresses the EOF. It is believed that the behavior observed in Figure 2-3B results from the buffer anion interacting with the micelle layer to a greater extent than the buffer cation. For example, since ClO_4^- (highly chaotropic) interacts with the quaternary amine more strongly than K^+ (not chaotropic) interacts with the outer sulfonate group (Figure 2-4), the overall charge on the surface would be negative. This would account for the increasingly cathodic EOF as the concentration of anion in the buffer increases and as the chaotropic character of the buffer anion increases. For the separation of proteins, the ideal anion buffer additive would
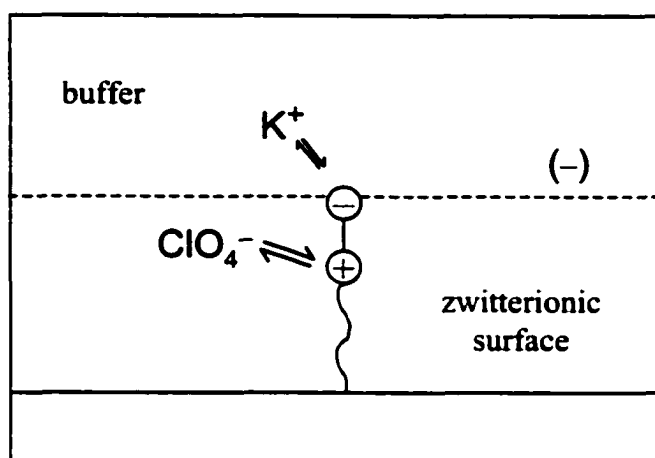
Figure 2-4. Effect of adding potassium perchlorate to a buffer in contact with a zwitterionic surface. Potassium weakly interacts with the negative functional group while perchlorate strongly interacts with the positive functional group. The overall surface charge will be negative. Figure adapted from reference (18).

generate the strongest cathodic EOF and would not absorb in the UV range. The cathodic EOF would allow simultaneous separation of cationic and anionic proteins. Since perchlorate is not UV active, and gives a strong EOF (+2.7 x 10^{-4} cm²/Vs), it was chosen for the protein separations.

2.3.2 Effect of perchlorate on protein separations

Interaction of anions with the micelle layer makes it negatively charged. Thus, intuitively it would not be expected that this surfactant coating would prevent cationic protein adsorption. Despite this, high efficiencies and quantitative recoveries were observed for cationic proteins using CAS U [11]. If the cationic proteins do not adhere to the wall in the presence of perchlorate, the increased EOF generated by the perchlorate should enable simultaneous determination of anionic proteins. Anionic proteins would not be expected to adsorb onto the wall due to their electrostatic repulsion from the negatively charged micelle coating.

In Figure 2-3B, the strongest cathodic EOF were observed using 30 mM-90 mM perchlorate. However, at these high perchlorate concentrations, only a broad, tailed lysozyme peak was observed upon injection of the cationic protein mixture. The other proteins (ribonuclease A, α-chymotrypsinogen A) were not even observed. Satisfactory peak shapes for the cationic proteins were only obtained at low perchlorate concentrations (1-7 mM). As shown in Figure 2-5, from 1-3 mM ClO_4^-, a baseline artifact was present in the anionic region, and the efficiencies were as low as 350 000 plates/m. Between 4 and 5 mM ClO_4^-, the efficiencies were maximum (~500 000 plates/m) and the baseline in the anionic region was smoother. Above 5 mM perchlorate, the efficiencies again dropped off (down to 300 000 plates/m at 7 mM ClO_4^- for
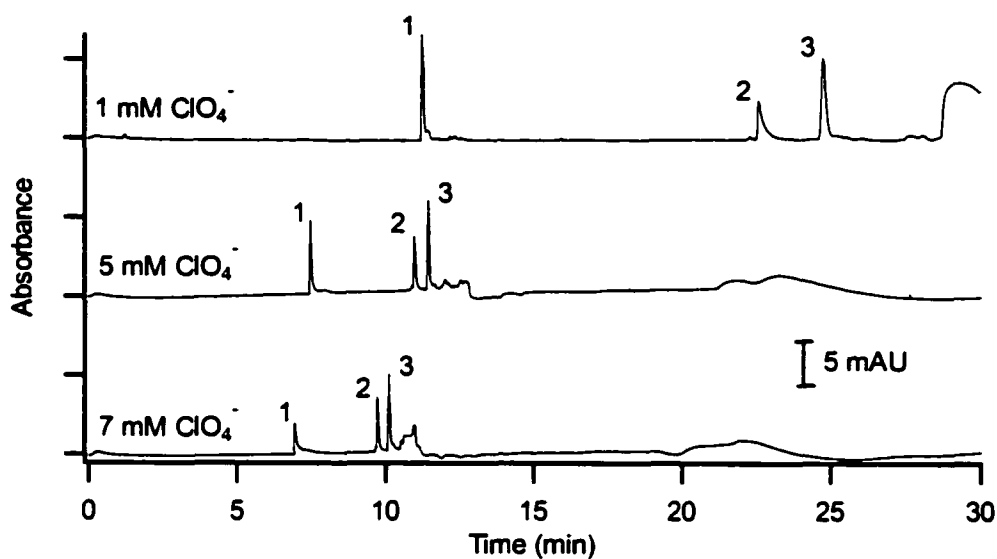
Figure 2-5. Cationic protein separation in the presence of different perchlorate concentrations. Peaks: (1) lysozyme; (2) ribonuclease A; (3) α-chymotrypsinogen A. Experimental conditions: applied voltage, 15 kV; temperature, 25°C; capillary length, 47 cm (40 cm to detector), 50 μm ID; buffer, 10 mM phosphate and 2 mM CAS U containing 1, 5, or 7 mM perchlorate, pH 7.2; sample, 0.15 mg/ml of each protein.

lysozyme). It was reasoned that the more negatively charged capillary wall caused band broadening by attracting the cationic proteins to the wall [20]. Since the strongest EOF possible is desired for separating anionic proteins, 5 mM perchlorate is optimal.

2.3.3 Effect of CAS U on protein separations

All previous electrophoretic separations were performed with 2 mM CAS U in the buffer. Keeping the perchlorate concentration constant at 5 mM and varying the CAS U concentration from 0.25 to 2 mM resulted in the behaviour shown in Figure 2-6. The baseline in the anionic region improved as the CAS U concentration decreased. However, the efficiencies of the cationic proteins decreased when the CAS U concentration was below 1 mM to a low of 380 000 plates/m at 0.25 mM CAS U. Thus, low concentrations of surfactant do not prevent protein interaction with the wall to the same extent as higher concentrations. Indeed this is consistent with what has been previously reported using CAS U where EOF suppression only became constant at concentrations above 1 mM CAS U [11]. The baseline was reasonable at 1 mM CAS U and the efficiencies were optimal, in excess of 560 000 plates/m. Thus these conditions were used for further separations.

2.3.4 Separation of cationic and anionic proteins

In the absence of CAS U in the separation buffer (10 mM phosphate, 5 mM $KClO_4$, pH 7.2), the proteins lysozyme, ribonuclease A, and α-chymotrypsinogen A are not observed in the CE electropherogram indicating that the cationic proteins are irreversibly adsorbed to the capillary wall. A myoglobin peak is present in the electropherogram since it is anionic at pH 7.2 and does not interact with the wall very strongly. However, a mixture of cationic (lysozyme, ribonuclease A and α-
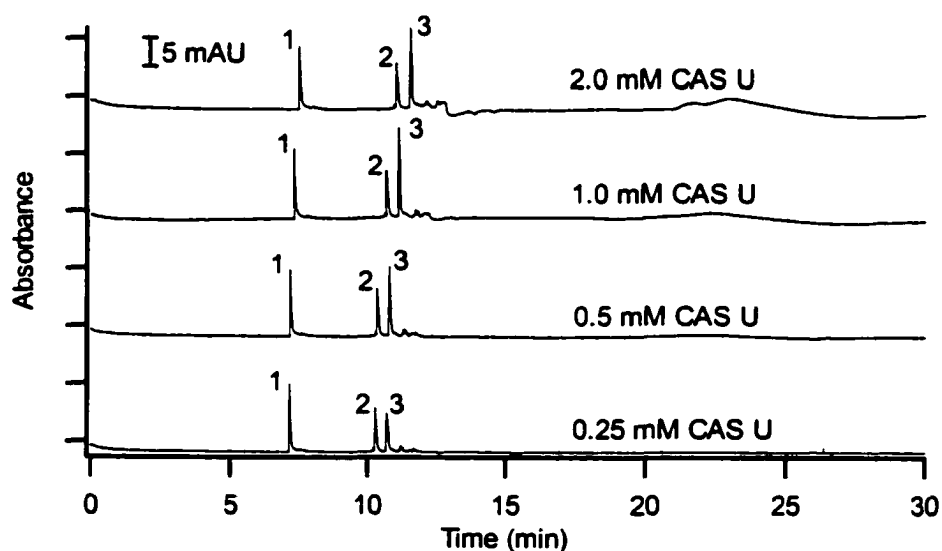
Figure 2-6. Cationic protein separation in the presence of different CAS U concentrations. Peaks: (1) lysozyme; (2) ribonuclease A; (3) α-chymotrypsinogen A. Experimental conditions: applied voltage, 15 kV; temperature, 25°C; capillary length, 47 cm (40 cm to detector), 50 μm ID; buffer, 10 mM phosphate and 5 mM perchlorate containing 0.25, 0.5, 1.0, or 2.0 mM CAS U, pH 7.2; sample, 0.15 mg/ml of each protein.

chymotrypsinogen A) and anionic (myoglobin) proteins was separated at pH 7.2 (10 mM phosphate) using the optimized buffer containing 5 mM $KClO_4$ and 1.0 mM CAS U. Figure 2-7 and Table 2-1 show that all four proteins were separated in less than 15 minutes with efficiencies ranging from 560 000 to 840 000 plates/m. Myoglobin eluted after the EOF confirming its anionic character under these buffer conditions. The anionic protein α-lactalbumin (pI ~ 4.8) was also injected, but could not be observed after a 40 min run time. This protein was not seen because its mobility was greater than that of the EOF.

Protein recoveries were determined by measuring the difference in peak area between protein peaks observed using two different lengths of capillaries. This approach is explained further in Section 2.2.5. The protein recoveries observed for injections from water were near quantitative, as shown in Table 2-1. The amount of α-chymotrypsinogen A recovered (91%) was nearly as good as that reported by Towns and Regnier (95%) [15] and was improved from the 80% previously seen in our laboratory [11].

Migration time should be reproducible if proteins do not adsorb onto the wall during the separations. Run-to-run and day-to-day migration time reproducibility are presented in Table 2-1. These are comparable to those achieved previously with CAS U (0.6-1.3 % and 2.3-4.5 %, respectively) [11], but not as impressive as that seen by Srinivasan et al. [9] whose permanent polymer coating held up for 500 runs with an RSD within 2%.

To judge the versatility of the coating, separations were performed over a range of pH values. The coating was effective at preventing protein adsorption between pH 5.5 and 9. Below pH 5.5, the lysozyme peak broadened and was severely tailed (N<35 000
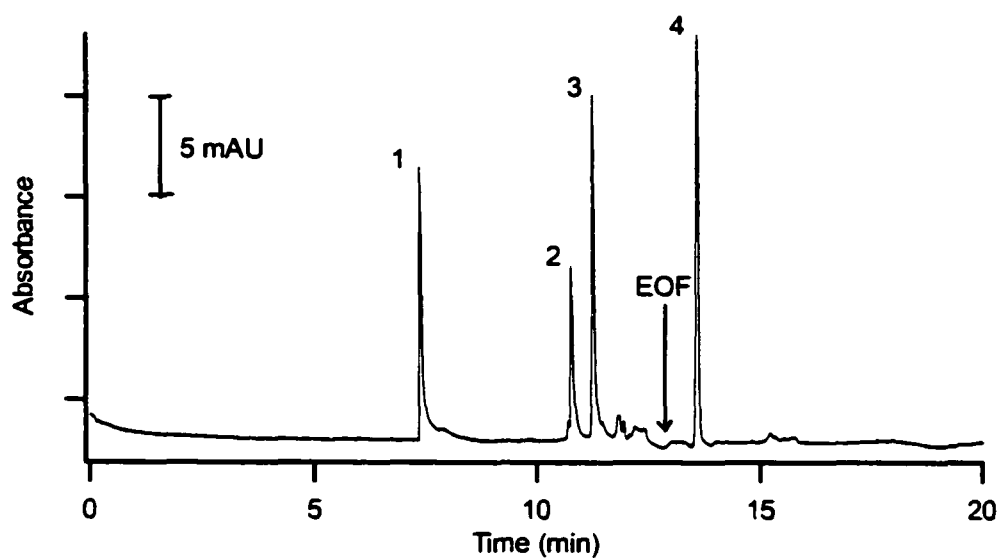
Figure 2-7. Separation of cationic and anionic proteins at pH 7.2. Peaks: (1) lysozyme; (2) ribonuclease A; (3) α-chymotrypsinogen A; (4) myoglobin. Experimental conditions: applied voltage, 15 kV; temperature, 25 °C; capillary length, 47 cm (40 cm to detector), 50 μm ID; buffer, 10 mM phosphate, 1 mM CAS U, 5 mM perchlorate; sample, 0.15 mg/ml of each protein.

Table 2-1. Efficiency, recovery, and migration time reproducibility for cationic and anionic proteins separated using the optimal buffer conditions.*

protein	pI	efficiency (plates/m)	recovery (%)	%RSD of migration time within 1 day	%RSD of migration time day to day
lysozyme	11	560 000	100	0.7	2.5
ribonuclease A	9.6	560 000	96	1.1	2.4
α-chymotrypsinogen A	8.7	840 000	91	1.1	2.9
myoglobin	7.0	620 000	94	1.6	4.6

* optimal conditions as in Figure 2-7

plates/m). Myoglobin was not even observed. Ribonuclease A and α-chymotrypsinogen A retained a Gaussian shape, but their efficiencies were lower than 100 000 plates/m. Figure 2-8A shows a separation of the four proteins at pH 4. Decreasing the pH increases the positive charge of a protein. Perhaps the electrostatic attraction to the negatively charged coating was too great. Decreasing the concentration of perchlorate in the pH 4 phosphate buffer to 0.5 to 1 mM resulted in some improvement in peak shape, but the efficiencies were still poorer than at pH 7.2 (lysozyme, N=250 000 plates/m at 0.5 mM $KClO_4$). Above pH 9, all protein peaks degraded except that of lysozyme. However, as shown in Figure 2-8B, a second component was separated from α-chymotrypsinogen A at pH 8, and efficiencies now exceeded 1.5 million plates/m.

2.4 Conclusions

The zwitterionic surfactant CAS U forms a dynamic wall coating which is effective at preventing protein adsorption and suppressing the EOF. In analogy to electrostatic ion chromatography, chaotropic ions interact with this zwitterionic wall coating. The addition of the chaotropic anion perchlorate to the buffer generates a cathodic EOF strong enough for the fast separation of both anionic and cationic proteins in the same run. Protein efficiencies were as high as 1.5 million plates/m. This buffer system generates an ideal CZE coating possessing the desired coating characteristics of high protein efficiencies, high protein recovery, excellent migration time reproducibility, and a strong cathodic EOF, while simultaneously being inexpensive and quick and easy to apply.
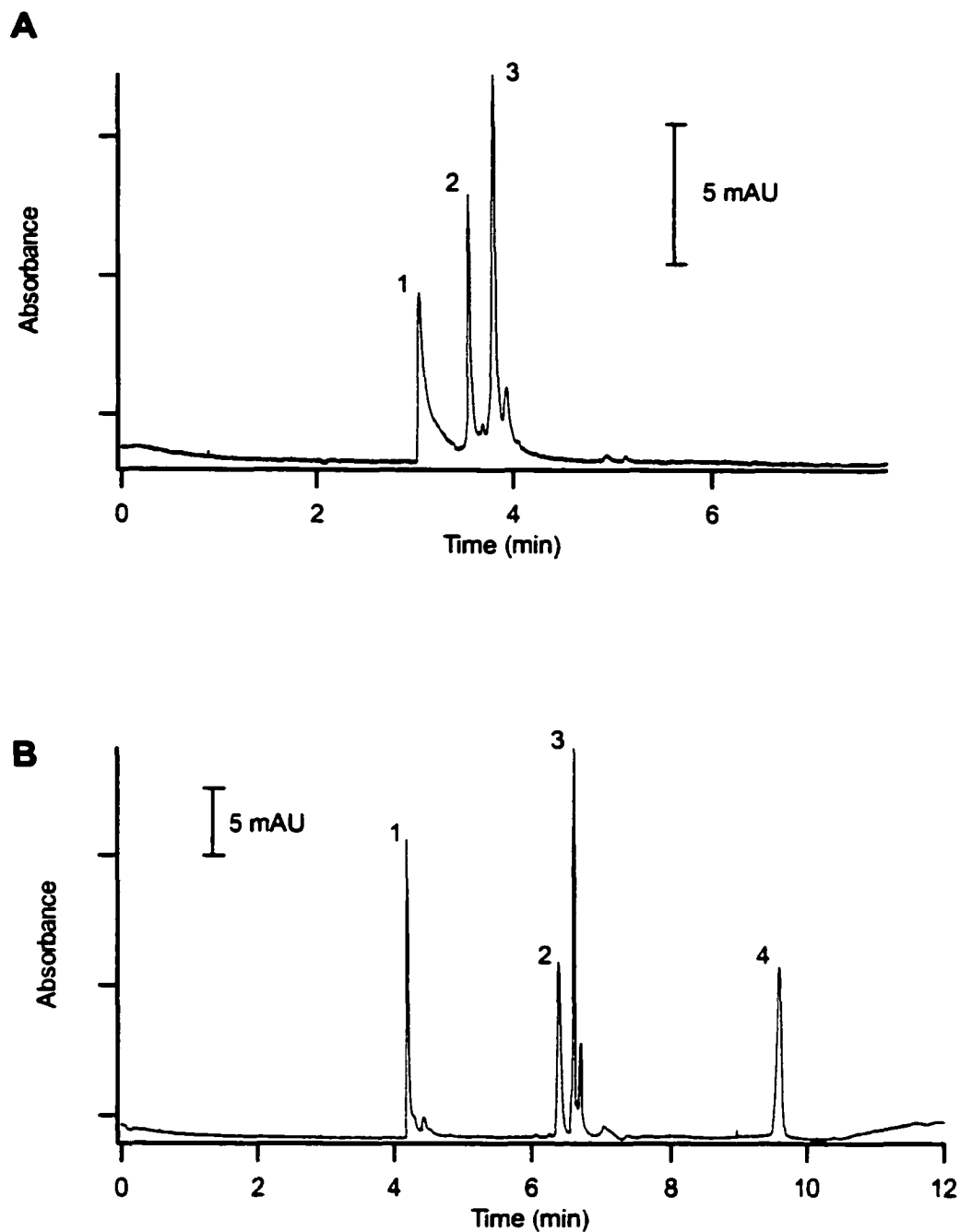
Figure 2-8. Separation of proteins at (A) pH 4 and (B) pH 8. Peaks: (1) lysozyme; (2) ribonuclease A; (3) α-chymotrypsinogen A; (4) myoglobin. Experimental conditions as in Figure 2-7, except: applied voltage, 8 kV; capillary length, 27 cm (20 cm to detector), 50 μm ID.

2.5 References

(1)   Towns, J. K.; Regnier, F. E. *Anal. Chem.* **1992,** *64*, 2473.

(2)   Bushey, M. M.; Jorgenson, J. W. *J. Chromatogr.* **1989,** *480*, 301.

(3)   Rodriguez, I.; Li, S. F. Y. *Anal. Chim. Acta* **1999,** *383*, 1.

(4)   Hjerten, S. *J. Chromatogr.* **1985,** *347*, 191.

(5)   Tsuji, K.; Little, R. J. *J. Chromatogr.* **1992,** *594*, 317.

(6)   Schmalzing, D.; Pigee, C. A.; Foret, F.; Carrilho, E.; Karger, B. L. *J. Chromatogr.*
         1993, *652*, 149.

(7)   Chiari, M.; Dell'Orto, N.; Gelain, A. *Anal. Chem.* **1996,** *68*, 2731.

(8)   Huang, M.; Bigelow, M.; Byers, M. *Am. Lab.* **1996,** *28*, 32.

(9)   Srinivasan, K.; Pohl, C.; Avdalovic, N. *Anal. Chem.* **1997,** *69*, 2798.

(10)   Giles, M.; Kleemiss, G.; Shomburg, G. *Anal. Chem.* **1994,** *66*, 2038.

(11)   Yeung, K. K.-C.; Lucy, C. A. *Anal. Chem.* **1997,** *69*, 3435.

(12)   Mazzeo, J.R.; Krull, I.S. In *Handbook of Capillary Electrophoresis*, Landers, J.
         P. ed. ; CRC Press: Boca Raton, FL, 1994; p.495.

(13)   Hult, E. L.; Emmer, A.; Roeraade, J. *J. Chromatogr. A* **1997,** *757*, 255.

(14)   Williams, B. A.; Vigh, G. *Anal. Chem.* **1996,** *68*, 1174.

(15)   Towns, J. K.; Regnier, F. E. *Anal. Chem.* **1991,** *63*, 1126.

(16)   Yeung, K. K.-C.; Lucy, C. A. *Electrophoresis* **1999,** *20*, 2554.

(17)   Yeung, K. K.-C.; Lucy, C. A. *Anal. Chem.* **1998,** *70*, 3286.

(18)   Cook, H. A.; Hu, W.; Fritz, J. S.; Haddad, P. R. *Anal. Chem.* **2001,** *73*, 3022.

(19)   Hu, W.; Haddad, P. R.; Hasebe, K.; Tanaka, K. *Anal. Commun.* **1999,** *36*, 97.

(20)   Schure, M. R.; Lenhoff, A. M. *Anal. Chem.* **1993,** *65*, 3024.

CHAPTER THREE. pH Independent Large-Volume Sample Stacking of Positive or Negative Analytes in Capillary Electrophoresis[*]

The primary object of the work in Chapter Two was to prevent protein adsorption while recovering the EOF. However, a by-product of these studies was the ability to control the magnitude of suppressed EOF independently of the pH. In this chapter, I demonstrate the usefulness of this ability by performing pH-independent large volume sample stacking of positive or negative analytes. This is an on-line sample concentration technique that had previously been restricted to very low pH. Using my technique, I was able to improve detection limits up to 85 fold, while retaining the ability to use buffer pH to optimize the separation.

3.1 Introduction

Capillary electrophoresis (CE) is an excellent analytical technique for the separation of charged species. Among the advantages of CE are its simple instrumentation, rapid separations, and high-resolution capabilities. UV detection is the most commonly employed detection method in CE. Unfortunately, detection sensitivity is limited because of the small injection volumes and the short optical path length associated with on-column UV detection. To overcome this problem, more sensitive detection methods have been employed such as electrochemical detection [1] and laser-induced fluorescence (LIF) detection [2]. However, electrochemical detection requires a lengthy, difficult alignment procedure of the electrodes with the capillary, while LIF

---

[*] A version of this chapter has been published. Baryla, N.E.; Lucy, C.A. *Electrophoresis* **2001**, *22*, 52-58.

detection often requires derivatization of the sample with a fluorescent or fluorogenic probe.

In the early nineties sample stacking was introduced as a simple, on-line concentration technique in CE [3,4]. An extensive review of this technique has recently been published [5] and the concept explained in detail in Section 1.1.6.1. In sample stacking, the capillary is initially filled with a higher conductivity buffer. A plug of low conductivity sample solution is then introduced into the capillary hydrodynamically. When high voltage is applied across the capillary, the sample ions experience a higher field strength than the buffer ions due to the difference in conductivity between the zones. This causes the sample ions to migrate quickly to the sample-buffer interface. Here the ions experience a lower field strength and slow down, causing a narrow zone of analytes to be formed at this boundary.

The volume of sample that can be injected into a capillary column is limited in conventional stacking because of the zone broadening effect caused by the mismatch of local electroosmotic velocities [6]. The EOF in the sample plug will be greater than the EOF in the rest of the capillary. This causes a pressure difference between the zones and generates a laminar flow inside the capillary. The laminar flow broadens the sharp zone generated by the stacking process and leads to reduced resolution. In order to inject large volumes of sample, and to avoid this problem, the low conductivity sample matrix must be removed immediately after the stacking process has occurred.

Several methods to remove the sample matrix for large-volume sample stacking (LVSS) have been proposed. One technique that was used by many groups involves hydrodynamically injecting a large volume of sample and then reversing the polarity to

remove the matrix plug [7-12]. However, the polarity switch used in this technique is not possible in most commercial CE instruments. The polarity switching method was later simplified by Burgi [13] when he performed LVSS of inorganic anions. Addition of electroosmotic flow (EOF) modifiers such as diethylenetriamine [13] or tetradecylammonium bromide [14] to the buffer suppressed the EOF. By suppressing the EOF, the sample matrix will be pumped out the injector end of the capillary [13]. After the matrix plug is removed, the stacked ions separate while migrating toward the detector end of the capillary without ever having switched the polarity. However, to employ LVSS without polarity switching, the electrophoretic mobility of the sample ions must be opposite and greater than the EOF.

Palmarsdottir *et al.* [15, 16] described a double stacking procedure for cationic analytes that increases sensitivity 400-fold. This method involves simultaneously applying high voltage and a back pressure in order to balance the EOF and prevent the analyte from moving too fast towards the capillary outlet. However, as with polarity reversal, most commercial CE instruments are not able to apply a back pressure and high voltage simultaneously. As well, the entire double stacking procedure takes 15 minutes before the separation step begins.

Recently, Quirino and Terabe [17] and He and Lee [18] used LVSS without polarity switching by using a low pH buffer to suppress the EOF. They achieved 100- and 300-fold sensitivity enhancement for small anions, respectively. Quirino and Terabe [19] extended this idea to LVSS of cations, particularly drugs and organic amines, by suppressing the EOF with low pH buffer and reversing the EOF by adding cetyltrimethylammonium bromide. Over 100-fold improvements in detection sensitivity

were obtained. While these methods are simple and convenient, the restriction to low pH can hamper a separation since optimal selectivity may not be achieved under these constrained buffer conditions.

Using the zwitterionic surfactant Rewoteric AM CAS U as a wall coating is an effective means of suppressing the EOF. This suppressed EOF can be adjusted to be in either the normal or reversed directions as was demonstrated in Chapter Two. In this chapter I demonstrate that large-volume sample stacking can be performed at any buffer pH if the zwitterionic surfactant CAS U is used to suppress the EOF. Further, it is possible to stack either positively or negatively charged analytes in this manner. Sensitivity enhancements of up to 85-fold are achieved for cationic antihistaminic drugs and anionic catecholamines.

3.2 Experimental

3.2.1 Apparatus

A P/ACE 2100 System (Beckman Instruments, Fullerton, CA) with a UV absorbance detector was used for all experiments. Untreated silica capillaries (PolymicroTechnologies, Phoenix, AZ) with an inner diameter of 50 μm, outer diameter of 365 μm, and total length of 47 cm (40 cm to detector) were used. Data acquisition (5 Hz) and control was performed using P/ACE Station Software (Beckman) for Windows 95 on a Pentium 120 MHz microcomputer.

New capillaries (50 μm; 47 cm total length) were pretreated by rinsing at high pressure (20 psi) with 0.1 M NaOH for 10 min. Prior to each run, the capillary was

rinsed at high pressure (20 psi) with 0.1 M NaOH for 2 min, H_2O for 2 min, and buffer for 3 min.

3.2.2 Chemicals

All solutions were prepared in Nanopure ultra-pure water (Barnstead, Chicago, IL). Buffers were prepared from reagent grade orthophosphoric acid (BDH, Darmstadt, Germany) or boric acid (BDH) and adjusted to the desired pH with sodium hydroxide (BDH). L-ascorbic acid and ethylenediaminetetraacetic acid disodium salt (EDTA) were obtained from BDH. The zwitterionic surfactant coco (amidopropyl) ammoniumdimethylsulfobetaine $(RCONH(CH_2)_2N^+(CH_3)_2CH_2CH(OH)CH_2SO_3^-$, R = $C_8H_{17}-C_{18}H_{37}$; Figure 2-1) (Rewoteric AM CAS U; Goldschmidt Chemical, Oakville, ON) was used as received. All buffers containing CAS U were prepared fresh each day and stored in Nalgene bottles. The antihistaminic drugs diphenhydramine hydrochloride, doxylamine succinate, chlorpheniramine maleate, brompheniramine maleate, and pheniramine maleate were purchased from Sigma. Catecholamines DL-3,4-dihydroxyphenylalanine (DOPA) and 3,4-dihydroxyphenylacetic acid (DOPAC) were purchased from Sigma. Analytes were prepared in a 1:10 dilution of buffer.

3.2.3 EOF measurements

The electroosmotic flow generated by the prepared buffers was measured using the three-injection method introduced by Williams and Vigh [20], described in Section 2.2.3. The first mesityl oxide marker was injected using low pressure (0.5 psi) for 1.0 s. This band was pushed through the capillary for 2 min using low pressure. The second mesityl oxide marker was then introduced by an identical low pressure injection and the two bands were pushed with low pressure for 2 min. A constant voltage of 15 kV was

applied for 3 min causing the two markers to move within the capillary. A third marker

was then injected and all the bands were eluted by applying low pressure for 12 min.

Detection was at 254 nm.

3.2.4 Separation of cationic anti-histaminic drugs

The electrophoretic buffers were 100 mM and 25 mM phosphate adjusted to pH

2.15 and 4.0, respectively, with sodium hydroxide. The buffers contained 2 mM CAS U.

The conventional injection and subsequent separation conditions were as follows. A

sample of 1 mM each of diphenhydramine hydrochloride, doxylamine succinate,

chlorpheniramine maleate, brompheniramine maleate, and pheniramine maleate was

prepared in 1:10 dilution of buffer and injected using low pressure (0.5 psi) for 1.0 s. The

applied voltage was 20 kV, detector rise time was 1.0 s, and detection was at 214 nm.

The LVSS of the drugs was performed by using a 1.0-min, low-pressure injection of a

1:100 dilution of the initial drug sample. A voltage of 10 kV was applied for 3 min with

a ramp time of 1 min. The voltage was then increased to 20 kV with a ramp time of 2

min. This procedure is used to prevent instability and subsequent loss of current as

discussed in section 3.3.3. The detector rise time was 1.0 s and detection was at 214 nm.

Migration time and peak area reproducibility were determined by performing 12

replicate injections of the 5 μM drug sample using the above conditions.

3.2.5 Separation of anionic catecholamines

The buffer used was 50 mM borate, 0.5mM EDTA, 1.0 mM ascorbic acid, and

2mM CAS U adjusted to pH 10.0 with sodium hydroxide. The conventional injection and

subsequent separation conditions were as follows. A sample of 1 mM each of DL-3,4-

dihydroxyphenylalanine (DOPA) and 3,4-dihydroxyphenylacetic acid (DOPAC) was

prepared in 1:10 dilution of buffer and injected using low pressure (0.5 psi) for 1.0 s. The

applied voltage was -15 kV, detector rise time was 1.0 s, and detection was at 214 nm.

The LVSS of a 1:100 dilution of the original catecholamine sample was performed by

using a 1.5-min, low-pressure injection. A voltage of -10 kV was applied for 3 min with

a ramp time of 1 min. The voltage was then increased to -15 kV with a ramp time of 2

min. The detector rise time was 1.0 s and detection was at 214 nm.

Migration time and peak area reproducibility were determined by performing 12

replicate injections of the 10 μM catecholamine sample using the above conditions.

3.2.6   Quantification

To determine the limits of detection for all analytes, the method specified by the

U.S. Environmental Protection Agency (U.S. EPA) was followed [21]. This method gives

the minimum concentration of a substance that can be reported with 99% confidence to

be greater than the blank (noise). One in ten dilutions of the 1 mM samples were

prepared and run using the CE procedures described in Sections 3.2.4 and 3.2.5 until the

detection limit was estimated. A calibration curve was constructed. A sample whose

concentration was 1-5 times that of the detection limit was prepared and run 7 times. The

concentration of the replicate samples was determined from the calibration curve and the

standard deviation (s) was computed for the 7 measurements. The detection limit equals

the standard deviation multiplied by the value of t corresponding to n-1 degrees of

freedom and 98% confidence (t = 3.143 at 98% confidence with 6 degrees of freedom).

3.3 Results and Discussion

3.3.1 EOF control using a zwitterionic surfactant

The zwitterionic surfactant, CAS U, is postulated to adsorb onto the capillary wall to form a micelle layer [22] as shown in Figure 1-4B in analogy to cationic surfactants adsorbing to a fused-silica surface [23]. This will be confirmed in Section 4.5.2. This coating shields the silanol groups from the bulk solution and thus suppresses the EOF. Phosphate buffers (with no salt added) containing CAS U produce a low, reversed EOF as seen in Figure 2-3B. The EOF can be tuned from -5×10^{-5} cm^2/Vs to 25×10^{-5} cm^2/Vs in 2×10^{-5} cm^2/Vs increments simply by adding various concentrations of salts containing different anions. In analogy to electrostatic ion chromatography [24], anions may be retained by the zwitterionic micelle layer present on the capillary wall. As described in Chapter Two, the retention order is dependent on the chaotropic character of the anions, with more chaotropic anions (e.g., ClO_4^-) being most strongly retained. Less chaotropic anions such as the phosphate (25 mM) and borate (50 mM) used herein are more weakly retained. Thus, variation of the concentration of these buffer anions allowed alteration of the magnitude and direction of the EOF.

3.3.2 LVSS of cationic analytes

Large-volume sample stacking (LVSS) requires an EOF that is slower than the electrophoretic mobility of the analytes and opposite in direction. Thus, for cationic analytes, a suppressed and reversed EOF is necessary. The mechanism of LVSS of positive analytes is shown in Figure 3-1. In Step I, the capillary is coated with CAS U prepared in a high conductivity buffer prior to sample injection. The sample is then introduced hydrodynamically (1 min injection) and the high voltage is applied. Step II
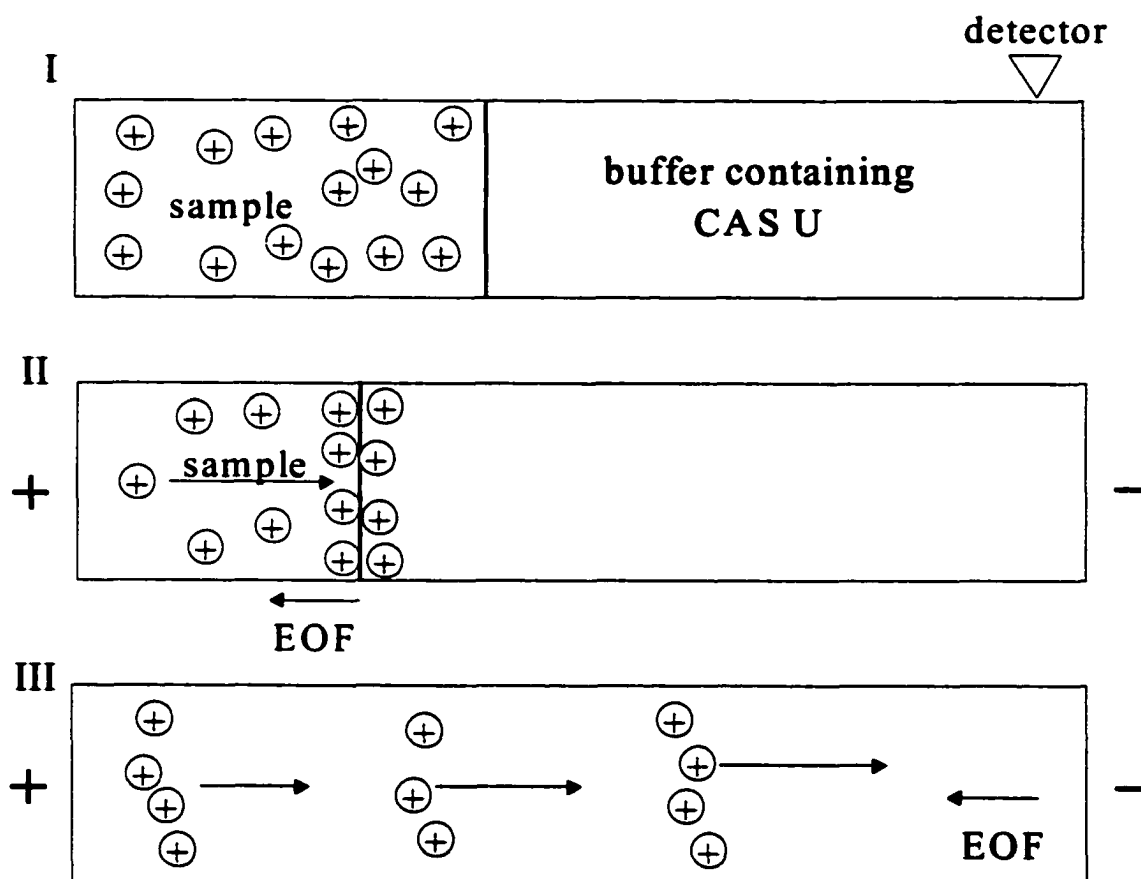
Figure 3-1. Mechanism for LVSS of cationic analytes. (I) sample is introduced hydrodynamically for 1 min. (II) sample accelerates to the buffer-sample matrix interface while the EOF pushes out the sample matrix plug. (III) sample is separated on the basis of difference of electrophoretic mobilities. See section 3.3.2 for further explanation.

shows how the cations stack at the boundary between the sample plug and buffer. The cations rush to this boundary due to the difference in conductivity between the sample matrix and the buffer in the capillary. While stacking is occurring, the slow reversed EOF slowly pumps the water plug out the inlet end of the capillary. After the sample matrix plug is removed (Step III), the electric field becomes constant along the capillary and the stacked analytes separate based on their electrophoretic mobilities and are detected.

3.3.2.1 LVSS of cationic anti-histaminic drugs

The above method can be applied to the separation of samples of cationic anti-histaminic drugs. This separation illustrates the necessity of being able to adjust the pH to obtain optimum separation selectivity. Figure 3-2 shows the separation from a conventional 1-s injection of the 5 drugs in 100-mM phosphate and 2 mM CAS U, adjusted to pH 2.15. The EOF generated by this buffer was calculated to be -2.42×10^{-5} cm^2/Vs. At pH 2.15, chlorpheniramine ($pKa_1 = 4.0$) is not baseline separated from brompheniramine ($pKa_1 = 4.05$). As well, the doxylamine ($pKa_1 = 4.4$) and pheniramine ($pKa_1 = 4.2$) peaks are closely spaced. In contrast, if the separation is done at pH 4.0, the resolution of the peaks is substantially improved, as shown in Figure 3-3A. Under these buffer conditions, chlorpheniramine and brompheniramine are nearly baseline separated. Doxylamine and pheniramine are also spaced farther apart.

Addition of 2 mM of CAS U to the 25-mM (pH 4.0) phosphate buffer yields a weak reversed EOF (-0.531×10^{-4} cm^2/Vs) which is suitable for LVSS of these anti-histaminic drugs. Adjusting the concentration of phosphate in the buffer optimized the low reversed EOF. A 1-min injection of the drugs is shown in Figure 3-3B. This sample
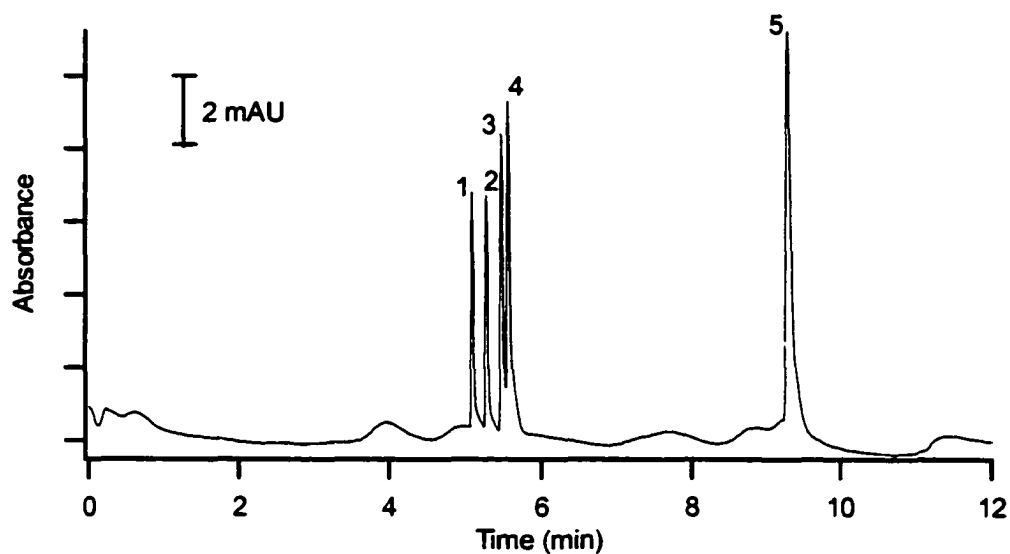
Figure 3-2. Separation of drugs at pH 2.15. Peaks: (1) pheniramine; (2) doxylamine; (3) chlorpheniramine; (4) brompheniramine; (5) diphenhydramine. Experimental conditions: applied voltage, 20 kV; 1-s hydrodynamic injection; temperature, 25°C; capillary length, 47 cm (40 cm to detector), 50 μm ID; buffer, 100 mM phosphate and 2 mM CAS U, pH 2.15; sample, 1 mM of each drug.

A)

B)
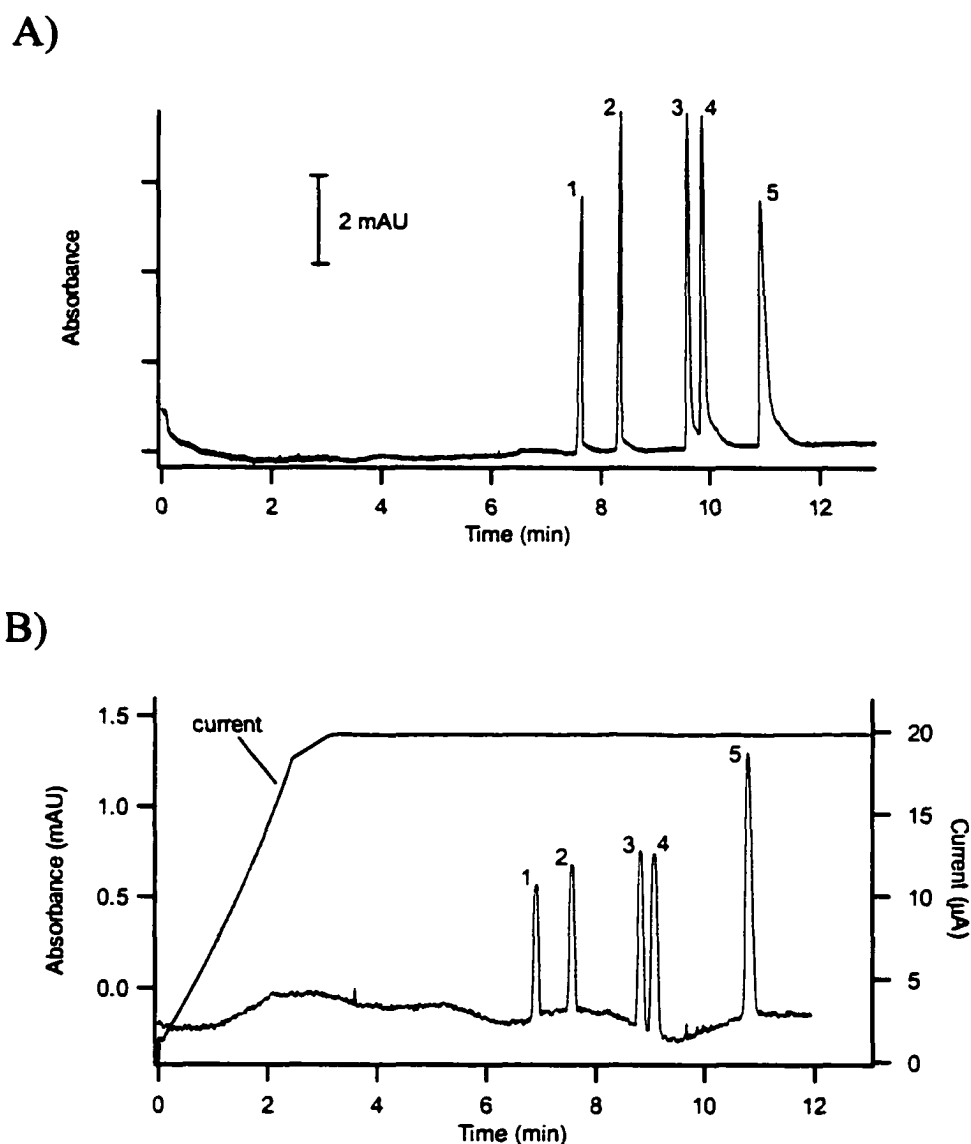
Figure 3-3. A) Separation of drugs at pH 4.0 with conventional injection. Peaks: (1) doxylamine; (2) pheniramine; (3) chlorpheniramine; (4) brompheniramine; (5) diphenhydramine. Experimental conditions: applied voltage, 20 kV; 1s hydrodynamic injection; temperature, 25°C; capillary length, 47 cm (40 cm to detector), 50 μm ID; buffer, 25 mM phosphate and 2 mM CAS U, pH 4.0; sample, 1 mM of each drug. B) Separation of drugs at pH 4.0 with LVSS. The current trace is overlaid. Peak identities as in 3-3A. Experimental conditions: applied voltage, 10 kV for 3 min, increased to 20 kV; 1 min hydrodynamic injection; temperature, 25 °C; capillary length, 47 cm (40 cm to detector), 50 μm ID; buffer, as in 3A; sample, 200-fold dilution of 3-3A.

is a 200-fold dilution of the sample solution in Figure 3-3A. There is slight broadening of the peaks due to some separation occurring before the sample matrix plug is removed (efficiency up to 140 000 plates in 3-3A versus efficiency up to 52 000 plates in 3-3B). However, given the excellent separation afforded by optimizing the pH, this broadening did not hamper the separation. Injections longer than 1-1.5 min could have been used to increase sensitivity. However, injections longer than 1.5 min compromised the separation and so were not used. The % RSD of migration time was less than 0.8 % for all the drugs while % RSD of corrected peak area was less than 1.3 % over 12 replicate runs. Peak height reproducibility ranged from 0.8-2.0 %. This data is summarized in Table 3-1.

Finally, LVSS was not demonstrated at pH below 4.0. The zwitterionic surfactant CAS U has been demonstrated to suppress the EOF at pH as low as 2.0 [22]. Thus, it is believed that CAS U could be used for LVSS under such acidic conditions. However since the procedures of Quirino and Terabe [17, 19] and He and Lee [18] are effective at this pH range, the use of CAS U at low pH was not investigated.

3.3.2.2 Overcoming loss of current

A 1-s injection filled 0.63 mm of the capillary while a 1-min injection filled 3.8 cm. When a substantial portion of the capillary is filled with sample and high voltage is applied, instability and eventual loss of the current is observed since the sample matrix is primarily water (1:10 dilution of buffer). The loss of current is shown in Figure 3-4. This problem was circumvented by increasing the ramp time of the voltage from the conventional 0.17-min to 1-2 min [25]. A lower voltage with a slow ramp time was first applied for a few minutes, and then slowly ramped to the final high voltage. This allowed

Table 3-1. Reproducibility of migration time, corrected peak area and peak height for anti-histaminic drugs and catecholamines.

compound	% RSD migration time	% RSD corrected peak area	% RSD peak height
ANTIHISTAMINES			
doxylamine	0.6	1.1	1.6
pheniramine	0.8	1.3	1.7
chlorpheniramine	0.6	1.1	2.0
brompheniramine	0.4	0.7	2.0
diphenhydramine	0.7	0.6	0.8
CATECHOLAMINES			
DOPA	1.3	3.7	4.8
DOPCA	1.6	1.4	4.9
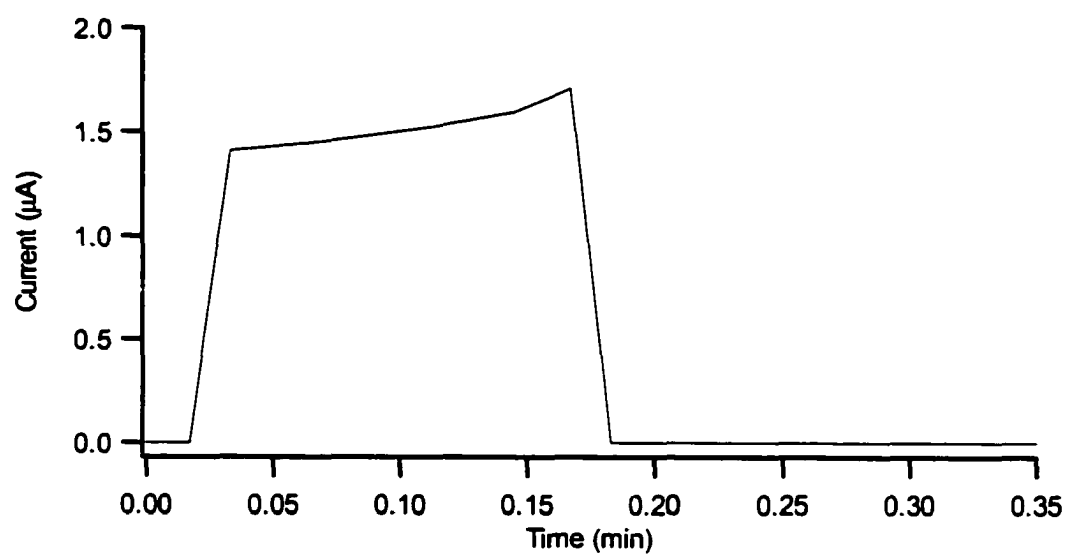
Figure 3-4. Current trace observed with a 0.17-min voltage ramp time and a long (>1 min) sample injection.

for a good portion of the matrix plug to be pumped out before the final high voltage was reached. The current, as shown in Figure 3-3B, was a useful indicator of when the matrix plug was removed. Initially the current would gradually rise as the voltage ramped to its maximum value. After this, the current gradually rose to an asymptotic value. The time at which the current became constant indicated when the sample plug had been entirely pumped out the inlet end by the EOF. In Figure 3-3B, the current indicates that the plug was entirely removed at 3.2 min.

3.3.3 LVSS of anionic catecholamines

The mechanism for LVSS of negative analytes is identical to that for positive analytes, except that the EOF and sample are moving in opposite directions to those described in Section 3.3.2 and Figure 3-1. The EOF must be suppressed and in the forward direction. The separation takes place by applying negative potential, and detection of the analytes occurs at the anodic end of the capillary.

As with the anti-histaminic drugs, catecholamines are not well separated under the acidic conditions (pH 2.15) required by the Quirino-Terabe procedures [17, 19] for LVSS. Even at a pH of 5.4, the catecholamines can not all be separated [26, 27]. Indeed, under neutral pH conditions, sodium dodecyl sulfate (SDS) is required to achieve the separation [26]. Only above pH 9, where the catecholamines are negatively charged, can they be adequately resolved [26]. In this work, two catecholamine-related compounds, DOPA and DOPAC, are used to illustrate LVSS of anions.

Since LVSS requires the analyte ions to have a mobility that is greater than and in the opposite direction of the EOF, the more highly charged the ions are, the better and faster the separation will be. At a pH of 10.0, DOPA and DOPAC are negatively

charged. Working with a borate buffer can increase this negative charge by the complexation of the tetrahydroxyborate ion with the ortho-dihydroxy groups of DOPA and DOPAC [28]. A 50 mM borate buffer containing 2 mM of CAS U adjusted to pH 10.0 was used as the separation buffer. At this high pH, DOPA and DOPAC are easily oxidized. To prevent oxidation, ascorbic acid and EDTA were added to the buffer and sample solutions. The EOF generated by the buffer was +0.328 x 10^{-4} cm^2/Vs.

Electropherograms obtained from a 1-s injection (0.63 mm of the capillary filled) and a 1.5-min injection (5.67 cm of the capillary filled) of the sample are shown in Figure 3-5A and 3-5B respectively. The sample in Figure 3-5B is a 100-fold dilution of Figure 3-5A. There is some broadening of the peaks (efficiency was reduced to 20 000 plates in 3-5B from 120 000 plates in 3-5A), but again the separation was not affected. The % RSD of migration time was less than 1.6 % for the catecholamines while % RSD of corrected peak area was less than 3.7 % over 12 replicate runs. Peak height reproducibility ranged from 4.8-4.9 %. This data is summarized in Table 3-1.

The borate buffer used at pH 10.0 enhanced the negative charge on the catecholamines and improved the separation. LVSS of these compounds was not tried at a higher pH since borate is not a suitable buffer above pH 10.2. LVSS should, however, be possible above this pH since CAS U is known to suppress the EOF up to a pH of 13.0 [22].

3.3.4 Quantification

For all compounds, the response was linear over two orders of magnitude-from 1 μM to 100 μM for large-volume injections and from 10 μM to 1 mM for conventional injections. The sensitivity enhancement achieved for the anti-histaminic drugs was up to
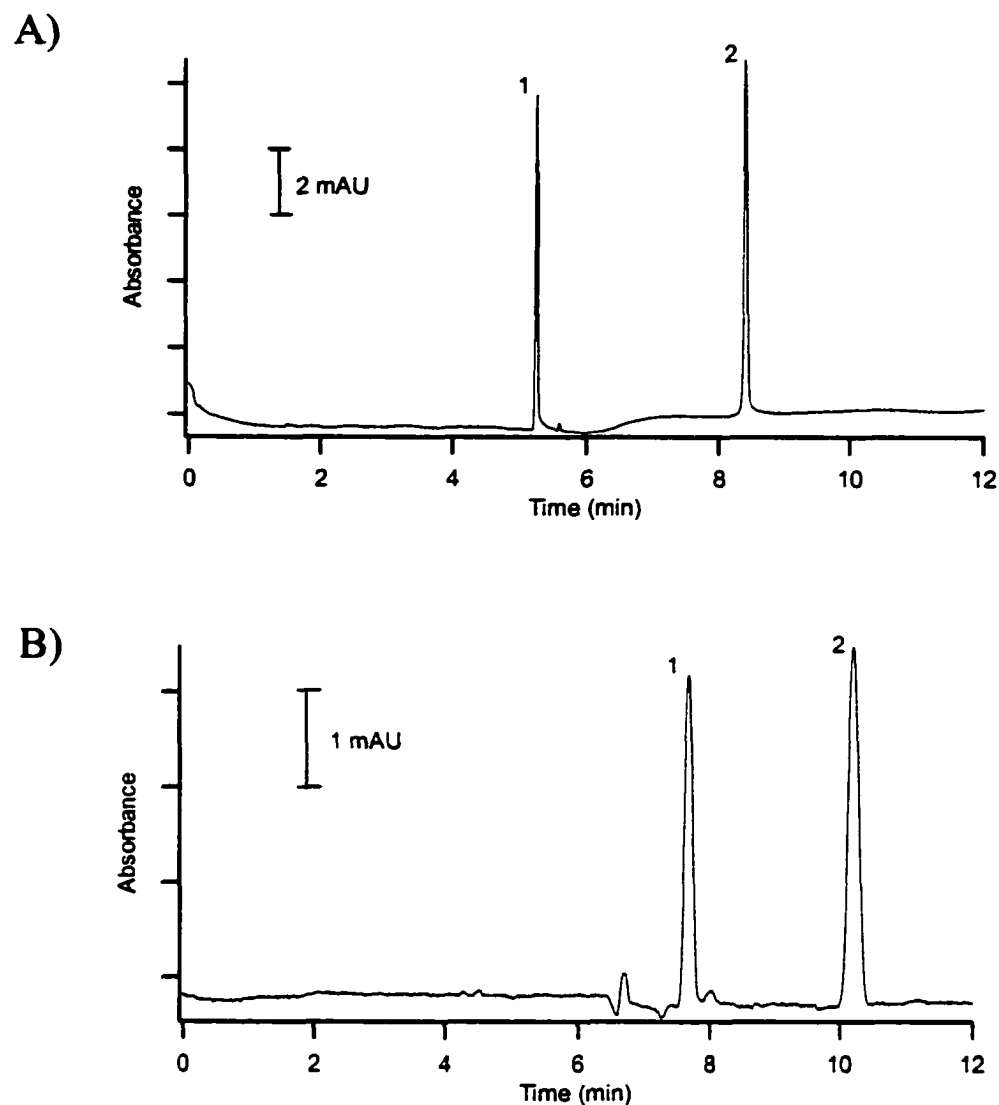
Figure 3-5. (A) Separation of catecholamines at pH 10.0 with conventional injection. Peaks: (1) DOPAC; (2) DOPA. Experimental conditions: applied voltage, -15 kV; 1-s hydrodynamic injection; temperature, 25°C; capillary length, 47 cm (40 cm to detector), 50 μm ID; buffer, 50 mM borate and 2 mM CAS U containing 1 mM ascorbic acid and 0.5 mM EDTA, pH 10.0; sample, 1 mM of each compound.

(B) Separation of catecholamines at pH 10.0 with LVSS. Peak identities as in 3-5A. Experimental conditions: applied voltage, -10 kV for 3 min, increased to -15 kV; 1.5 min hydrodynamic injection; temperature, 25 °C; capillary length, 47 cm (40 cm to detector), 50 μm ID; buffer, as in 3-5A; sample, 100-fold dilution of 3-5A.

85-fold and that for the catecholamines was up to 50-fold. Table 3-2 lists the detection limits for both the anti-histaminic drugs and the catecholamine-related compounds. For comparison, detection limits achieved using other CE methods are also listed.

Ong *et al.* [29] separated nine anithistamines CE using on-column UV detection. Included in the sample of antihistamines were pheniramine, doxylamine and chlorpheniramine. They achieved detection limits of 3-7 x10^{-5} M for 1-s injections of sample.

Britz-McKibbin and Chen [30] achieved 250-fold enhancement for the catecholamine epinephrine using a dynamic pH junction. In this technique a sample is stacked at the junction between sample and buffer solutions of differing pH. In order to be stacked in this manner, the analytes must possess a functional group that exists in two distinct states, each with a different mobility in the capillary. Such was the case of epinephrine, for which the detection limit was lowered to 4 x 10^{-8} M from 1 x 10^{-5} M. However, DOPA does not possess an appropriate functionality and so was not focused significantly by the dynamic pH junction.

Alternatively, Zhu and Kok [26] achieved detection limits for catecholamines on the order of 10^{-7} M using a post-column terbium complexation of catecholamines and luminescence detection. Chang and Yeung [27] detected catecholamines using laser-induced native fluorescence detection. They worked at a pH of 5.4 and could not baseline separate all compounds using CE. Their detection limits were also roughly 10^{-7} M.

Table 3-2. Detection limit values for conventional injection and large-volume injection* and comparison to literature detection limits.

compound	conventional injection	large volume injection	literature detection limits
ANTIHISTAMINES			30-70 μM [29]
doxylamine	6 μM	0.1 μM	
pheniramine	8 μM	0.13 μM	
chlorpheniramine	4 μM	0.1 μM	
brompheniramine	6 μM	0.07 μM	
diphenhydramine	5 μM	0.07 μM	
CATECHOLAMINES			0.04-10 μM [30], 0.1 μM [26][27]
DOPA	3.9 μM	0.075 μM	
DOPCA	3 μM	0.058 μM	

* see section 3.2.6 for details of detection limit calculation.

3.4 Conclusions

Large-volume sample stacking (LVSS) without polarity switching is demonstrated over a wide pH range (4.0-10.0) using the zwitterionic surfactant Rewoteric AM CAS U to suppress the EOF. This method provides a simple and effective stacking approach to improve detection sensitivity of cationic and anionic compounds. The separations are not restricted to low pH, which allows pH to be used as a tool to obtain optimal selectivity. Up to 85-fold enrichment in sensitivity was obtained for cationic anti-histaminic drugs and anionic catecholamine-related compounds using LVSS. Thus, this technique is capable of achieving detection limits comparable to other approaches with the advantage of being compatible with commercial instruments.

3.5 References

(1)   Wallingford, R. A.; Ewing, A. G. *Anal. Chem.* **1987**, *59*, 1762.

(2)   Gozel, P.; Gassmann, E.; Michelson, H.; Zare, R. N. *Anal. Chem.* **1987**, *59*, 44.

(3)   Burgi, D. S.; Chien, R.-L. *Anal. Chem.* **1991**, *63*, 2042.

(4)   Burgi, D. S.; Chien, R.-L. *J. Microcolumn Sep.* **1991**, *3*, 199.

(5)   Shihabi, Z. K. *J. Chromatogr. A* **2000**, *902*, 107.

(6)   Chien, R.-L.; Burgi, D. S. *Anal. Chem.* **1992**, *64*, 1046.

(7)   Burgi, D. S.; Chien, R.-L. *Anal. Biochem.* **1992**, *2*, 306.

(8)   Albert, M.; Debusschere, L.; Demesmay, C.; Rocca, J. L. *J. Chromatogr. A* **1997**, *757*, 281.

(9)   Harland, G. B.; McGrath, G.; McClean, S.; Smyth, W. F. *Anal. Commun.* **1997**, *34*, 9.

(10)   McGrath, G.; Smyth, W. F. *J. Chromatogr. B* **1996**, *681*, 125.

(11)   Smyth, W. F.; Harland, G. B.; McClean, S.; McGrath, G.; Oxspring, D. *J. Chromatogr. A* **1997**, *772*, 161.

(12)   Geldart, S. E.; Brown, P. R. *Am. Lab.* **1997**, *29*, 48.

(13)   Burgi, D. S. *Anal. Chem.* **1993**, *65*, 3726.

(14)   Albert, M.; Debusschere, L.; Demesmay, C.; Rocca, J. L. *J. Chromatogr. A* **1997**, *757*, 291.

(15)   Palmarsdottir, S.; Edholm, L.-E. *J. Chromatogr. A* **1995**, *693*, 131.

(16)   Palmarsdottir, S.; Mathiasson, L.; Jonsson, J. A.; Edholm, L.-E. *J. Chromatogr. B* **1997**, *688*, 127.

(17)   Quirino, J. P.; Terabe, S. *J. Chromatogr. A* **1999**, *850*, 339.

(18)   He, Y.; Lee, H. K. *Anal. Chem.* **1999,** *71,* 995.

(19)   Quirino, J. P.; Terabe, S. *Electrophoresis* **2000,** *21,* 355.

(20)   Williams, B. A.; Vigh, G. *Anal. Chem.* **1996,** *68,* 1174.

(21)   Grant, C. L.; Hewitt, A. D.; Jenkins, T. F. *Am. Lab.* **1991,** *23,* 15.

(22)   Yeung, K. K.-C.; Lucy, C. A. *Anal. Chem.* **1997,** *69,* 3435.

(23)   Manne, S.; Gaub, H. E. *Science* **1995,** *270,* 1480.

(24)   Hu, W.; Haddad, P. R.; Hasebe, K.; Tanaka, K.; Tong, P.; Khoo, C. *Anal. Chem.* **1999,** *71,* 1617.

(25)   Chevigne, R. In *P/ACE Setter,* 1999; Vol. 3, pp 8.

(26)   Zhu, R.; Kok, W. T. *Anal. Chem.* **1997,** *69,* 4010.

(27)   Chang, H.-T.; Yeung, E. S. *Anal. Chem.* **1995,** *67,* 1079.

(28)   In *High Performance Capillary Electrophoresis: Theory, Techniques, and Applications;* Khaledi, M. G., Ed.; John Wiley and Sons, Inc.: New York, 1998.

(29)   Ong, C. P.; Ng, C. L.; Lee, H. K.; Li, S. F. Y. *J. Chromatogr.* **1991,** *588,* 335.

(30)   Britz-McKibbin, P.; Chen, D. D. Y. *Anal. Chem.* **2000,** *72,* 1242.

CHAPTER FOUR. Characterization of Surfactant Coatings in Capillary Electrophoresis by Atomic Force Microscopy[*]

4.1 Introduction

Dynamic coatings are becoming particularly attractive as wall coatings in CE due to their versatility and simplicity. With the introduction of multi-capillary instruments (up to 96) [1,2], lengthy and costly derivatization procedures are not always feasible (Section 1.2.1). Thus replaceable surfactant-based coatings provide an economically attractive alternative. In dynamic coatings, a surfactant that has an affinity for the negatively charged capillary surface is added to the background electrolyte. Surfactant molecules then adsorb to the capillary surface in a particular fashion, thus altering the charge on the surface and shielding the silanol groups from the bulk solution. Traditionally, these coatings have been employed primarily for EOF reversal for small anion analyses [3,4]. Despite their simplicity and high performance, these coatings have seen only limited use, particularly in the area of proteins and peptides. A major shortcoming associated with traditional surfactant coatings is that free surfactant molecules are present in the background electrolyte and may interfere with the separation and/or detection scheme. However, perhaps the most critical drawback of surfactant coatings is their apparent lack of robustness and irreproducibility from laboratory-to-laboratory. In particular, minor alterations to the electrophoretic buffer appear to drastically alter the coating performance. Thus an understanding of the mechanism by

which surfactants adsorb at the capillary surface is essential in explaining and then avoiding these anomalies.

This chapter describes my studies of the use of didodecyldimethylammonium (DDAB, Figure 4-1A) versus cetyltrimethylammoinum bromide (CTAB, Figure 4-1B) for coating capillaries in CE. I observe dramatic advantages in the behavior of this double-chained surfactant relative to more commonly used single-chained surfactants. These differences are due to the different aggregation properties of single and double-chained surfactants, which lead to different adsorption mechanisms onto silica surfaces such as the capillary walls. Atomic force microscopy (AFM) is used to directly visualize surfactant adsorption on fused silica to gain an understanding of the behavior of surfactant coatings in capillary electrophoresis. The coating morphology of different types of surfactants is elucidated and explained. Further, the effects of surfactant concentration, pH, and ionic strength on surfactant assembly are investigated and related to CE. Finally, coating morphology and the degree of surface coverage are correlated to the EOF and the degree of inhibition of protein adsorption in capillary electrophoresis.

4.2 Background

4.2.1 Aggregation properties of single- and double-chained surfactants in solution

Surfactants form aggregates in aqueous solution due to the low energy of interaction between the surfactant hydrocarbon chains and water (the hydrophobic effect). Thus, surfactant hydrocarbon chains will tend to interact with one another due to an entropically favorable process. However, this interaction is limited by the repulsion

A
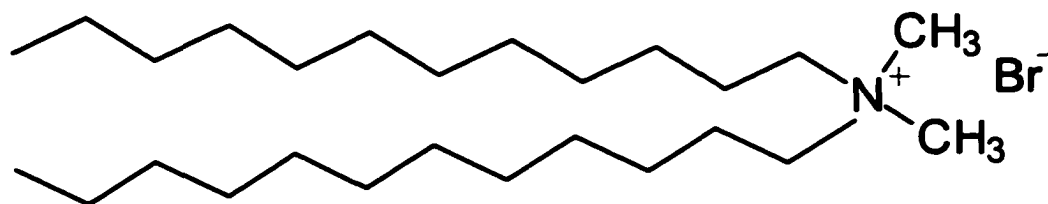
B
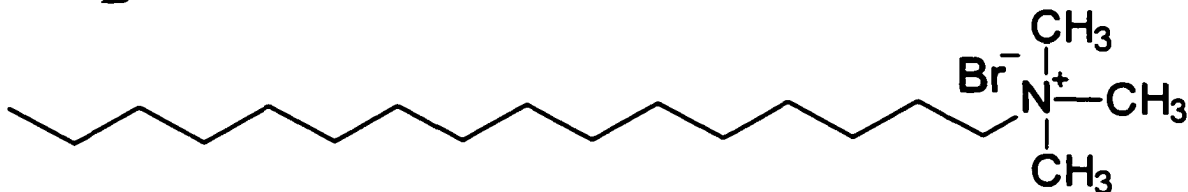
Figure 4-1. Structures of A) double-chained surfactant didodecyldimethylammonium bromide (DDAB) and B) single-chained surfactant cetyltrimethylammonium bromide (CTAB).

between the surfactant head groups. The balance of these two opposing forces will dictate the degree of aggregation as well as the morphology of the aggregates.

Single-chained surfactants such as CTAB form spherical micelles at concentrations above a critical micelle concentration (CMC), as shown in Figure 4-2. The CMC value for CTAB is known to be 0.9 mM in water [5] and 0.1 mM in phosphate buffer (50 mM ionic strength) at neutral pH [6]. The decreased CMC value associated with increasing ionic strength is due to the decreased head group repulsion (ionic screening) between adjacent surfactants in the micelle.

Contrary to single-chained surfactants, double-chained surfactants aggregate in solution to form bilayer structures or vesicles (Figure 4-2). This is attributed to the increased tail-group cross-sectional area. Vesicle formation has been studied extensively [7-9]. Israelachvili et al. [10] introduced the packing parameter

$$P = \frac{V_c}{l_c a_h}$$ (Eqn. 4-1)

where V_c and l_c are the volume and length of the hydrocarbon chain and a_h is the cross-sectional area of the head-group. When this value is such that $\frac{1}{2} < P < 1$, vesicles are favored over micelles [10]. For instance, the double-chained surfactant didocyldimethylammonium bromide (DDAB, Figure 4-1A) has a P-value of 0.620 [11], well within the vesicle region. Alternatively, CTAB (Figure 4-1B) has a packing parameter of 0.329 [11], which is indicative of micelle formation.

Double-chained surfactants form aggregates at concentrations above a critical vesicle concentration (CVC). The CVC for DDAB in water at 25°C is 0.035 mM [12]. Above this concentration, only small vesicles exist [12]. A transition occurs in the phase diagram at roughly 1 mM where large multilayer aggregates or liposomes are formed and

(A)

Micelle

(B)

Bilayer or Vesicle
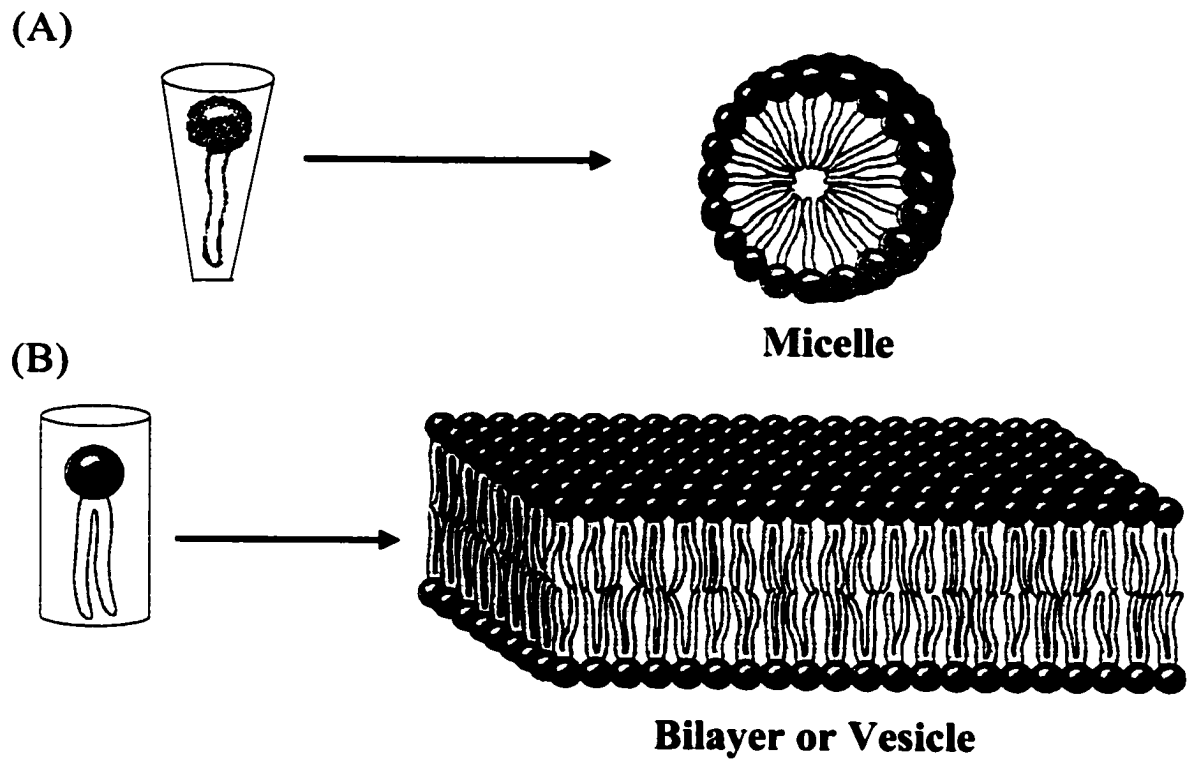
Figure 4-2. Aggregate structures of (A) single-chained surfactants and (B) double-chained surfactants.

coexist with the small vesicles [12]. Above roughly 10 mM, only liposomes are observed [12].

The single-chained analogue of DDAB, dodecyltrimethylammonium bromide (DTAB) has a CMC of 15 mM in water. This is roughly 400 times higher than the CVC of DDAB. Thus aggregation of double-chained surfactants in water appears to be much more favorable than for single-chained surfactants.

4.2.2 Adsorption of surfactants in solution onto silica surfaces

The exact mechanism by which surfactants adsorb onto silica surfaces is a topic of considerable debate. Conventionally, the adsorption of single-chained surfactants onto silica has been depicted as a bilayer. It has been assumed that a monolayer is initially formed into which tail-groups from a second layer become intertwined, resulting in a flat bilayer structure [13, 14]. However, this model is counter-intuitive since bilayer structures are strongly disfavored for single-chained surfactants (larger head-group area than tail area; Figure 4-2).

Recently, Liu and Ducker have confirmed through atomic force microscopy (AFM) imaging that single-chained surfactants form spherical aggregates at silica surfaces [5]. Images of silica surfaces in the presence of 1.8 mM CTAB in water (twice the CMC) at 25°C show spherical aggregates spaced uniformly over the surface. However, the AFM image does not reveal the structure beneath the outer layer of the surfactant, so the image could result from half-micelles on top of a flat monolayer instead of full micelles [5]. Regardless of the exact nature of the spherical aggregates, the roughly symmetrical dots of the AFM image confirmed a micellar structure at the surface as

opposed to a bilayer structure. These results are consistent with previous AFM imaging studies of quaternary ammonium surfactants adsorbed at silica surfaces [15].

Although few studies have investigated the adsorption of double-chained surfactants at surfaces, little debate surrounds their surface-aggregate morphology. Since double-chained surfactants are capable of forming bilayers in solution, one would expect them to form bilayers at surfaces. Not surprisingly, Manne and Gaub confirmed this by observing a uniform and featureless AFM image of DDAB on mica [15]. This was indicative of a flat bilayer, which was consistent with previous interpretations of the adsorption of double-chained surfactants [16]. To the best of my knowledge, adsorption studies by AFM of double-chained surfactants on silica have yet to be published.

4.3   Principles of atomic force microscopy (AFM)

4.3.1   Historical background and development of atomic force microscopy

Scanning probe microscopes (SPMs) are a family of instruments used for studying surface properties of materials from the atomic to the micron scale. The idea behind these techniques dates back to the early 1970's with the work of Young, Ward, and Scire [17]. Together, they developed the *topographiner*. This low-resolution instrument (3 nm in the vertical direction and 400 nm in the horizontal direction) contained a piezoelectric scanner and feedback system to control tip-sample distances. It was not until the early 1980's that Binning, Rohrer, and Gerber of IBM Zurich refined the topographiner and developed scanning tunneling microscopy (STM) [18, 19]. Five years later they were awarded the Nobel Prize in Physics for its invention.

The STM was the first instrument to generate real-space images of surfaces with atomic resolution. STMs use a sharp, conducting tip with a bias voltage applied between the tip and the sample. When the tip is brought close to the sample, electrons from the sample begin to "tunnel" through the gap into the tip or vice versa, depending upon the sign of the bias voltage. The resulting tunneling current varies exponentially with tip-to-sample spacing. It is this signal that is used to create a STM image. However, STM was limited by the requirement that both the sample and tip must be conductors or semi-conductors.

To circumvent this limitation, the atomic force microscope (AFM) was introduced in 1986 as a tool to image non-conductive surfaces such as polymeric materials and biological specimens [20]. In AFM, a sharp tip located at the free end of a cantilever scans the surface. Forces between the tip and the sample cause the cantilever to bend, or deflect. A detector measures the cantilever deflection as the tip is scanned over the sample, or the sample is scanned under the tip. The measured cantilever deflections allow a computer to generate a map of surface topography.

4.3.2 AFM instrumentation

A schematic diagram of an atomic force microscope is shown in Figure 4-3. The sharp tip is commonly made of silicon nitride and is 2-5 μm long and often less than 100 Å in diameter. The tip is located at the end of a reflective cantilever that is 100-200 μm long. The sample is placed on a piezoelectric scanner, which allows the sample to be scanned in a raster pattern under the tip.

An AFM image of a surface is generated by maintaining a constant force between the tip and the sample. A laser beam is reflected off the back of the cantilever and
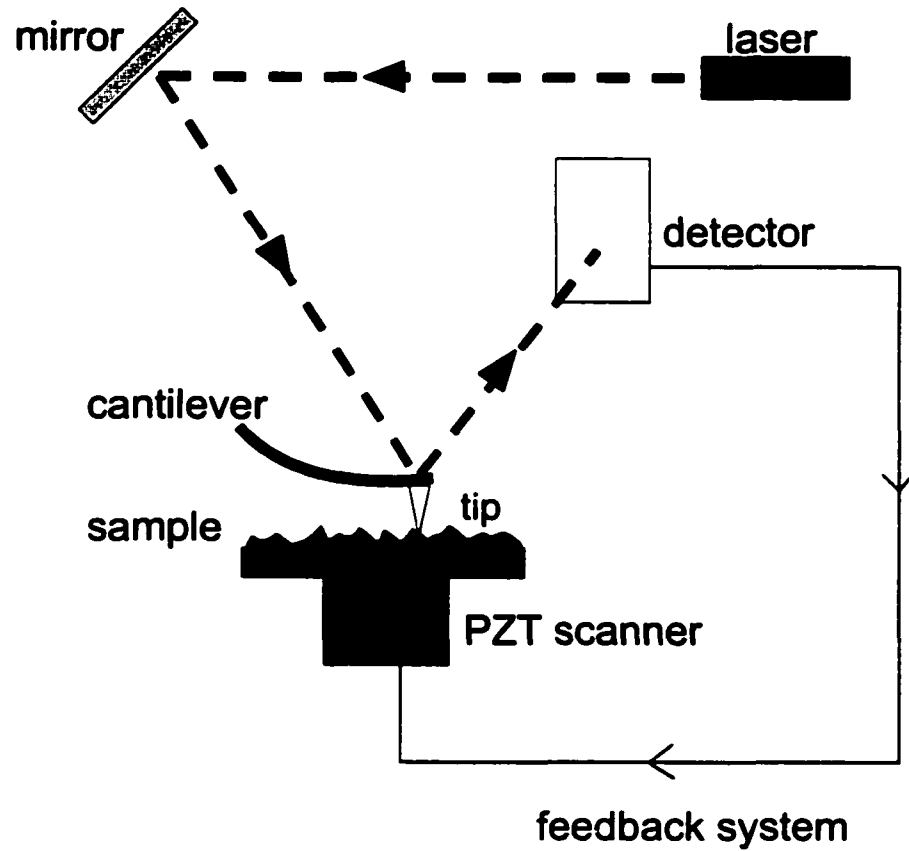
Figure 4-3. Schematic of an atomic force microscope.

directed onto a position-sensitive photodetector to monitor cantilever deflection in order to control the applied force. A computer collects the cantilever deflections and a topographical image is generated.

4.3.3 Modes of operation

Several forces typically contribute to the deflection of an AFM cantilever. The force most commonly associated with atomic force microscopy is an interatomic force called the van der Waals force. The dependence of the van der Waals force upon the distance between the tip and the sample is shown in Figure 4-4. Three main regions are labeled on Figure 4-4: 1) the contact region; 2) the non-contact region; and 3) the intermittent-contact region. In the contact region, the cantilever is held less than a few angstroms from the sample surface, and the interatomic force between the cantilever and the sample is repulsive. In the non-contact region, the cantilever is held on the order of tens to hundreds of angstroms from the sample surface, and the interatomic force between the cantilever and sample is attractive. In the intermittent-contact region, the tip is oscillated close to the sample so that at the bottom of its travel it just "taps" the sample surface. My use of AFM deals only with modes of operation within the contact (repulsive) region of the force-distance curve (Figure 4-4). Thus, only contact modes will be discussed in detail.

4.3.3.1 Contact AFM

In contact AFM mode, the AFM tip makes physical contact with the sample. The tip is attached to the end of a cantilever with a low spring constant (< 2 nN/nm). As the scanner moves the sample under the tip, the contact force causes the cantilever to bend to accommodate changes in topography. At the right side of the curve in Figure 4-4, a large
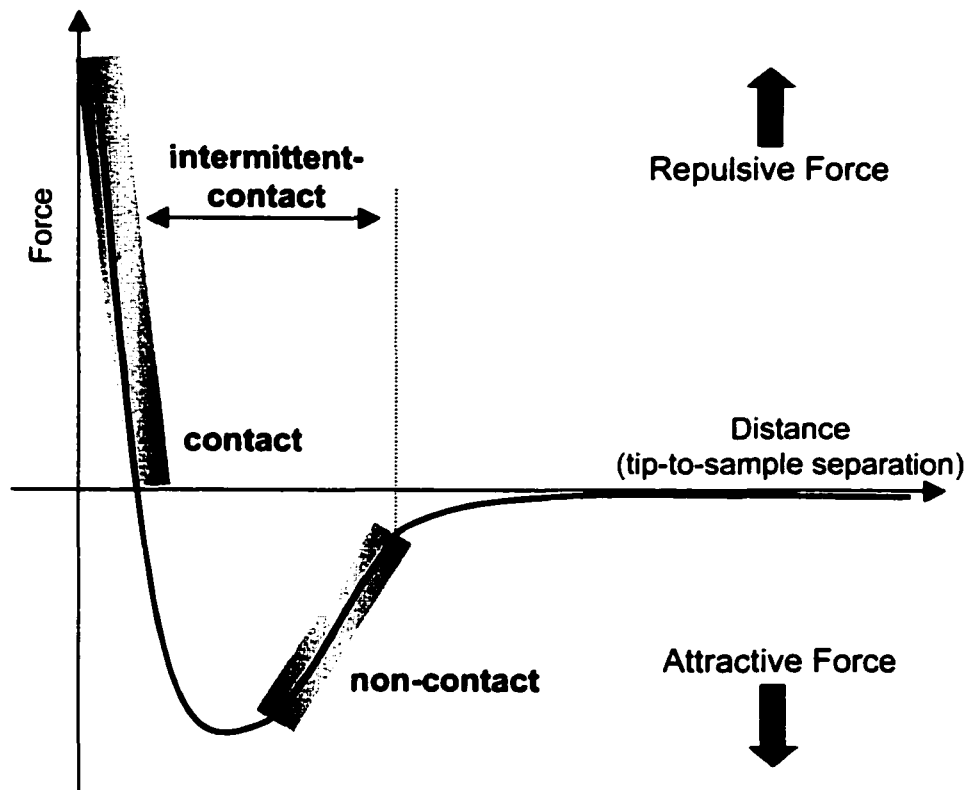
Figure 4-4. Dependence of van der Waals force upon the tip-to-sample separation.

distance separates the tip and the sample. As the tip and the sample are gradually brought together, they first weakly attract each other (attractive region). This attraction increases until the atoms of the tip and the atoms of the sample are so close together that their electron clouds begin to electrostatically repel each other (bottom of the force curve in Figure 4-4). This electrostatic repulsion progressively weakens the attractive force as the interatomic separation continues to decrease. The force goes to zero when the distance between the atoms reaches a few angstroms. When the total van der Waals force becomes positive (repulsive), the atoms (and thus the tip and sample) are considered to be in contact. Also under aqueous imaging conditions, there is a force exerted by the tip on the sample, in addition to the van der Waals force. The force exerted by the tip is like the force of a compressed spring.

In practice, force-distance curves are used to measure the normal force (F_N) that the tip applies to the surface while a contact-AFM image is being collected. Figure 4-5 shows an idealized raw force-distance curve obtained by monitoring the detector signal (volts) as the sample approaches the tip (nm) and is then subsequently retracted. Following the solid line from right to left, a flat line indicating no cantilever deflection is initially observed. As the sample approaches the tip, the attractive forces acting between the tip and sample pull the two into contact. Further movement of the sample towards the tip results in a repulsive tip-sample interaction causing the cantilever to bend. The slope of this region is the detector sensitivity (S, volts/nm) to cantilever bending in the z-direction. During the reverse scan (dashed line) where the sample is moved away from the tip, the sample must sometimes be retracted further to pull the tip off the surface. The point where the tip is pulled off the surface is called the breakaway point ($V_{breakaway}$,
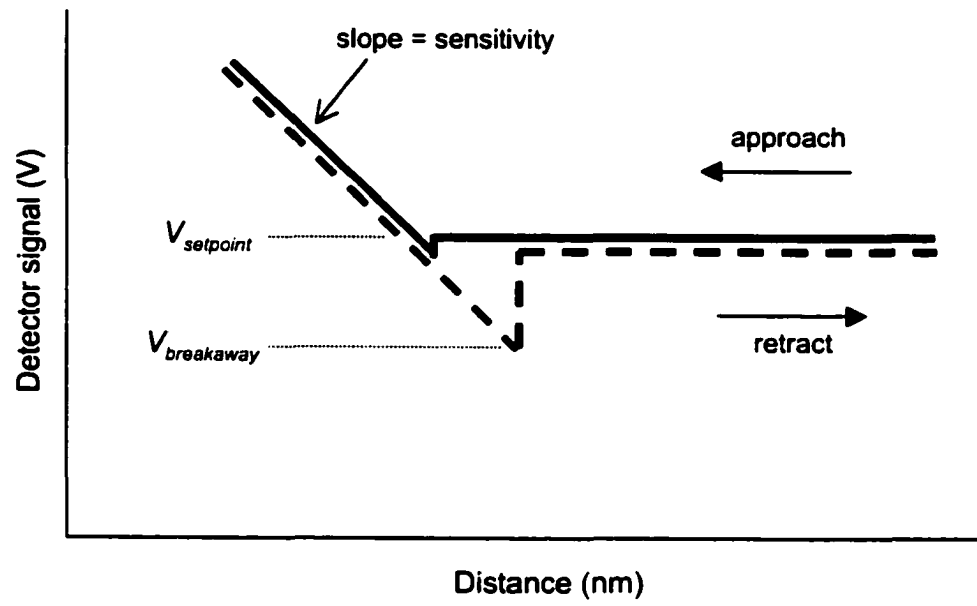
Figure 4-5. Typical force-distance curve obtained as the sample approaches the tip (———) and is subsequently retracted (- - -).

volts). Once the tip is off the surface, the detector signal returns to the level initially observed at the beginning of the approach. Typically, the user defines the setpoint ($V_{setpoint}$, volts) at which an image will be captured and the force (F_N) can be calculated according to:

$$F_N = \left(\frac{V_{setpoint} - V_{breakaway}}{S} \right) \times k \qquad \text{(Eqn. 4-2)}$$

where k is the cantilever spring constant (nN/nm).

4.3.3.1.1 Height mode AFM

Once the AFM has detected the cantilever deflection, it commonly generates the topographic data by operating in height mode. In height mode, a feedback loop keeps the deflection of the cantilever, and thus the applied force, constant by changing the height of the sample with a varying voltage applied to the z-electrode of the piezoelectric scanner. The magnitude of the feedback signal needed to raise or lower the sample to keep the force constant is proportional to the topography of the surface. For example, a voltage required to lower the sample indicates a step in the surface, and the applied voltage is proportional to the height of the step.

4.3.3.1.2 Deflection (error signal) mode AFM

The information content of the feedback signal in height mode is limited due to the frequency response of the feedback loop. The feedback loop can be considered as a high-pass filter where low spatial frequencies are filtered out by the action of the piezoelectric scanner. High spatial frequencies, however, are not affected by the feedback loop and can pass without change in amplitude. These frequencies cause the

cantilever to deflect. Thus, the error signal in the feedback loop is not equal to zero. The fine detail of a sample surface is not captured within the feedback loop and is therefore not present in the image when imaging in height mode. The information on the fine structure is available, but not acquired. This information is acquired using deflection (error signal) mode AFM [21]. The high spatial frequency components that are not filtered out by the feedback loop are displayed in this mode. Deflection mode is preferred when imaging soft biological samples that contain a high level of structural detail [21].

4.4   Experimental

4.4.1   Apparatus

AFM images were obtained with a Nanoscope III (Digital Instruments, Santa Barbara, CA, USA) equipped with a fluid cell. Oxide-sharpened silicon nitride cantilevers (Digital Instruments, Santa Barbara, CA, USA) with nominal spring constants of 0.06 N/m were used. The AFM substrates used were polished fused silica plates (Heraeus Amersil Inc., Duluth, GA, USA). The silica substrates were cleaned by heating in hot concentrated sulfuric acid overnight followed by rinsing thoroughly with water.

Capillary electrophoresis was performed on either a Beckman P/ACE MDQ system (Fullerton, CA, USA) or Beckman P/ACE 2100 system (Fullerton, CA, USA) equipped with a UV absorbance detector. Untreated fused silica capillaries (PolymicroTechnologies, Phoenix, AZ, USA) with inner diameters of 50 μm, outer diameters of 365 μm, and total lengths of 30 cm (20 cm to detector) were used unless otherwise stated. Data acquisition (4 Hz) and control were performed using P/ACE

Station Software for Windows 95 (Beckman Instruments, Fullerton, CA, USA) on a Pentium 300 MHz IBM computer.

Surface tension measurements were taken using a Fisher Surface Tensiometer Model 20 (Fisher Scientific, Pittsburgh, PA, USA). The platinum-iridium ring used was cleaned in 2-butanone and then heated in a gas flame to ensure it was free of any oil residue. The glass sample beaker was also washed with 2-butanone and rinsed with water prior to measurements.

4.4.2 Chemicals

All solutions were prepared in Nanopure 18 MΩ ultrapure water (Barnstead, Chicago, IL, USA). Buffers were prepared from reagent grade orthophosphoric acid (BDH, Darmstadt, Germany) and adjusted to the desired pH with sodium hydroxide (BDH). The surfactants cetyltrimethylammonium bromide (CTAB; Sigma, St. Louis, MO, USA), coco (amidopropyl) ammoniumdimethylsulfobetaine (Rewoteric AM CAS U; Goldschmidt Chemical, Oakville, ON), and didodecyldimethylammonium bromide (DDAB; Aldrich, Milwaukee, WI, USA) were used as received. Mesityl oxide (Aldrich, Milwaukee, WI, USA) was used as a neutral marker for the EOF measurements. The proteins ribonuclease A (bovine pancreas), lysozyme (chicken egg white), α-chymotrypsinogen A (bovine pancreas), cytochrome c (bovine heart), and myoglobin (horse skeletal muscle) were used as received (Sigma, St. Louis, MO, USA).

4.4.3 EOF measurements

New capillaries were used for each surfactant and each surfactant concentration. Each capillary was pretreated with 0.1 M NaOH or H_2SO_4 for 5 min (20 psi rinse) and water for 5 min (20 psi rinse). H_2SO_4 was used to condition the capillary prior to

electrophoretic runs that were used for comparison to AFM images. Thus the surface charge would be similar to the charge on the fused silica plates used for imaging (which were cleaned with H_2SO_4). However, we found that preconditioning the capillary with NaOH prior to electrophoretic runs did not affect migration times. Before each run, the capillary was rinsed at high pressure (20 psi) with buffer for 2 min. Mesityl oxide (1 mM) was introduced as a neutral marker using a 3-s, low-pressure (0.5-psi) hydrodynamic injection. Detection was at 254 nm. The capillary was thermostated to 23°C and a constant voltage of ±10 kV was applied (depending on the direction of the EOF). The magnitude of the EOF (μ_{EOF}) was calculated using the migration time of mesityl oxide under constant voltage according to Eqn. 1-4.

4.4.4 AFM imaging

Contact AFM images were captured in deflection mode at 23°C [21]. Images of the fused silica surface in buffer were captured in order to compare the surface before and after surfactant was added. CTAB (0.5 mM) and DDAB (0.1 mM) solutions were prepared in phosphate buffer of pH 3, 5, 7 or 11 (constant ionic strength of 20 mM) at concentrations above their critical micelle (or vesicle) concentration. The surfactant solution was introduced and held in the fluid cell, sealed with a silicon O-ring, and allowed to equilibrate for 5 min. Integral and proportional gains were set to 0.75 and 1.0 respectively, while scan rates were set at 6.10 Hz. To eliminate drift before imaging, the scanner was left scanning over a 10-μm^2 area for 1 hour. After this time period, the tip was allowed to barely touch the surface, then the voltage was increased in small increments until a clear image was obtained. The imaging force was always less than 1 nN. This type of imaging is known as "soft contact" or "double-layer" imaging [5,22,23].

The normal force, F_N, was estimated from the force-distance plots (Figure 4-5) and represents the total imaging force, with $F_N = 0$ nN designated as the point where the tip "breaks away" from the surface. Features observed in the images were confirmed to be real and not artifacts due to drift by obtaining identical images independent of scan direction.

Friction measurements were obtained with the fast scan axis perpendicular to the principal axes of the cantilever while systematically varying the normal force (F_N). Frictional forces were measured from trace/retrace cycles along a single scan line (friction loops). The frictional signal is the raw detector signal in volts which changes as the tip twists due to friction. The detector signal was not converted into frictional force for comparisons between surfaces. This is acceptable since the same cantilever and tip were used for all these studies. Hysteresis in the friction was not observed when cycling F_N.

Aspect ratios of the aggregates were calculated by measuring the length and width of the aggregates using the cross-section tool in the Digital Instruments image analysis software version 4.43r8. Nearest-neighbour distances were also measured using the cross-section tool in the Digital Instruments image analysis software version 4.43r8.

4.4.5 Surface tension measurements

Surface tension measurements were taken in 10 mM phosphate buffer, pH 7 containing increasing concentrations of CTAB (from 0.01-0.5 mM) or DDAB (from 0.0001-0.1 mM). The break in a plot of the log of the concentration versus the surface tension occurs at the critical aggregation concentration of the surfactant in this buffer.

4.4.6 Protein separations

New 50 cm (40 cm to detector) capillaries were used for the separations. The electrophoretic buffer consisted of 25 M phosphate containing 0.5 mM CTAB, 0.1 mM DDAB, or no surfactant. The buffer was adjusted to pH 3 with NaOH. The capillary was pretreated with 0.1 mM NaOH for 10 min (20 psi rinse) and water for 10 min (20 psi rinse). Prior to each separation, the capillary was rinsed for 5 min (20 psi rinse) with electrophoretic buffer.

A mixture of 0.1 mg/ml of ribonuclease A, lysozyme, α-chymotrypsinogen A, cytochrome c, and myoglobin in water was injected at low pressure (0.5 psi) for 3.0 s. Separation was performed using -15 kV (coated capillary) or $+15$ kV (bare capillary), and the proteins detected at 214 nm. Efficiencies were calculated by the P/ACE Station Software using the peak width at half height method.

4.4.7 Protein recovery studies

Protein recoveries were determined using the procedure of Towns and Regnier [24] modified for a one-detector CE [25] as described in Section 2.2.5. In this procedure, 4 replicate separations of the proteins ribonuclease A, lysozyme, α-chymotrypsinogen A, cytochrome c, and myoglobin (0.1 mg/ml) were performed using 25 mM phosphate buffer containing 0.5 mM CTAB or 0.1 mM DDAB at pH 3 on a 50 cm (40 cm to detector) capillary. Each capillary was pretreated as before with 0.1 M NaOH for 10 min (20 psi rinse) and water for 10 min (20 psi rinse). Before each run, the capillary was rinsed at high pressure (20 psi) with buffer for 5 min. The proteins were introduced into the capillary using a low-pressure (0.5 psi) injection for 3 s and were separated using a field strength of -300 V/cm. Detection was at 214 nm. The capillary was then shortened

to 31 cm (21 cm to detector) and the injections were repeated. The applied voltage, rinse times, and injection time were reduced accordingly for the short capillary. Benzyl alcohol was used as an internal standard to correct for injection volume variation. The percent recoveries of the proteins were determined by comparing the peak area between the long and short capillaries.

4.5 Results and Discussion

4.5.1 Evaluation of coating stability

Measurements of the EOF in CE under a variety of conditions can be used as an indirect test of the stability of capillary coatings [26]. The EOF was measured after an initial rinse (5 min at 20 psi) with surfactant-containing buffer followed by a second rinse (3 min at 0.5 psi) with the separation buffer (no surfactant). The second rinse was used to flush out excess surfactant in the bulk solution. The time required to flush the entire length of capillary was determined by measuring the time required for an injection of mesityl oxide to be pushed to the detector and then allowing for the length of capillary after the detector.

Figure 4-6 displays reversed EOF (cathode to anode) as a function of time for CTAB and DDAB measured by consecutive injections of mesityl oxide. Electrophoretic buffers consisted of 10-mM phosphate at pH 7.2. Excellent stability was observed for DDAB over 30 runs (2.5 min for each run). The EOF decreased only 3 % over the 75 minutes of this test. The stability of CTAB was significantly lower, as seen by the sharp decline in reversed EOF.
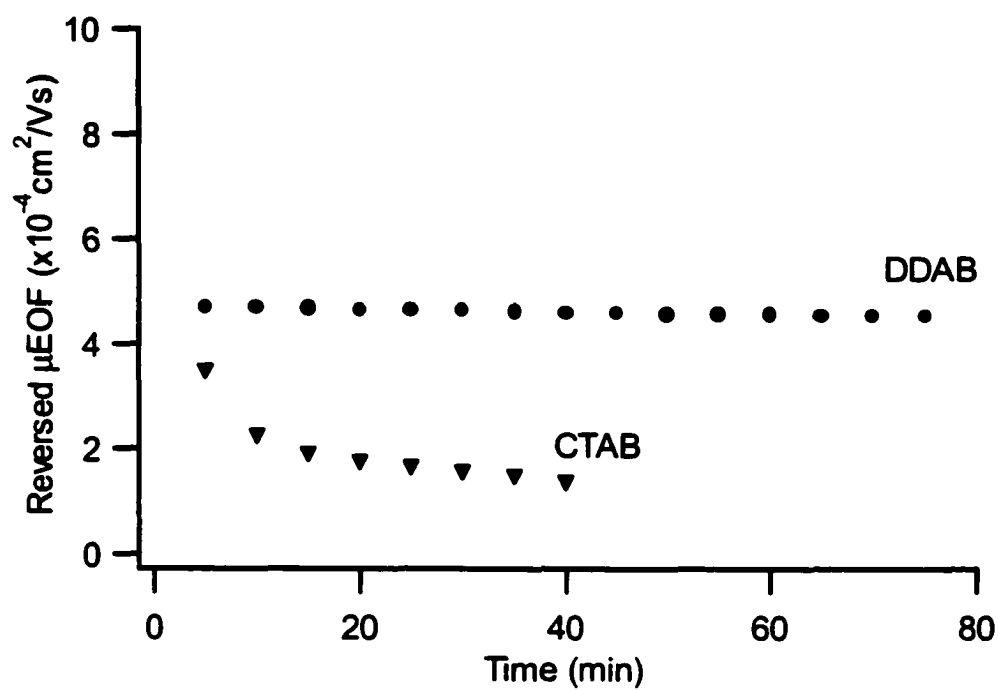
Figure 4-6. Coating stability of CTAB and DDAB as reflected by the reversed EOF as a function of time. Successive injections performed after an initial flushing of excess surfactant from the capillary. No rinses performed between runs.

These results support the theory that single-chained surfactants such as CTAB form dynamic coatings. By removing the free-surfactant from the bulk solution, the system is pushed far from equilibrium. The adsorbed surfactants then desorb from the surface to re-establish equilibrium with the bulk solution, resulting in lower surface coverage. The fact that this phenomenon was not observed with DDAB suggests that its adsorption behaviour is less dynamic. However, as indicated by the slight decline in the observed reversed EOF in Figure 4-6, it cannot be said that DDAB forms a permanent coating either. Thus this type of coating falls into the class of adsorbed cationic polymer coatings (Polybrene, see Section 1.2.2). These semi-permanent coatings must be recoated quite frequently to achieve reproducible results. Thus, the short equilibration times associated with DDAB coatings makes this approach particularly attractive.

The effect of pH on the stability of CTAB and DDAB was also studied. EOF measurements were performed over the pH range of 2 to 11.5 for both surfactants. Little relative difference in the reversed EOF was observed above pH 4. However, between pH 2 to 4 DDAB performed significantly better. At pH 2, DDAB produced a 60 % faster reversed EOF than CTAB. Thus it appears that the DDAB coatings are more stable under acidic conditions.

4.5.2 Structure of surfactants adsorbed on fused silica

As explained in Section 4.2.2, literature images of single-chained quaternary ammonium surfactants (C_{14} [15] and C_{16} [5]) revealed the presence of spherical aggregates spaced uniformly over the silica surface. It was concluded that these aggregates were adsorbed micelles [5]. To determine if this micellar-type coating forms on the capillary surface during CE, I employed AFM imaging to study surfactant adsorption in a

commonly used electrophoretic buffer. Fused silica plates were used as the imaging substrate to mimic the inside wall of a capillary. Figure 4-7A is an AFM image of 0.5-mM CTAB (a concentration known to produce a reversed EOF; see below) in a 10-mM phosphate buffer at pH 7. The CTAB image shows spherical aggregates uniformly spaced over the 150 nm x 150 nm surface. Diameters of the aggregates were found to be 4.5 ± 0.4 nm using the Digital Instruments image analysis software. This agrees very well with previous studies [5] and suggests that these spherical aggregates are indeed CTAB micelles adsorbed to the silica surface. Similarly, the single-chained zwitterionic surfactant coco (amidopropyl) ammoniumdimethylsulfobetaine (CAS U) used in Chapter Two was investigated and yielded the image shown in Figure 4-7C. The diameters of the CAS U aggregates measured 4.1 ± 0.2 nm using the Digital Instruments software. Identical images and aggregate diameters (within error) were obtained for 0.5 mM CTAB at pH 7 when sharper AFM probe tips (silicon ESP tips, Digital Instruments) were used for imaging rather than the oxide-sharpened silicon nitride tips (4.5 ± 0.4 nm versus 4.1 ± 0.5 nm). This indicates that the tip is not convoluting the image.

As shown in Section 4.5.1, the double-chained DDAB produces a much more stable coating than the single-chained CTAB. I speculated that this increased stability might have been due a different adsorption mechanism for DDAB onto silica than CTAB. Figure 4-7B shows an AFM image of 0.1 mM DDAB (concentration known to reverse the EOF) in 10-mM phosphate buffer at pH 7. The flat featureless image is indicative of a uniform bilayer. Although this image does not differ significantly from the blank (no surfactant), 0.1 mM DDAB produces a strong reversed EOF in CE (Figure 4-6) which suggests that the coating is intact on the silica substrate.

50 nm

A

50 nm

B

50 nm

C
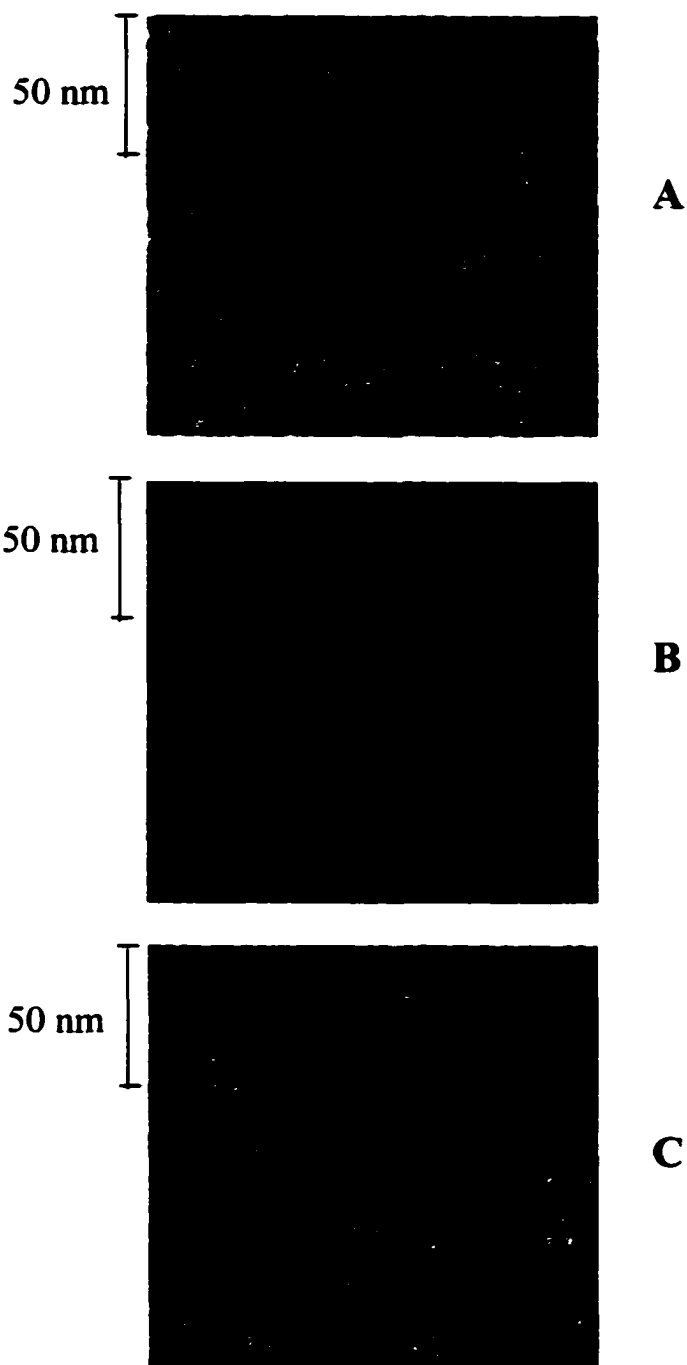
Figure 4-7. AFM images (150 nm x 150nm) of (A) 0.5 mM CTAB in 10 mM phosphate buffer, pH 7 on fused silica, (B) 0.1 mM DDAB in 10 mM phosphate buffer, pH 7 on fused silica, and (C) 2 mM CAS U in 10 mM phosphate buffer, pH 7 on fused silica. Note that images captured in deflection mode do not provide height information, thus z-scale is not indicated here.

To confirm the presence of a DDAB coating on the surface, friction measurements as a function of applied normal force were taken on the bare silica flushed with buffer and compared to measurements taken on the silica flushed with DDAB-containing buffer. A plot of detector signal in volts (proportional to friction; see Section 4.4.4) versus normal force applied on each surface is shown in Figure 4-8. As is evident, the friction at any one applied normal force on bare silica is larger than that on the DDAB-coated silica, demonstrating that indeed DDAB coats the surface. I also tried to scratch a hole in the coating with the AFM tip by applying a large force (~100 nN) to the surface. Immediately after scratching the hole, I zoomed out and re-imaged the area. There was no evidence of a hole. This is likely because the DDAB has such a high affinity for the surface that it re-coated the substrate very quickly.

The formation of bilayer structures by the double-chained surfactant DDAB is consistent with the theoretical aggregate structure expected for a surfactant with a packing parameter between ½ and 1 (Section 4.2.1). The cylindrical shape of a double-chained surfactant, as opposed to the conical shape of a single-chained surfactant, accounts for its different aggregate structure.

4.5.3 Effect of surfactant concentration on surface aggregation

AFM was employed to directly observe the onset of aggregation of CTAB on a silica surface upon increasing surfactant concentration. These images were then correlated to the direction and magnitude of the EOF observed in CE experiments using the same buffer. At CTAB concentrations of 0.1 mM and below in a 10-mM phosphate buffer (pH 7), a featureless image was obtained. At 0.15 mM and above (up to 0.5 mM), spherical aggregates were observed as in Figure 4-7A. No change in the AFM image was
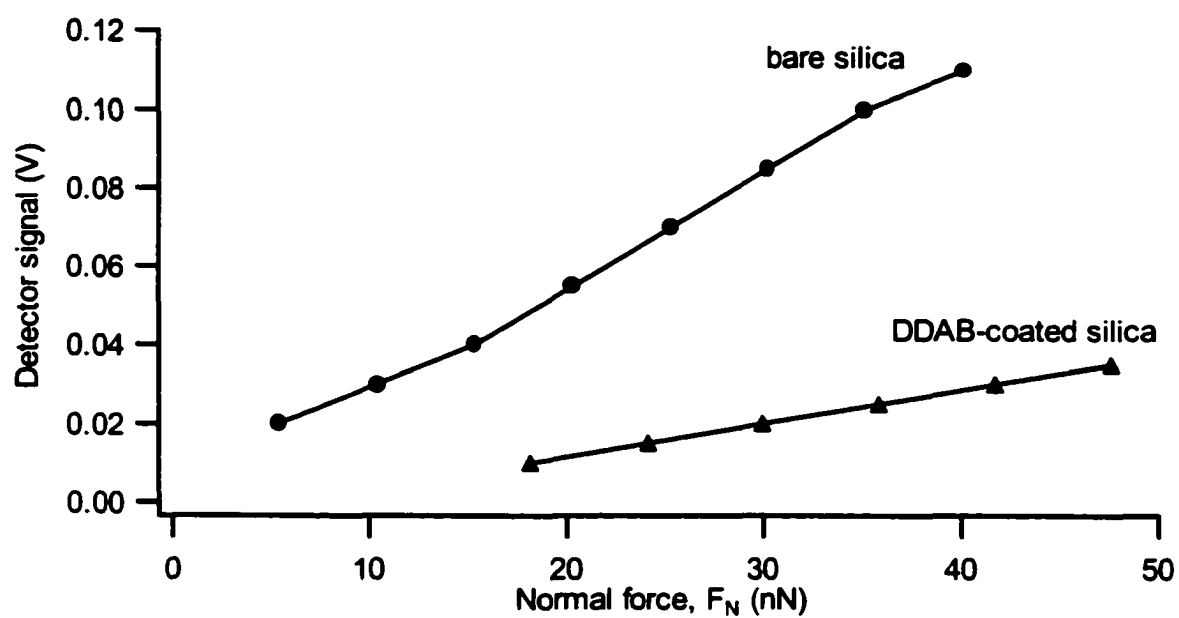
Figure 4-8. Plots of detector signal vs normal force for bare silica and DDAB-coated silica in 10 mM phosphate buffer, pH 7. Note that the detector signal is proportional to friction (see section 4.4.4). Lines through points act only as a guide to the eye.

observed upon increasing the CTAB concentration from 0.15 to 0.5 mM. Figure 4-9

shows the plot of EOF as a function of CTAB concentration. A relatively sharp transition

from normal to reverse EOF occurs between 0.05 and 0.1 mM. Thus it appears that the

onset of the micellar coating formation approximately coincides with the onset of the

reversed EOF.

The onset of the micellar coating formation also approximately coincides with the

critical micelle concentration (CMC) of CTAB, measured to be 0.20 mM in a 10-mM

phosphate buffer at pH 7. Adsorbed micelles were first observed at 0.15 mM by AFM,

just below the CMC of the surfactant, consistent with previous AFM studies in which Liu

and Ducker first observed adsorbed micelles at 1/2 to 1/3 of the CMC of CTAB in

distilled water (0.9 mM) [5]. The authors suggested that the formation of micelles at the

surface at sub-CMC levels may be the result of electrostatic attraction of the surfactant by

the silica creating a 'surface excess' [5]. Thus, the higher concentration of surfactant at the

surface would make it appear that the surface induces micelle formation at lower

concentrations than the bulk solution.

A similar set of experiments was performed for the double-chained surfactant

DDAB. However, AFM imaging could not verify the onset of coating formation since

the DDAB coating looks quite similar to the bare silica surface (blank). The onset of

reversed EOF did fall near the region of the critical aggregation concentration of DDAB,

measured to be 0.004 mM in a 10-mM phosphate buffer at pH 7. However, the reversed

EOF measured at these low concentrations was highly dependent upon the rinse time

with the surfactant-containing buffer prior to the EOF measurement. The data suggested

that the total amount of surfactant flushed through the capillary, rather than the
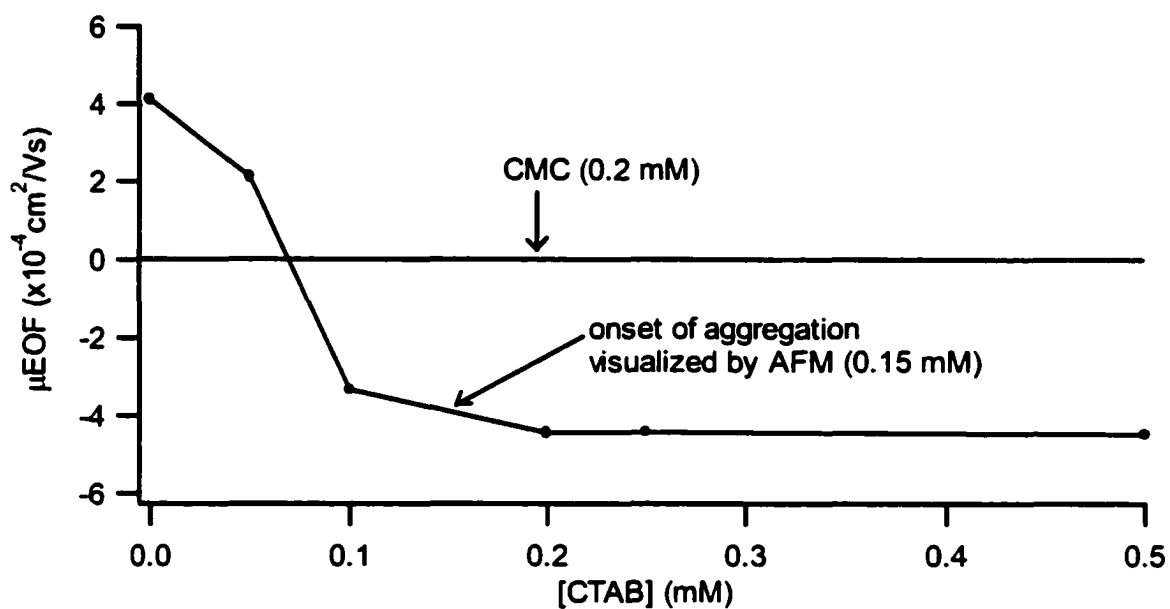
Figure 4-9. Effect of CTAB concentration on the EOF in 10 mM phosphate, pH 7 buffer. Experimental conditions: applied voltage, ± 10 kV; temperature, $23^{\circ}C$; capillary length, 30 cm (21 cm to detector). Line through points acts only as a guide to the eye.

concentration of surfactant present in the buffer during the EOF measurement, dictated the direction and magnitude of the EOF. Thus the behavior of DDAB was not as easily interpreted as that of CTAB, and suggests that the DDAB coating is more permanent in nature rather than dynamic. This is consistent with the studies using DDAB in Section 4.5.1.

4.5.4 Effect of pH on surface aggregation

CTAB was imaged on fused silica in different pH buffers to study the effect of pH on surface aggregation. Figure 4-10 shows images of 0.5 mM CTAB in phosphate buffers of pH 3 (A), 7 (B), and 11 (C). The ionic strength of the buffers was kept constant at 20 mM by altering the phosphate concentration. Spherical aggregates, spaced uniformly over the imaging surface, are seen in all images.

To quantify the spacing of the aggregates on the surface, the nearest neighbour distance was measured. The nearest neighbour distance is defined as the distance between the center point of adjacent spherical aggregates (or micelles). Manne and Gaub [15] found that the nearest neighbour distance varied inversely with solution pH for tetradecyltrimethylammonium bromide on silica. Table 4-1 shows how the nearest neighbour distance changes as a function of pH for CTAB. As seen in Figure 4-10, the micelles are spaced closer together as the pH increases from 3 (13.1 ± 0.4 nm) to 11 (7.4 ± 0.2 nm). The nearest neighbour distance became constant above pH 7 (7.5 ± 0.2 nm) as would be expected, since the silanol groups are fully ionized above this pH (pKa = 5.7 [27]).

A similar image was taken of 0.1 mM DDAB on silica at pH 3. As seen for 0.1 mM DDAB in 10 mM phosphate buffer at pH 7 (Figure 4-7B), a flat, featureless image

A

50 nm

B

50 nm

C
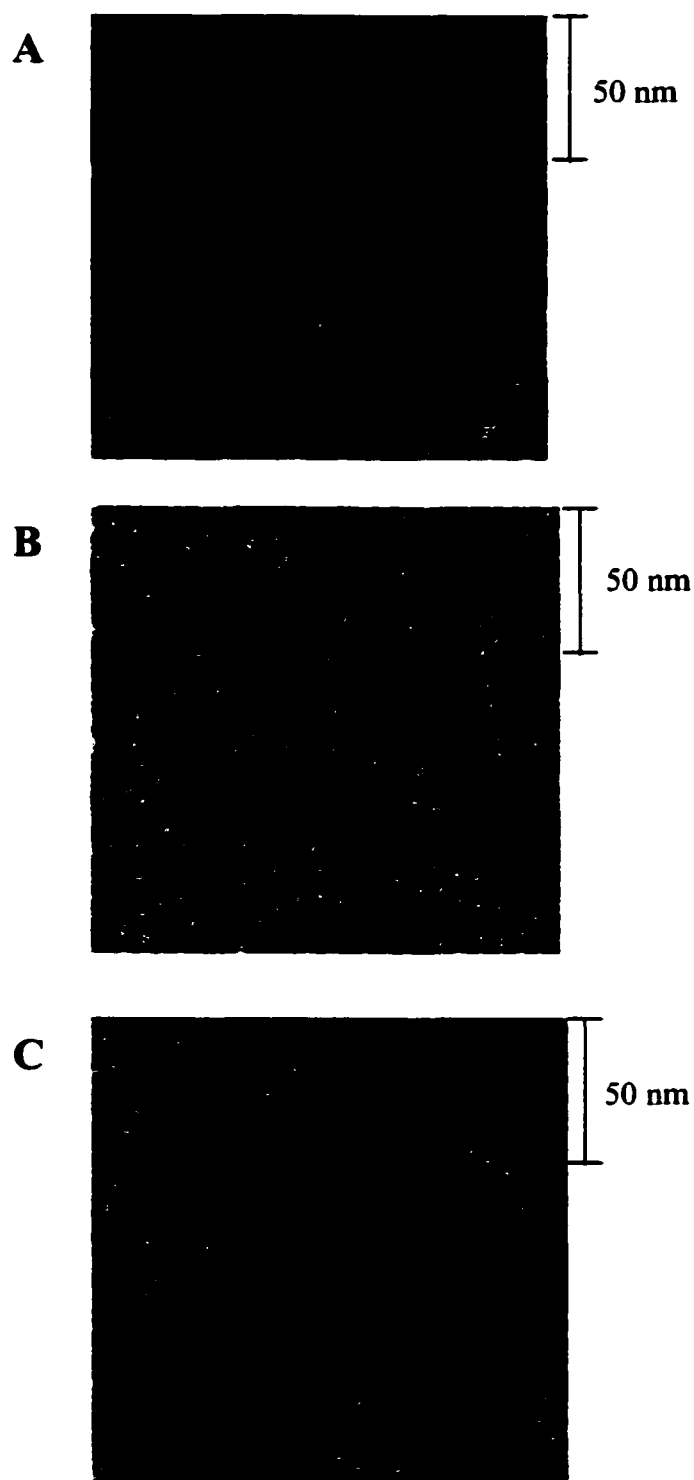
50 nm

Figure 4-10. AFM images (150 nm x 150 nm) showing the effect of pH on the surface aggregation of 0.5 mM CTAB in phosphate buffer (ionic strength constant at 20 mM). (A) pH 3; (B) pH 7; (C) pH 11. Note that images captured in deflection mode do not provide height information, thus z-scale is not indicated here.

Table 4-1. Nearest neighbour distance for cetyltrimethylammonium bromide (CTAB) aggregates in different pH buffers.

buffer pH	nearest neighbour distance (nm)
3	13.1 ± 0.4
5	8.3 ± 0.3
7	7.5 ± 0.2
11	7.4 ± 0.2

was observed. As explained in Section 4.5.1, 0.1 mM DDAB strongly reverses the EOF at a pH as low as 2. In order to see a reversed EOF under these conditions, DDAB must aggregate to produce a positively charged wall. This confirms the presence of a flat bilayer at pH 3. Even though there is less charge on the capillary wall at pH 3 (reflected in the low EOF of +0.232 x 10^{-4} cm^2/Vs on a bare capillary), DDAB still forms a bilayer coating. The hydrophobic interactions between the hydrocarbon chain groups of DDAB must still be sufficient to keep the bilayer intact despite the loss of some electrostatic attraction to the wall.

4.5.5 Effect of buffer ionic strength on surface aggregation

The effect of ionic strength on the surface assembly of CTAB was studied by capturing AFM images of CTAB which had been dissolved in increasing ionic strength phosphate buffers of pH 3 and 7. Table 4-2 summarizes the results found using AFM imaging. In pH 7 phosphate buffers of 20 mM and 50 mM ionic strength, CTAB forms spherical aggregates on fused silica. At pH 7 the nearest neighbour distance of CTAB aggregates decreased from 7.5 ± 0.2 nm in a buffer of 20 mM ionic strength to 5.2 ± 0.2 nm in a buffer of 50 mM ionic strength. The mean aspect ratio of the spheres was 1.14 ± 0.05. Increasing the ionic strength to 100 mM at pH 7 caused a change in CTAB aggregate structure. As seen in Figure 4-11, a combination of short rods and spherical aggregates are observed, rather than the complete coverage by spherical aggregates observed at lower ionic strengths (Figure 4-7A). We will define short rods as aggregates whose aspect ratio is greater than 1.5 but less than 15. The mean aspect ratio of the spheres circled in Figure 4-11 is 1.13 ± 0.08 while the aspect ratios of the circled rods

Table 4-2. Effect of ionic strength on cetyltrimethylammonium bromide (CTAB) aggregate shape and nearest neighbour distances at pH 3 and pH 7.

Ionic strength (mM)	pH 3		pH 7	
	nearest neighbour distance (nm)	aggregate shape	nearest neighbour distance (nm)	aggregate shape
20	13.1 ± 0.4	sphere	7.5 ± 0.2	sphere
50	8.5 ± 0.3	sphere	5.2 ± 0.2	sphere
100		cylinder		short rods/ spheres
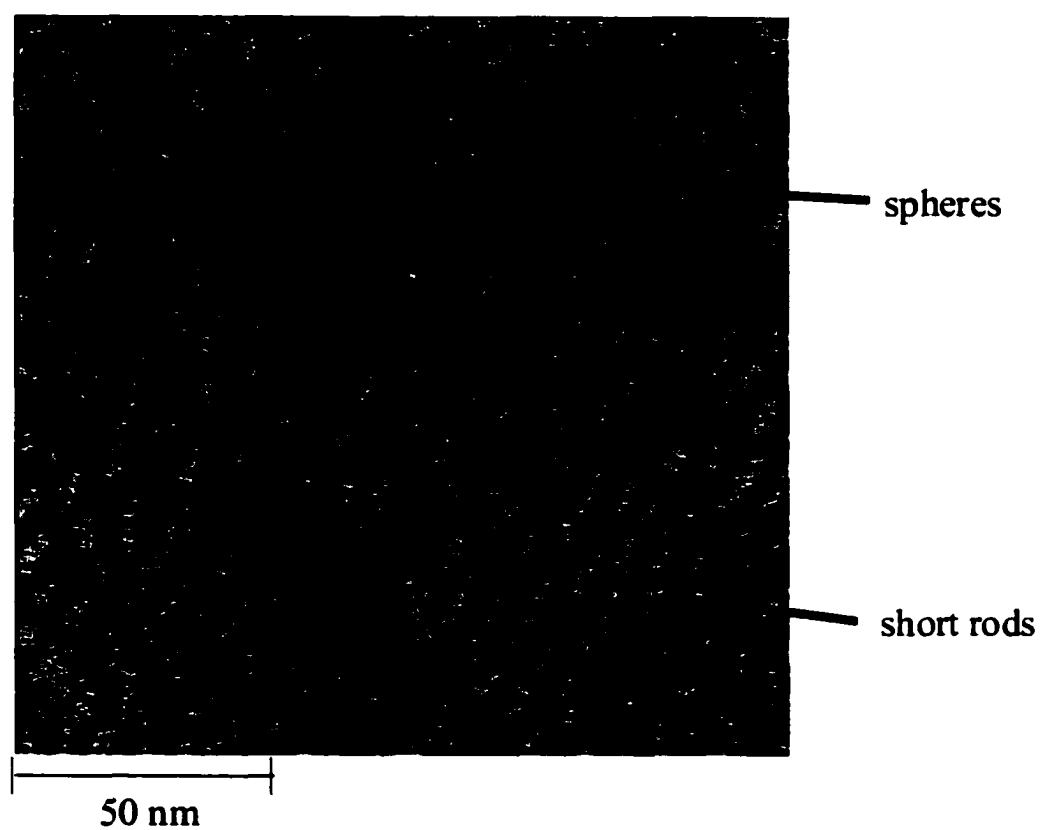
Figure 4-11. AFM image (150 nm x 150 nm) showing the effect of high ionic strength (100 mM) on aggregate shape of 0.5 mM CTAB in phosphate buffer, pH 7 on fused silica. (spheres/short rods). Note that images captured in deflection mode do not provide height information, thus z-scale is not indicated here.

range from 5 – 10. The image in Figure 4-11 shows approximately 30% short rods and 70% spheres.

In aqueous solution, surfactant monomers form aggregates due to the hydrophobic interactions between the long hydrocarbon chains and water. The favorable attraction of the hydrocarbon tail groups is limited by the unfavorable, electrostatic repulsion between the polar head groups. Increasing the ionic strength of the buffer minimizes the repulsion between adjacent headgroups by ionic screening of this electrostatic repulsion [28]. As cited by Ducker and co-workers [5, 29] and Velegol et. al. [30], surfactants will assemble at the surface in a different fashion under high salt conditions, as they are able to overcome electrostatic repulsion. Patrick *et al.* explain that the area occupied per headgroup is typically 65 A^2 for trimethyl headgroup surfactants [31]. In this case, the packing parameter, P, is less than 1/3 (Eqn. 4-1), which indicates sphere formation. With addition of electrolyte (such as an increase in phosphate buffer), the effective headgroup area decreases since electrostatic repulsion decreases. The value of a_h in the packing parameter relationship decreases, thereby increasing P. When P has a value of 1/3 to 1/2, cylindrical micelles [32] form. The ionic screening and decreased effective headgroup area account for the transition from spherical aggregates to cylindrical micelles on the surface in a 100 mM ionic strength buffer at pH 7.

The trend is similar for CTAB in low pH buffers. At a silica surface in pH 3 phosphate buffers of 20 mM and 50 mM ionic strength, CTAB forms spherical aggregates (aspect ratio 1.06 ± 0.03). At pH 3 the distance between adjacent aggregates decreases from 13.1 ± 0.4 nm in a buffer of 20 mM ionic strength to 8.5 ± 0.3 nm in a buffer of 50 mM ionic strength. At an ionic strength of 100 mM, electrostatic repulsion

between the headgroups is overcome and meandering stripes, which are cylindrical micelles, are observed in the AFM image. Cylindrical micelles are defined as aggregates with an aspect ratio greater than 15. There is no evidence of spherical aggregates at this ionic strength.

The change in surfactant coverage at the silica surface is reflected in the changes in EOF observed in identical buffers of increasing ionic strength. The magnitude of the EOF, μ_{cof}, is generally described by the Smoluchowski equation (Eqn. 1-2). As explained in Section 1.1.4, the zeta potential is the potential slightly off the silica and is a function of the deprotonation of the silanols, ion adsorption onto the surface, and the ionic strength of the buffer. Therefore, the zeta potential is a function of the surface charge and as a consequence the EOF is also related to surface charge. At high ionic strengths, cylindrical aggregates were observed in the AFM images suggesting that more of the surface was covered with the positively charged surfactant. This would also imply that the reversed EOF should be stronger in higher ionic strength buffers containing CTAB. However, since increasing ionic strength slows the EOF, this must be accounted for in order to correlate the strength of reversed EOF to the surface coverage of CTAB. To take into account the effect of ionic strength, EOF values obtained in the presence of CTAB were "normalized" by taking a ratio of the EOF measured with CTAB to the EOF measured on a bare capillary in an identical buffer without CTAB.

The "normalized" reversed EOF increased from -18 ($-4.20\times10^{-4}/0.23\times10^{-4}$) to -29 ($-3.80\times10^{-4}/0.13\times10^{-4}$) on going from the 20 mM ionic strength buffer to the 100 mM ionic strength buffer at pH 3. This indicates that there is an increased positive charge present on the silica surface when CTAB is in high (100 mM) ionic strength buffers of

low pH (pH 3). The cylindrical micelles observed provide more surface coverage. The formation of cylindrical micelles at high ionic strength implies that it is the headgroup repulsion and not the charge on the wall that is the limiting factor governing CTAB aggregation at low pH.

The trend is not as pronounced with the pH 7 buffers. The "normalized" reversed EOF remains approximately constant at -0.8 (e.g. $-4.0 \times 10^{-4}/4.8 \times 10^{-4}$ for the 100 mM ionic strength buffer), indicating that the charge on the wall is not significantly altered as a result of changing the ionic strength of the buffers containing CTAB from 20 mM to 100 mM. The positive charge density on the surface does not noticeably change with the formation of some short rods in 100 mM ionic strength buffers at pH 7. This would indicate that the spherical CTAB aggregates formed at lower ionic strength provide similar coverage as the combination of short rods and spherical aggregates observed at higher ionic strength.

4.5.6 Implications of surfactant coating morphology in CE

To assess the ability of CTAB- and DDAB-coated capillaries to prevent protein adsorption, protein analysis using these coatings was investigated. A separation of basic (cationic) proteins lysozyme, ribonuclease A, α-chymotrypsinogen A, cytochrome c, and myoglobin was performed at pH 7 and 3. At pH 7, the separation of the proteins using a CTAB coated capillary was comparable to the separation using a DDAB coated capillary. However, the two coatings were not comparable at pH 3. At pH 3, the proteins are highly positively charged (pI range from 7 to 11). As well, the surface still carries a significant negative charge as indicated by a positive EOF value ($+0.23 \times 10^{-4}$ cm^2/Vs). To confirm that it is necessary to shield the proteins from the wall at this pH, the separation was first

performed on a bare capillary. Separation of the five cationic proteins on a bare capillary at pH 3 is shown in Figure 4-12A. It is evident that two of the five proteins were irreversibly adsorbed to the wall since there are only three peaks present. Further, the lysozyme, ribonuclease A, and α-chymotrypsinogen A peaks are broad and tailed, indicative of wall adsorption.

The separation of the cationic proteins using a CTAB-coated capillary is shown in Figure 4-12B. Three of the proteins were separated in less than 15 min with efficiencies of 500 000 plates/m. The other two proteins, cytochrome c and myoglobin, were not detected, even after run times of 40 min, which should have been sufficient time for the proteins to migrate to the detector. The spacing between adjacent micelles at this pH is roughly 9 nm while the dimensions of lysozyme, for example, are 4.5 nm x 3 nm x 3 nm [33]. The gaps present between the adjacent CTAB micelles at the capillary surface (seen in Figure 4-10A) are most likely responsible for the unwanted adsorption of proteins. The extent of protein adsorption of the detected proteins (lysozyme, α-chymotrypsinogen A, and ribonuclease A) was quantitatively determined by performing a recovery study. Protein recoveries were determined as described in Section 4.4.7. The recoveries of lysozyme, α-chymotrypsinogen A, and ribonuclease A were 81% ± 3%, 79% ± 5%, and 77% ± 8% respectively.

The separation of the same basic proteins using a DDAB-coated capillary is shown in Figure 4-12C. All five proteins are separated in less than 6 min with efficiencies of 500 000 plates/m. The degree of protein adsorption to the capillary wall was measured as before using a recovery study. The recovery of α-chymotrypsinogen A and lysozyme were quantitative (uncertainty includes 100%) while the recovery of
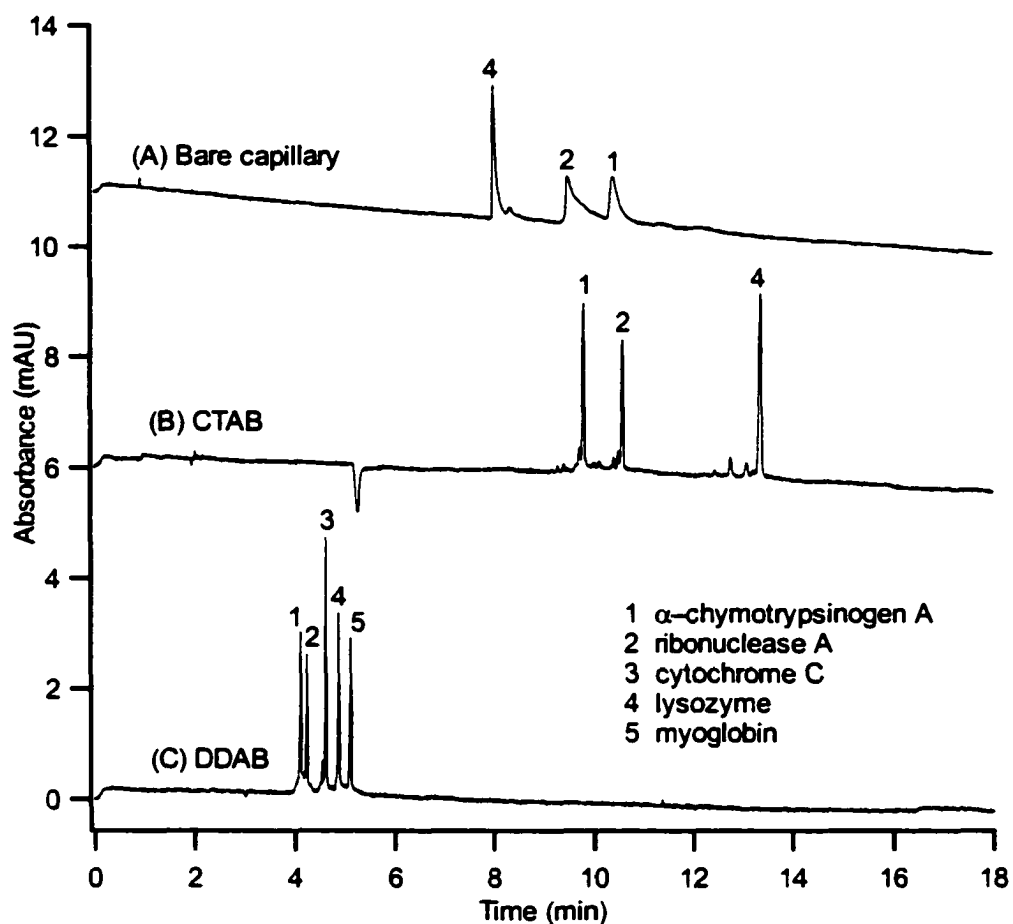
Figure 4-12. Separation of five basic proteins at pH 3 using (A) bare capillary (offset 11 mAU), (B) CTAB-coated capillary (offset 6 mAU); and (C) DDAB-coated capillary. CE conditions: 50 cm capillary (40 cm to detector); UV detection at 214 nm; +15 kV applied voltage (A) -15 kV applied voltage (B, C); buffer, 25 mM phosphate buffer at pH 3.0 containing (A) no surfactant, (B) 0.5 mM CTAB, or (C) 0.1 mM DDAB. Note that the myoglobin peak was not observed after a 40 min run time in (B).

ribonuclease A, cytochrome c, and myoglobin was nearly quantitative (96% ± 3%, 91% ± 4%, and 85% ± 1% respectively). This indicates that the increased surface coverage provided by DDAB is effective in the prevention of protein adsorption.

4.6   Conclusions

An ideal coating technology for CE must balance performance, cost, and speed. Future endeavors such as proteomic and combinatorial analytical chemistry place even greater demands on the simplicity and convenience of the coating procedure. Double-chained surfactants such as didodecyldimethylammonium bromide (DDAB) combine the stability of permanent coatings with the versatility of dynamic coatings.

Atomic force microscopy studies are useful for studying interfacial surfactant aggregation and have lead to an improved understanding of self-assembly at the capillary wall. At a fused silica surface, AFM has shown that the surfactant cetyltrimethylammonium bromide (CTAB) forms spherical aggregates while the surfactant DDAB forms flat bilayers in common electrophoretic buffers. The observed nearest neighbour distance between CTAB aggregates varies inversely with the buffer pH. DDAB forms a flat, uniform coating at both low (pH 3) and neutral pH (pH 7). Increasing the buffer ionic strength allows CTAB aggregates at the surface to pack closer together. The morphology of surfactant aggregates at the capillary wall and the change in surface coverage has implications in CE separations of strongly adsorbing analytes such as proteins. It appears as if AFM imaging is a useful tool for the understanding and development of new capillary coatings in CE in the future.

4.7 Post-script

Based on the studies described in this chapter, Yeung et al. [34] performed capillary electrophoresis separations of cytochrome c protein mixtures using a DDAB-coated capillary. The separation was coupled off-line with matrix-assisted laser desorption ionization mass spectrometry (MALDI-MS). Due to its semi-permanent nature, the DDAB coating was compatible with the MALDI-MS measurements. They achieved highly efficient separations (600 000 plates/m) with good detection sensitivity (23 fmol).

4.8 References

(1)   Kang, S. H.; Gong, X. Y.; Yeung, E. S. *Anal. Chem.* **2000**, *72*, 3014.

(2)   Ma, L. J.; Gong, X. Y.; Yeung, E. S. *Anal. Chem.* **2000**, *72*, 3383.

(3)   Huang, X.; Luckey, J. A.; Gordon, M. J.; Zare, R. N. *Anal. Chem.* **1989**, *61*, 766.

(4)   Jones, W. R.; Jandik, P. *J. Chromatogr.* **1991**, *546*, 445.

(5)   Liu, J.-F.; Ducker, W. A. *J. Phys. Chem. B* **1999**, *103*, 8558.

(6)   Lucy, C. A.; Underhill, R. S. *Anal. Chem.* **1996**, *68*, 300.

(7)   Ninham, B. W.; Evans, D. F.; Wel, G. J. *J. Phys. Chem.* **1983**, *87*, 5020.

(8)   Talmon, Y.; Evans, D. F.; Ninham, B. W. *Science* **1983**, *221*, 1047.

(9)   Brady, J. E.; Evans, D. F.; Kachar, B.; Ninham, B. W. *J. Am. Chem. Soc.* **1984**, *106*, 4279.

(10)   Israelachvili, J. N.; Mitchell, D. J.; Ninham, B. W. *J. Chem. Soc., Faraday Trans. 2* **1976**, *72*, 1525.

(11)   Warr, G. G.; Sen, R.; Evans, D. F. *J. Phys. Chem.* **1988**, *92*, 774.

(12)   Svitova, T. F.; Smirnova, Y. P.; Pisarev, S. A.; Berezina, N. A. *Colloids Surf. A* **1995**, *98*, 107.

(13)   Bijsterbosch, B. H. *J. Colloid Interface Sci.* **1974**, *47*, 186.

(14)   Yeskie, M. A.; Harwell, J. H. *J. Phys. Chem.* **1988**, *92*, 2346.

(15)   Manne, S.; Gaub, H. E. *Science* **1995**, *270*, 1480.

(16)   Helm, C. A.; Israelachvili, J. N.; McGuiggan, P. M. *Science* **1989**, *246*, 919.

(17)   Young, R.; Ward, J.; Schire, F. *Phys. Rev. Lett.* **1971**, *27*, 922.

(18)   Binning, G.; Rohrer, H.; Gerber, C.; Weibel, E. *Phys. Rev. Lett.* **1982**, *49*, 57.

(19)   Binning, G.; Rohrer, H.; Gerber, C.; Weibel, E. *Phys. Rev. Lett.* **1983**, *50*, 120.

(20)   Binning, G.; Quate, C. F.; Gerber, C. *Phys. Rev. Lett.* **1986,** *12,* 930.

(21)   Putman, C. A. J.; Werf, K. O. v. d.; Grooth, B. G. d.; Hulst, N. F. v.; Greve, J.; Hansma, P. K. *Proc. SPIE-Int. Soc. Opt. Eng.* **1992,** *1639,* 198 *(Scanning Probe Microscopies).*

(22)   Manne, S.; Cleveland, J. P.; Gaub, H. E.; Stucky, G. D.; Hansma, P. K. *Langmuir* **1994,** *10,* 4409.

(23)   Senden, T. J.; Drummond, C. J.; Kekicheff, P. *Langmuir* **1994,** *10,* 358.

(24)   Towns, J. K.; Regnier, F. E. *Anal. Chem.* **1991,** *63,* 1126.

(25)   Yeung, K. K.-C.; Lucy, C. A. *Anal. Chem.* **1997,** *69,* 3435.

(26)   Cordova, E.; Gao, J.; Whitesides, G. M. *Anal. Chem.* **1997,** *69,* 1370.

(27)   Schwer, C.; Kenndler, E. *Anal. Chem.* **1991,** *63,* 1801.

(28)   Underwood, A. L.; Anacker, E. W. *J. Colloid Interface Sci.* **1987,** *117,* 242.

(29)   Subramanian, V.; Ducker, W. A. *Langmuir* **2000,** *16,* 4447.

(30)   Velegol, S. B.; Fleming, B. D.; Biggs, S.; Wanless, E. J.; Tilton, R. D. *Langmuir* **2000,** *16,* 2548.

(31)   Patrick, H. N.; Warr, G. G.; Manne, S.; Aksay, I. A. *Langmuir* **1999,** *15,* 1685.

(32)   Israelachvili, J. N. *Intermolecular and Surface Forces,* 2nd ed.; Academic Press: New York, 1991.

(33)   Blake, C. C. F.; Koenig, D. F.; Mair, G. A.; North, A. C. T.; Phillips, D. C.; Sarma, V. R. *Nature* **1965,** *206,* 757.

(34)   Yeung, K. K.-C.; Kiceniuk, A. G.; Li, L. *J. Chromatogr. A* **2001,** *931,* 153.

CHAPTER FIVE. Phospholipid Bilayer Coatings for the Separation of Proteins in Capillary Electrophoresis*

In Chapter Two I showed that a surfactant with a zwitterionic head group formed a capillary coating that allowed for the separation of both cationic and anionic proteins with minimal protein adsorption to the wall. Chapter Four demonstrated that a surfactant with a double-chained tail provided a highly stable coating at the wall with the most complete surface coverage. This chapter discusses the use of phosphatidylcholines (essentially double-chained, zwitterionic surfactants) for wall coatings in capillary electrophoresis.

5.1 Introduction

The bilayer structures of double-chained surfactants are attractive for wall coatings in capillary electrophoresis. The flatter and more homogeneous coatings observed with double-chained surfactants translate into greater surface coverage and stability, as seen in Chapter Four. Specifically, prevention of protein adsorption improves and a reproducible electroosmotic flow is achieved using the double-chained surfactant didodecyldimethylammonium bromide (DDAB). Due to its increased stability, DDAB was termed a semi-permanent coating as opposed to a dynamic coating. In comparison, the single-chained surfactant cetyltrimethylammonium bromide (CTAB) does not prevent protein adsorption to the same extent, most likely due to the incomplete surface coverage the coating provides at the capillary wall. Further, the coating was not

---

*A version of this chapter has been published. Cunliffe, J.M.; Baryla, N.E.; Lucy, C.A. *Analytical Chemistry* **2002**, *74*, 776-783.

as stable as indicated by the electroosmotic flow dropping dramatically following removal of surfactant from the buffer (Fig. 4-6).

Although a DDAB-coated capillary can efficiently separate cationic proteins, anionic protein adsorption is inevitable due to the cationic headgroup of DDAB. Holmlin *et al.* have shown that surfaces terminated in zwitterionic groups are resistant to protein adsorption [1]. Further, zwitterionic surfactants have been successful for the separation of both cationic and anionic proteins in capillary electrophoresis [2-5]. For example, as described in Chapter Two, the single-chained zwitterionic surfactant coco(amidopropyl)-hydroxyldimethylsulfobetaine, CAS U, forms a capillary coating that enables protein separations with efficiencies greater than 500 000 plates/m. In Chapter Four, atomic force microscopy (AFM) studies confirmed that the single-chained surfactant, CAS U, aggregates at the capillary wall as spherical micelles and therefore provides incomplete surface coverage. Also, this coating is unstable in the sense that the surfactant must be present in the separation buffer to keep the coating intact and therefore will not be compatible with MS detection.

The class of phospholipids termed phosphatidylcholines are essentially double-chained zwitterionic surfactants. They are often used to form supported phospholipid bilayers (SPB) in the study of biological membranes (see Section 5.2). Since phospholipids have proven to be protein resistant [1, 6-9] and exhibit great structural integrity, this may translate into a more permanent coating at the capillary wall in CE.

Here I present a capillary coating technique for CE using the phospholipid 1,2-dilauroyl-*sn*-phosphatidylcholine (DLPC, Figure 5-1 [10]). DLPC offers the stability of a
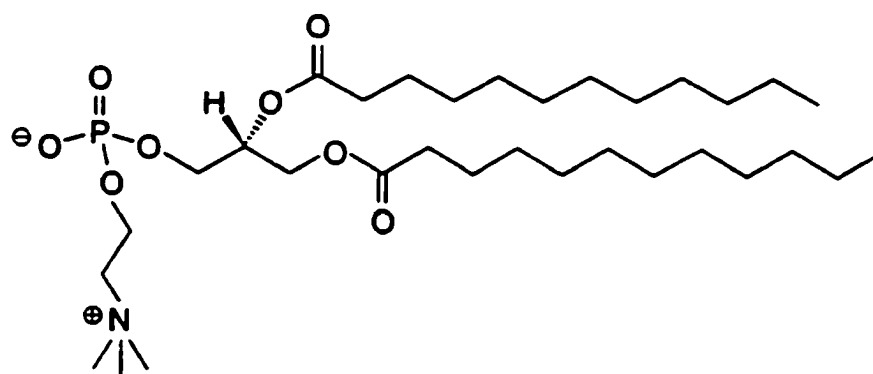
Figure 5-1. Structure of 1,2-dilauroyl-*sn*-phosphatidylcholine (DLPC). Conformation shown based on reference (10).

semi-permanent coating with the ability to separate both cationic and anionic proteins over a wide pH range.

5.2 Background

A phospholipid is defined as a molecule with a polar headgroup (containing a phosphate group) and a double-chained hydrophobic tail. Phospholipids aggregate to form a bilayer where two lipid monolayers combine to form a two-dimensional sheet. Phospholipid bilayers are fundamental to the structure of all biological membranes. Biological membranes define the external boundary of cells and are vital for the survival of living organisms as they regulate the molecular traffic across the boundary. Scientists have used supported phospholipid bilayers (SPB), a lipid bilayer adsorbed on a solid support, to study the physical behaviour of biological membranes and of membrane-bound macromolecules [11, 12].

A schematic identifying the steps in SPB formation is shown in Figure 5-2. When a phospholipid is suspended in water, a cloudy solution is obtained due to the presence of multilamellar vesicles, MLVs (Figure 5-2, step 1). MLVs form when stacks of bilayers become fluid, swell and finally self-close. Once formed, the size of the particles can be reduced by using sonic energy (sonication). Following sonication, small unilamellar vesicles, SUVs (Figure 5-2, step 2) are present in solution [13]. SPB formation is initiated by depositing a SUV solution over a substrate. Vesicle fusion, the formation of supported membranes on substrates from SUVs, is currently the most common and robust way of forming an SPB [14, 15]. Several mechanisms have been reported for the formation of SPB [15-19], all of which report steps of adsorption, fusion, and rupture (Figure 5-2, steps
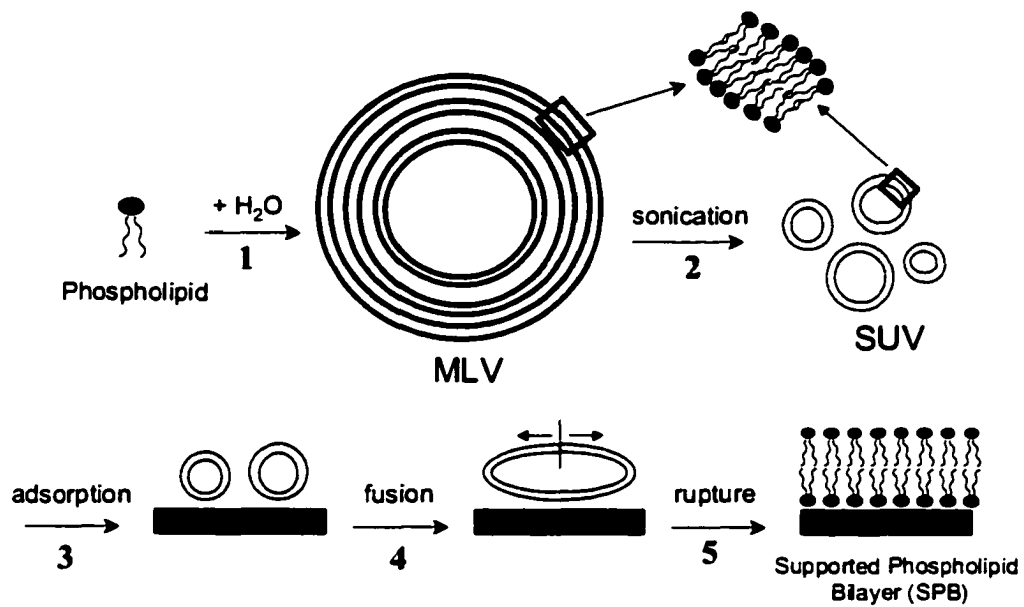
Figure 5-2. Steps in the formation of a supported phospholipid bilayer (SPB). See section 5.2 for details.

3-5). For example Reviakine and Brisson report a three-step process for formation of

SPB by vesicle fusion [19]. Their model of SPB formation involves an initial step of

vesicle adsorption to a surface, followed by fusion, which results in larger vesicles.

Finally, the larger vesicles flatten and rupture, leading to the formation of a single bilayer

adsorbed onto the surface. SPB formation is dependent on a number of factors including

lipid type, buffer, vesicle size, lipid concentration, and the presence or absence of Ca^{2+} [19,20]. Some of these factors have implications in the formation of capillary wall coatings

using phospholipids (see Section 5.4.1).

5.3 Experimental

5.3.1 Apparatus

Capillary electrophoresis was performed on a P/ACE MDQ Capillary

Electrophoresis System (Beckman Instruments, Fullerton, CA, USA) equipped with a UV

absorbance detector. Data acquisition and control were performed using P/ACE Station

software (Beckman) for Windows 95 on a 300 MHz IBM personal computer.

Efficiencies were calculated with the P/ACE Station software using the peak width at half

height method. All electropherograms were baseline subtracted due to a problem with

the P/ACE MDQ capillary cartridges. The untreated fused silica capillaries (Polymicro

Technologies, Phoenix, AZ, USA) had an inner diameter of 51 μm and an outer diameter

of 360 μm.

AFM images were obtained with a Nanoscope III (Digital Instruments, Santa

Barbara, CA, USA) equipped with a fluid cell. Oxide-sharpened silicon nitride

cantilevers (Digital Instruments, Santa Barbara, CA, USA) with nominal spring constants

of 0.06 N/m were used. The AFM substrates used were polished fused silica plates

(Heraeus Amersil Inc., Duluth, GA, USA). The silica substrates were cleaned by heating

in hot concentrated sulfuric acid overnight followed by rinsing thoroughly with water.

5.3.2 Chemicals

All solutions were prepared with Nanopure ultrapure water (Barnstead, Chicago,

IL, USA). Ultra Pure Tris (Tris(hydroxylmethyl)aminonmethane, Schwarz/Mann

Biotech) and CHES (2-(N-cyclohexylamino)ethanesulfonic acid, 99%, Sigma) were used

to prepare buffers. Tris buffers were adjusted to pH 3 or 7.4 using reagent grade

hydrochloric acid (Anachemia). CHES buffers were adjusted to pH 10 using reagent

grade sodium hydroxide (BDH). The phospholipids 1,2-dilauroyl-sn-

phosphatidylcholine (DLPC), 1,2-didecanoyl-sn-phosphatidylcholine (DDPC), and 1,2-

dimyristoyl-sn-phosphatidylcholine (DMPC) (all from Sigma) were used as received.

The aggregation process of the phospholipids was accelerated by the addition of calcium

chloride dihydrate (Molecular Biology grade, Sigma). Mesityl oxide (Aldrich) was used

as the neutral EOF marker. The proteins lysozyme (chicken egg white), cytochrome-c

(bovine heart), ribonuclease-A (bovine pancreas), α-chymotrypsinogen A (bovine

pancreas), insulin chain A oxidized (bovine insulin), trypsin inhibitor (soybean), and α-

lactalbumin (bovine milk) were used as received from Sigma. Benzyl alcohol (99%,

Aldrich) and benzoic acid (reagent grade, BDH) were used as internal standards for the

cationic and anionic protein recovery studies, respectively. Fresh chicken egg samples

were purchased from a local supermarket.

5.3.3 Preparation of solutions containing phospholipids

Preparation of the phospholipid solutions involved the addition of 20 mM $CaCl_2$ to the buffer, followed by the addition of the phospholipid. Once all of the reagents were combined, the solution was sonicated (Bransonic 220, Shelton, CT, USA) for 10 min periods. Between each 10-min period there was a 10 min "rest" interval where the solution was stirred at room temperature to cool [15]. This sonicate/stir cycle was repeated about 3 times or until the solution was clear. Solutions containing phospholipids were stored and used within 5 days. Migration time reproducibility and efficiency of protein separations were compromised after this period of time.

5.3.4 EOF measurements

New 50 cm (40 cm to the detector) capillaries were used for all coating studies. Each new capillary was pretreated with 0.1 M NaOH for 5 minutes (20 psi), followed by Nanopure water for 5 minutes (20 psi). Prior to each injection a solution of 0.1 mM DLPC in 20 mM Tris-HCl pH 7.4 buffer containing 20 mM $CaCl_2$ was rinsed through the capillary (20 psi) for 2 minutes. Mesityl oxide was hydrodynamically injected as the neutral EOF marker (0.5 psi for 3 seconds). A constant voltage of -20 kV (a negative voltage as the EOF was reversed due to the Ca^{2+} in the separation buffer) was applied and detection was at 254 nm. The capillary was thermostated to 25 °C. This procedure was repeated until a stable EOF was achieved (and hence the capillary was completely coated).

Once the coating procedure was complete, the capillary was rinsed with buffer (without calcium and phospholipid) for 1-minute intervals to determine the coating

stability. The strength of the EOF was measured after each 1-minute rinse as an indirect measure of the coating stability upon high-pressure rinsing and applied voltage.

Two methods were used to calculate the electroosmotic mobility (μ_{EOF}). When the μ_{EOF} was greater than 1.0×10^{-4} cm^2/Vs, a single injection method was used as described in Section 1.1.5, where mesityl oxide was directly injected and a constant voltage was applied. However, when μ_{EOF} is smaller than 1.0×10^{-4} cm^2/Vs, the above method was not used because migration times are very long. The method of Williams and Vigh [21] was implemented and is discussed in detail in Section 2.2.3. The first mesityl oxide marker was injected using low pressure (0.5 psi) for 3.0 s. This band was pushed through the capillary for 2 min using low pressure (0.5 psi). The second mesityl oxide marker was then introduced by an identical low-pressure injection and both markers pushed through the capillary for 2 min using 0.5 psi pressure. A constant voltage of 15 kV was applied for 3 min causing the 2 markers to move within the capillary. A third marker was then injected and all three bands were pushed to the detector using 0.5 psi pressure. Detection was at 254 nm.

5.3.5 Protein separations

A new capillary (L_d=40 cm, L_t=50 cm) was initially rinsed with 0.1 M NaOH (5 minutes, 20 psi) and Nanopure water (5 minutes, 20 psi). It was then coated with 0.1 mM DLPC in 20 mM Tris-HCl pH 7.4 buffer containing 20 mM $CaCl_2$ for 20 minutes (20 psi). The capillary was rinsed with 20 mM Tris-HCl pH 7.4 buffer (1 min, 20 psi) to flush excess phospholipid and calcium from the capillary before protein samples were introduced. All protein mixtures (0.1 mg/mL in water) were injected for 3 seconds at 0.5 psi. Separation of proteins occurred in 20 mM Tris-HCl pH 7.4 buffer void of calcium

and phospholipid. The applied voltage was 20 kV (+20 kV for cationic protein mixtures, -20 kV for anionic protein mixtures). Protein detection was performed at 214 nm. Between runs the capillary was rinsed with 0.1 mM DLPC in 20 mM Tris-HCl pH 7.4 buffer containing 20 mM $CaCl_2$ (5 min, 20 psi) followed by 20 mM Tris-HCl pH 7.4 (1 min, 20 psi). For the different pH conditions and different phospholipids, the same procedure was used with the appropriate buffer substitutions.

Migration time reproducibility was determined by performing 16 replicate injections on 3 different days. A variation of the method of Towns and Regnier [22] was used for protein recovery studies [5]. A new 30-cm (20 cm to the detector) capillary was used for the study. Six replicate injections of a protein mixture were performed as previously described (total distance proteins travel to the detector is 20 cm). The 10-cm portion of the capillary was then used for the second set of 6 protein separations. For the cationic proteins injection was from the outlet vial, the rinses were adjusted to flow from the outlet vial to the inlet vial, and a negative voltage was applied. These settings allowed the proteins to travel 10 cm to the detector (from the outlet to the inlet). An internal standard (benzyl alcohol for cationic proteins, benzoic acid for anionic proteins) was used to correct for injection volume variation. The percent recoveries of the proteins were determined by comparing the peak area between the long and short portions of the capillary.

5.3.6 Egg white protein analysis

A new capillary (L_d=40 cm, L_t=50 cm) was pretreated and coated with DLPC as described in Section 5.3.5. Egg white was diluted with 20 mM Tris-HCl pH 7.4 buffer in a 1:20 ratio and filtered through a Millex-HA 0.45 μm membrane (Millipore, Bedford,

MA, USA) before use. Egg white samples were injected for 3 seconds at 0.5 psi. Separation was performed in 20 mM Tris-HCl pH 7.4 buffer void of calcium and phospholipid. The applied voltage was 20 kV (+20 kV for lysozyme analysis, -20 kV for ovalbumin analysis). Detection was at 214 nm.

5.3.7 AFM imaging

Contact AFM images were captured in height mode at 23°C. Images of the fused silica surface in buffer were captured in order to compare the surface before and after phospholipid was added. DDPC (0.1 mM), DLPC (0.1 mM) and DMPC (0.1 mM) dispersions were prepared in 20 mM Tris-HCl buffer of pH 7.4 containing 20 mM $CaCl_2$. A 50 µL droplet of phospholipid solution was pipetted onto the silica substrate and allowed to sit for 20 min. The excess phospholipid and calcium was removed by replacing the droplet liquid with 20 mM Tris-HCl buffer by pipetting off the original drop and pipetting 50 µL of buffer onto the silica substrate. Integral and proportional gains were set to 0.75 and 1.0 respectively, while scan rates were set at 7.63 Hz. To eliminate drift before imaging, the scanner was left scanning over a 10-μm^2 area for 1 hour. After this time period, the tip was allowed to barely touch the surface, then the voltage was increased in small increments until a clear image was obtained. The imaging force was always less than 1 nN. A 5 µm x 5 µm image was captured. Then the scan size was reduced to 1 µm x 1 µm, and the coating in this region was scraped off by applying an excessive force (~100 nN) at fast scan rates (61 Hz). The 5 µm x 5 µm area was then imaged again.

5.4 Results and Discussion

5.4.1 Coating time and stability of DLPC

A capillary was coated by rinsing a DLPC solution through the capillary with high pressure. The EOF was used as an indirect measure of the completeness of the coating. The capillary was considered completely coated (refers to maximum coverage and is not necessarily 100%) when the magnitude of the EOF became constant, even after additional rinsing of the capillary with DLPC solution. Figure 5-3 shows that 0.1 mM DLPC in a pH 7.4 buffer of 20 mM $CaCl_2$ and 20 mM Tris-HCl requires no more than 4 minutes of high-pressure rinsing to obtain a constant EOF, and hence to coat the capillary wall. After 4 minutes of coating, the EOF remains constant at -1.4×10^{-4} cm^2/Vs. To ensure the capillary was always completely coated, new capillaries were coated for at least 20 minutes prior to use.

The weakly reversed EOF in Figure 5-3 is consistent with the analogy between electrostatic ion chromatography retention [23] and the EOF generated by zwitterionic coatings reported in Chapter Two. Hu et al. have demonstrated that divalent cations such as Ca^{2+} are retained by electrostatic ion chromatography columns prepared using N-dodecylphosphocholine, a single tailed analog of DLPC [24]. Thus, the weakly reversed EOF in Figure 5-3 results from the retention of Ca^{2+} by the DLPC coating on the walls of the capillary.

In the absence of Ca^{2+} in the coating buffer (and using a phosphate buffer), the time required to coat the capillary was excessively long (~ 75 minutes) as shown in Figure 5-4. The addition of Ca^{2+} to a solution containing phospholipids has been demonstrated to dramatically increase the rate of SPB formation [18, 19, 25-27]. The calcium
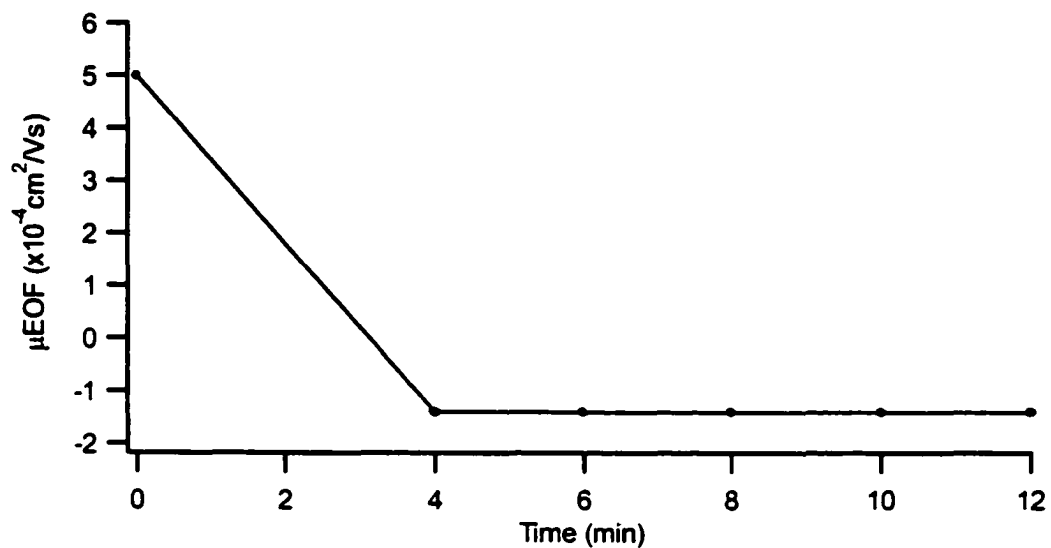
Figure 5-3. Time required to achieve a stable EOF by rinsing a capillary with 0.1 mM DLPC in 20 mM Tris-HCl pH 7.4 buffer containing 20 mM $CaCl_2$. Experimental conditions: 50-cm capillary (40 cm to detector); temperature, 25°C; separation buffer, 0.1 mM DLPC in 20 mM Tris-HCl pH 7.4 containing 20 mM $CaCl_2$; applied voltage, -20 kV; direct UV detection at 254 nm. EOF was measured after each 2-minute rinse until EOF became stable. Line through points acts only as a guide to the eye.

μEOF (x10⁻⁴cm²/Vs)

Time (min)
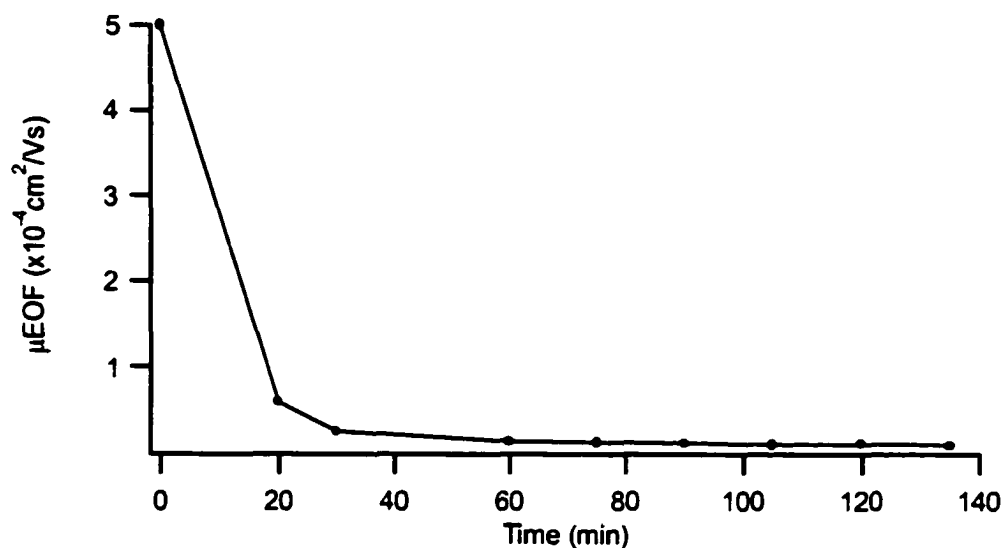
Figure 5-4. Time required to achieve a stable EOF by rinsing a capillary with 0.1 mM DLPC in 10 mM phosphate buffer, pH 7. Experimental conditions: 50-cm capillary (40 cm to detector); temperature, 25°C; separation buffer, 0.1 mM DLPC in 10 mM phosphate pH 7; applied voltage, +15 kV; direct UV detection at 254 nm. EOF was measured after each 15-minute rinse until EOF became stable. Line through points acts only as a guide to the eye.

ion is a strong fusogenic agent, which promotes the fusion of cells and vesicles [19, 28].

Further, it has been suggested that an increase in intracellular Ca^{2+} initiates fusion

between biological membranes [29]. Also documented is the effect of buffer on SPB

formation. Rapuano and Carmona-Ribeiro examined SPB formation on silica using

different buffers [20]. The authors concluded that the use of Tris buffer led to bilayer

formation over the largest surface area. They speculated that protonated amino groups on

Tris would be attracted to the negatively charged silanols at the silica surface.

Subsequently, the phosphate group of the phospholipid could form a hydrogen bond

bridge with the hydroxyl groups of Tris [20]. Thus, Tris buffers containing Ca^{2+} were used

for coating the capillaries with DLPC unless otherwise noted.

The stability of the wall coating in the absence of DLPC can be determined by

monitoring the EOF [30]. The capillary was first coated with DLPC as described in the

Experimental Section. The excess DPLC and Ca^{2+} were then rinsed from the capillary

with a series of 1-minute high-pressure rinses of Tris-HCl pH 7.4 buffer. Figure 5-5

shows the EOF observed after each rinse. Prior to the rinses with buffer void of DLPC

and Ca^{2+}, the EOF was weakly reversed, as described above. The EOF rapidly changes

from weakly reversed in the presence of Ca^{2+} to weakly forward ($+0.22 \times 10^{-4}$ cm^2/Vs).

This is equivalent to the EOF observed after coating a capillary with 0.1 mM DLPC

without Ca^{2+} for 75 min (Figure 5-4). After the first rinse, the EOF was stable over 35

runs (35 minutes of rinsing and 105 minutes of high voltage) as seen in Figure 5-5. The

EOF only slightly increased from $+0.22 \times 10^{-4}$ cm^2/Vs (first high-pressure rinse) to $+0.5 \times$

10^{-4} cm^2/Vs (thirty-fifth high-pressure rinse). This is comparable to what is observed

when the stability of the DLPC coating formed without calcium is measured. These
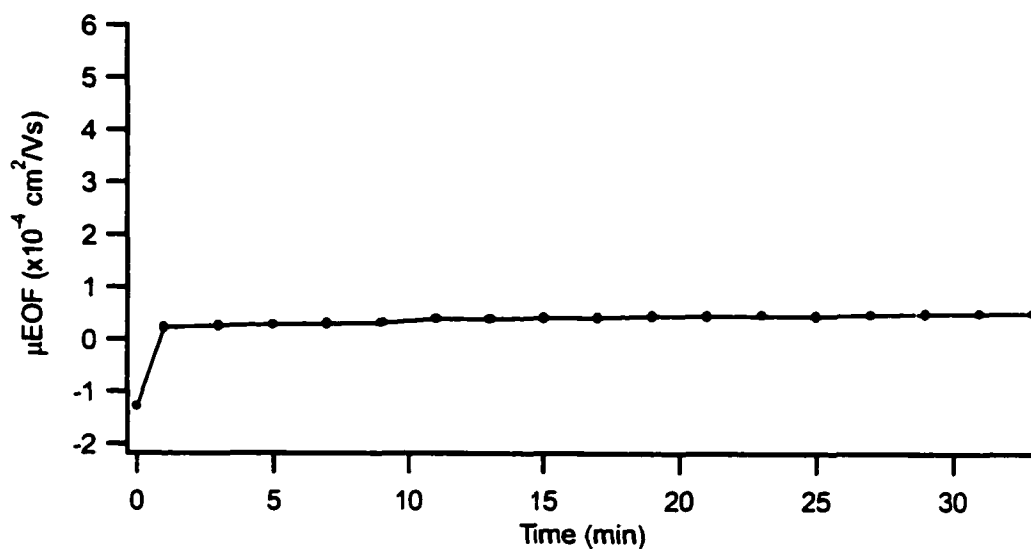
Figure 5-5. Coating stability of DLPC as reflected by the EOF as a function of time. Experimental conditions: 50-cm capillary (40 cm to detector); temperature, 25°C; separation buffer, 20 mM Tris-HCl pH 7.4; applied voltage, +15 kV (slow EOF, 3 peak injection method used, see section 5.3.4); direct UV detection at 254 nm. EOF measured after 1-min rinses with 20 mM Tris-HCl buffer. Line through points acts only as a guide to the eye.

results demonstrate that DLPC generates a semi-permanent coating, similar to the double chain surfactant DDAB. DLPC can therefore be removed from the electrophoretic buffer prior to performing a separation. Thus, unwanted buffer additive-analyte interactions that can deteriorate the separation are eliminated and detection schemes that are compromised in the presence of surfactants may be applied. For example, with DLPC in the separation buffer, numerous spikes in the electropherogram are present which interfere with analyte peaks.

5.4.2 Protein separations using a semi-permanent DLPC wall coating

When DLPC and calcium are removed from the buffer, the EOF generated in the capillary at pH 7.4 is suppressed ($\sim$ +0.3x10^{-4} cm^2/Vs). Thus, cationic analytes can be separated using a positive polarity and anionic analytes can be separated using a negative polarity. Both cationic and anionic proteins are efficiently separated using DLPC as a capillary wall coating at pH 7.4. Figure 5-6 shows the separation of 4 cationic proteins: lysozyme, cytochrome-c, ribonuclease-A, and α-chymotrypsinogen A in under 20 minutes. In theory, CE is capable of achieving protein efficiencies of 1-2 million plates/m. Efficiencies of the protein peaks obtained using a DLPC-coated capillary were between 780 000 plates/m and 1.4 million plates/m. These values exceed what has previously been achieved using a permanently coated capillary and are comparable to efficiencies obtained using dynamic, surfactant-based coatings as shown in Chapters Two and Four. Commonly used permanent coatings such as polyacrylamide give efficiencies of 50 000 to 600 000 plates/m for cationic proteins [31,32] while dynamic coatings have yielded efficiencies nearing 1 million plates/m. When performing protein separations
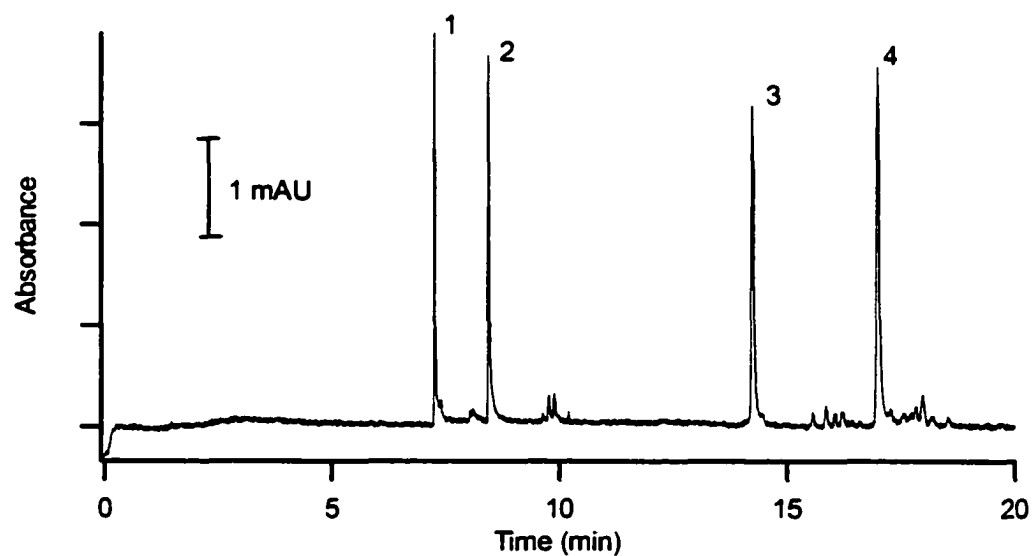
Figure 5-6. Separation of cationic proteins at pH 7.4. Peaks, (1) lysozyme, (2) cytochrome c, (3) ribonuclease A, (4) α-chymotrypsinogen A. Experimental conditions: 50-cm capillary (40 cm to detector); temperature, 25°C; separation buffer, 20 mM Tris-HCl at pH 7.4; sample, 0.1 mg/ml protein mixture in water; applied voltage, +20 kV; direct UV detection at 214 nm. Coating procedure: 20 min rinse with 0.1 mM DLPC in 20 mM Tris-HCl pH 7.4 buffer containing 20 mM $CaCl_2$ followed by a 1 min rinse with separation buffer to remove excess phospholipid; between runs phospholipid rinse time was shortened to 5 min.

using a DLPC-coated capillary formed without calcium in the buffer, efficiencies of up to only 200 000 plates/m were achieved.

The separation of 3 anionic proteins: insulin chain A, trypsin inhibitor, and α-lactalbumin at pH 7.4 using a DLPC-coated capillary is shown in Figure 5-7. Efficiencies of the anionic protein peaks ranged between 150 000 plates/m and 310 000 plates/m. Although lower than the theoretical 1-2 million plates/m, these efficiencies are consistent, if not superior to the efficiencies obtained with a common method used for anionic protein analysis, namely use of an uncoated capillary [33].

Migration time should be reproducible from run-to-run and from day-to-day if proteins do not adsorb onto the capillary. For the cationic and anionic proteins, the RSD of the migration times were as low as 0.2% (run-to run, n=16) and 2.8% (day-to-day, n=3). Table 5-1 summarizes the peak efficiencies and migration time reproducibilities achieved for the above proteins at pH 7.4.

Protein recovery studies (see Experimental) were conducted for lysozyme, cytochrome-c, ribonuclease-A, α-chymotrypsinogen A, insulin chain A, trypsin inhibitor, and α-lactalbumin at pH 7.4. For the cationic proteins (lysozyme, cytochrome-c, ribonuclease-A, α-chymotrypsinogen A), the recoveries were 64±5%, 76±6%, 83±7%, and 75±7% respectively. Since the recoveries are not quantitative, it is evident that protein adsorption is occurring at the capillary wall. Indeed, the cationic peaks exhibit some tailing (Figure 5-6), which is indicative of protein adsorption. Since the EOF is forward ($+0.3 \times 10^{-4}$ cm^2/Vs), the wall has a slight negative charge, and therefore electrostatic attraction could exist between any uncoated portions of the wall and the cationic proteins. Another possibility is that proteins are interacting with the zwitterionic
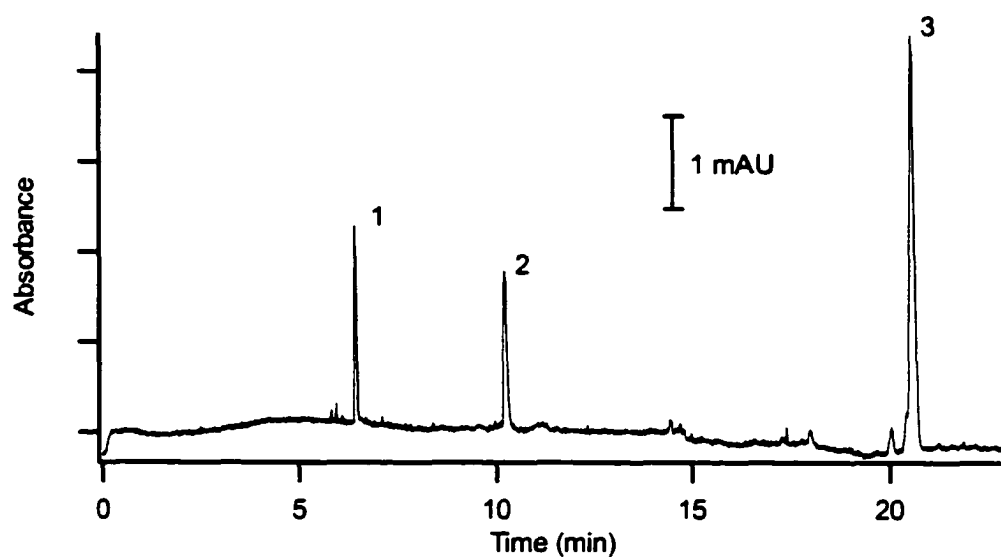
Figure 5-7. Separation of anionic proteins at pH 7.4. Peaks, (1) insulin chain A, (2) trypsin inhibitor, (3) α-lactalbumin. Experimental conditions: 50-cm capillary (40 cm to detector); temperature, 25°C; separation buffer, 20 mM Tris-HCl at pH 7.4; sample, 0.1 mg/ml protein mixture in water; applied voltage, -20 kV; direct UV detection at 214 nm. Coating procedure: 20 min rinse with 0.1 mM DLPC in 20 mM Tris-HCl pH 7.4 buffer containing 20 mM CaCl₂ followed by a 1 min rinse with separation buffer to remove excess phospholipid; between runs phospholipid rinse time was shortened to 5 min.

Table 5-1. Efficiency, migration time reproducibility and recovery of cationic and anionic proteins separated using a DLPC-coated capillary at pH 7.4.

Protein	pI	Efficiency (plates/m)	Migration Time Run-to-Run (%RSD)	Migration Time Day-to-Day (%RSD)	Recovery (%)
lysozyme	11	1 400 000	0.3	4.0	64 ± 5
cytochrome c	9.5	1 000 000	0.3	4.0	76 ± 6
ribonuclease A	9.6	780 000	0.4	4.0	83 ± 7
α-chymotrypsinogen A	8.7	880 000	0.4	3.8	75 ± 7
insulin chain A	3.8	170 000	0.2	3.4	93 ± 7
trypsin inhibitor	5.0	150 000	0.4	3.3	78 ± 6
α -lactalbumin	4.8	310 000	1.3	2.8	92 ± 8

headgroup. Holmlin *et al.* demonstrated that zwitterionic self-assembled monolayers (terminating in the phosphatidylcholine headgroup) prevented protein adsorption substantially more than monolayers terminated in a single charge [1]. They tested lysozyme (cationic) and fibrinogen (anionic) at pH 7.4 for adsorption. However, adsorption of proteins was not completely eliminated at a zwitterionic phosphatidylcholine-terminated surface [1], which is consistent with our protein recovery data.

The anionic proteins also partially adsorb to the capillary wall (again consistent with Holmlin *et al.*'s data [1]), but to a lesser degree than do the cationic proteins. For insulin chain A, trypsin inhibitor, and α-lactalbumin, the recoveries were $93\pm7\%$, $78\pm6\%$, and $92\pm8\%$ respectively. The results of the protein recovery studies are summarized in Table 5-1.

5.4.3 Effect of pH on the DLPC capillary coating

To judge the versatility of the coating, DLPC was tested for its ability to maintain a stable coating and minimize protein adsorption over a wide pH range. The phosphate group of the phosphatidylcholine headgroup has a pKa of approximately 1. Thus, to ensure DLPC will act as a true zwitterion, it is best to work at a pH greater than 3. At pH 3, the capillary wall still carries a slight negative charge as indicated by the positive EOF ($\sim +0.3 \times 10^{-4}$ cm^2/Vs) generated in a bare capillary at this pH. Consequently, cationic proteins adsorb to a bare capillary wall at pH 3 (Section 4.5.6). This indicates that a coating is necessary even when separating proteins at low pH.

EOF is normally quite variable at low pH in a bare capillary [34]. Therefore, a coating would be attractive if it produces a stable EOF at low pH. It required only 5 minutes of high-pressure rinsing of 0.1 mM DLPC in a 20 mM Tris-HCl pH 3 buffer

(containing 20 mM $CaCl_2$) to reach a stable EOF (-1.6 x 10^{-4} cm^2/Vs) and hence coat the capillary wall. The EOF upon rinsing the capillary (1 min) with 20 mM Tris-HCl pH 3 buffer (removing DLPC and calcium) is -1.4 x 10^{-4} cm^2/Vs. The EOF remained constant at this value after 10 minutes of identical rinses (%RSD= 3%, n=10) indicating that DLPC forms a stable coating on the capillary wall at low pH.

A mixture of cationic proteins (lysozyme, cytochrome c, ribonuclease A and α-chymotrypsinogen A) was separated at pH 3 (20 mM Tris-HCl) using a DLPC-coated capillary. Figure 5-8 shows that all four proteins were separated in less than 20 minutes with efficiencies ranging from 560 000 to 1 000 000 plates/m. The migration time RSD for the proteins was less than 1.8% (n=16). Table 5-2 summarizes the efficiency and migration time reproducibility obtained for each of these proteins at pH 3. Separating the anionic proteins insulin chain A, trypsin inhibitor, and α-lactalbumin using a negative voltage would not be practical because they would not be observed in a reasonable time. These proteins have a pI ~ 4 and would migrate very slowly, against the already suppressed EOF.

DLPC was used to coat a capillary at pH 10. 0.1 mM DLPC in 20 mM CHES pH 10 buffer (containing 20 mM $CaCl_2$) required 25 minutes of high-pressure rinsing to achieve a constant EOF of -1.3 x 10^{-4} cm^2/Vs and hence coat the wall as seen in Figure 5-9A. The coating time is much slower than was observed at pH 3 and 7.4, most likely due to the fact that CHES rather than Tris buffer was used (CHES has a better buffering capacity at pH 10). As discussed above, phospholipid dissolved in Tris buffer leads to improved bilayer formation over a silica surface [20]. Upon rinsing with CHES pH 10.0 buffer for 1 minute, the EOF changes to +1.1 x 10^{-4} cm^2/Vs. As seen in Figure 5-9B,
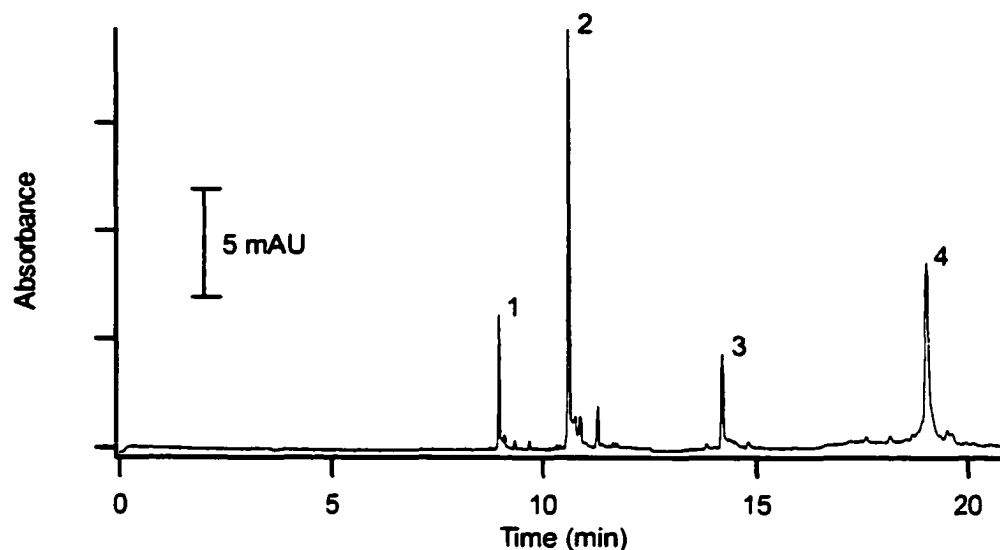
Figure 5-8. Separation of cationic proteins at pH 3. Peaks, (1) cytochrome c, (2) lysozyme, (3) ribonuclease A, (4) α-chymotrypsinogen A. Experimental conditions: 50-cm capillary (40 cm to detector); temperature, 25°C; separation buffer, 20 mM Tris-HCl pH 3; sample, 0.1 mg/ml protein mixture in water; applied voltage, +20 kV; direct UV detection at 214 nm. Coating procedure: 20 min rinse with 0.1 mM DLPC in 20 mM Tris-HCl pH 3 buffer containing 20 mM followed by a 1 min rinse with separation buffer to remove excess phospholipid; between runs phospholipid rinse time was shortened to 5 min.

Table 5-2. Efficiency and migration time reproducibility of proteins separated using a DLPC-coated capillary at pH 3.

Protein	Efficiency (plates/m)	Migration Time Run-to-Run (%RSD)
lysozyme	1 000 000	1.0
cytochrome c	1 000 000	0.7
ribonuclease A	790 000	1.3
α–chymotrypsinogen A	560 000	1.8
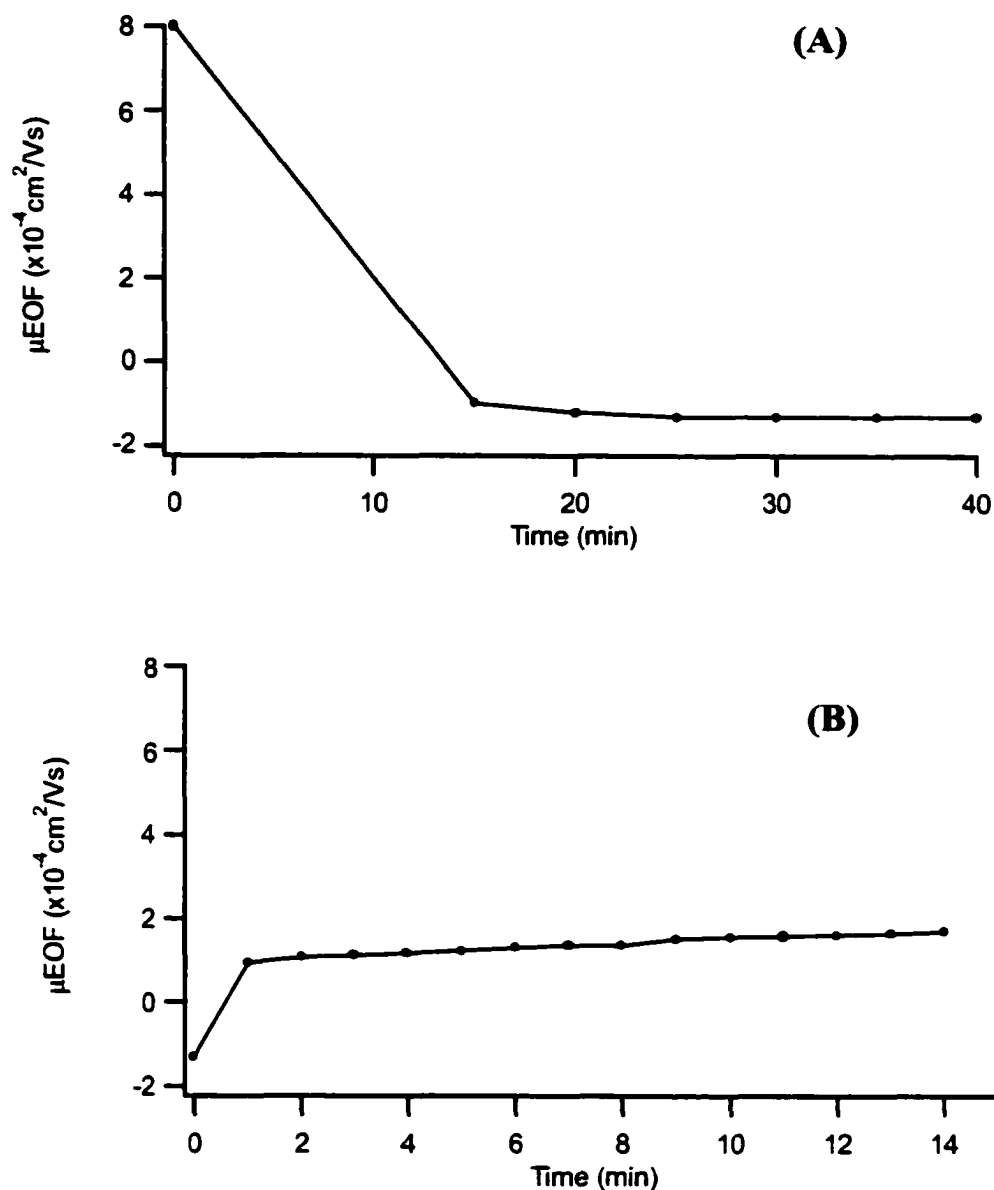
Figure 5-9. (A) Time required to achieve a stable EOF by rinsing a capillary with 0.1 mM DLPC in 20 mM CHES pH 10 buffer containing 20 mM CaCl$_2$. Experimental conditions as in Figure 5-3. (B) Coating stability of DLPC at pH 10 as reflected by the EOF as a function of time. Experimental conditions as in Figure 5-5. Lines through points act only as a guide to the eye.

upon 15 minutes of additional rinsing the EOF remains constant verifying the coating stability.

Figure 5-10 shows the separation of a mixture of three anionic proteins (insulin chain A, trypsin inhibitor, and α-lactalbumin). The proteins were separated in under 20 min with efficiencies up to 360 000 plates/m. The migration times for insulin chain A, trypsin inhibitor, and α-lactalbumin also proved to be quite reproducible over 16 runs, yielding RSD values less than 2.3%. Efficiencies and migration time RSD of the proteins using DLPC at pH 10 are summarized in Table 5-3. As with the anionic proteins at pH 3, the cationic proteins lysozyme, cytochrome c, ribonuclease A, and α-chymotrypsinogen A were not separated at pH 10. This would not be practical since they all have a pI ~ 9 and would approximately migrate with the suppressed EOF, making the separation time extremely long.

5.4.4 Analysis of egg white proteins

The major protein components of egg white are lysozyme (pI~11) and ovalbumin (pI~5). At biological pH (7.4), lysozyme is positively charged while ovalbumin is negatively charged. Thus separation of both proteins on a bare capillary is impossible. CE methods used for the analysis of egg white proteins involve working with high salt buffers (e.g. >300 mM phosphate) at neutral [35] or high pH [36], or with low pH buffer conditions using polyethylene glycol additives [37]. Efficiencies were never reported for the protein peaks in these previously reported methods. However, on the basis of their electropherograms, it is estimated that the efficiencies were less than 10 000 plates/m. Using a DLPC-coated capillary at pH 7.4, lysozyme and ovalbumin were analyzed in an egg white sample. Figure 5-11 shows the electropherograms for analysis of A)
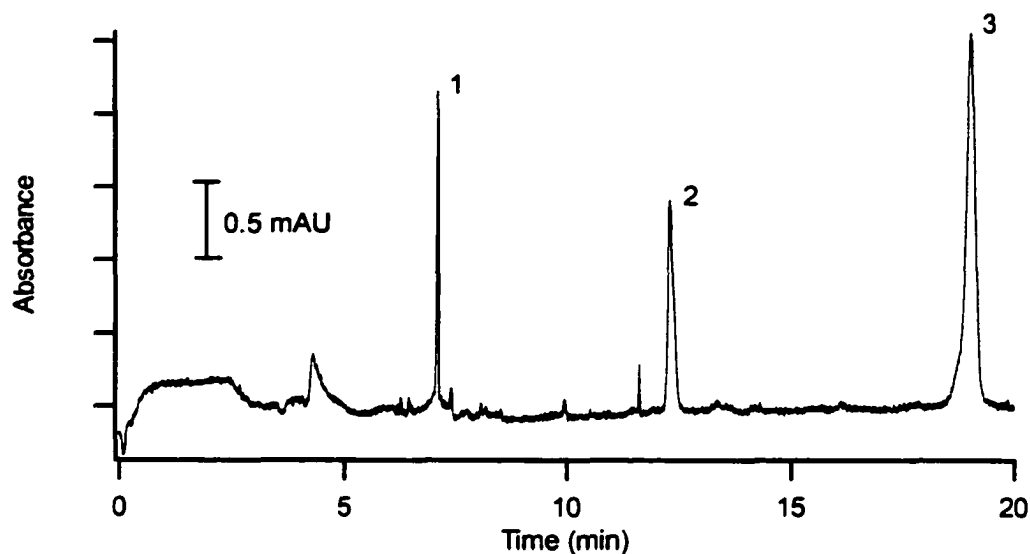
Figure 5-10. Separation of anionic proteins at pH 10. Peaks, (1) insulin chain A (2) trypsin inhibitor (3) α-lactalbumin. Experimental conditions: 50-cm capillary (40 cm to detector); temperature, 25°C; separation buffer, 20 mM CHES pH 10; sample, 0.1 mg/ml protein mixture in water; applied voltage, -20 kV; direct UV detection at 214 nm. Coating procedure: 20 min rinse with 0.1 mM DLPC 20 mM CHES pH 10 buffer containing 20 mM CaCl₂, followed by a 1 min rinse with separation buffer to remove excess phospholipid; between runs phospholipid rinse time was shortened to 5 min.

Table 5-3. Efficiency and migration time reproducibility of proteins separated using a DLPC-coated capillary at pH 10.

Protein	Efficiency (plates/m)	Migration Time Run-to-Run (%RSD)
insulin chain A	360 000	0.9
trypsin inhibitor	96 000	1.1
α -lactalbumin	100 000	2.3
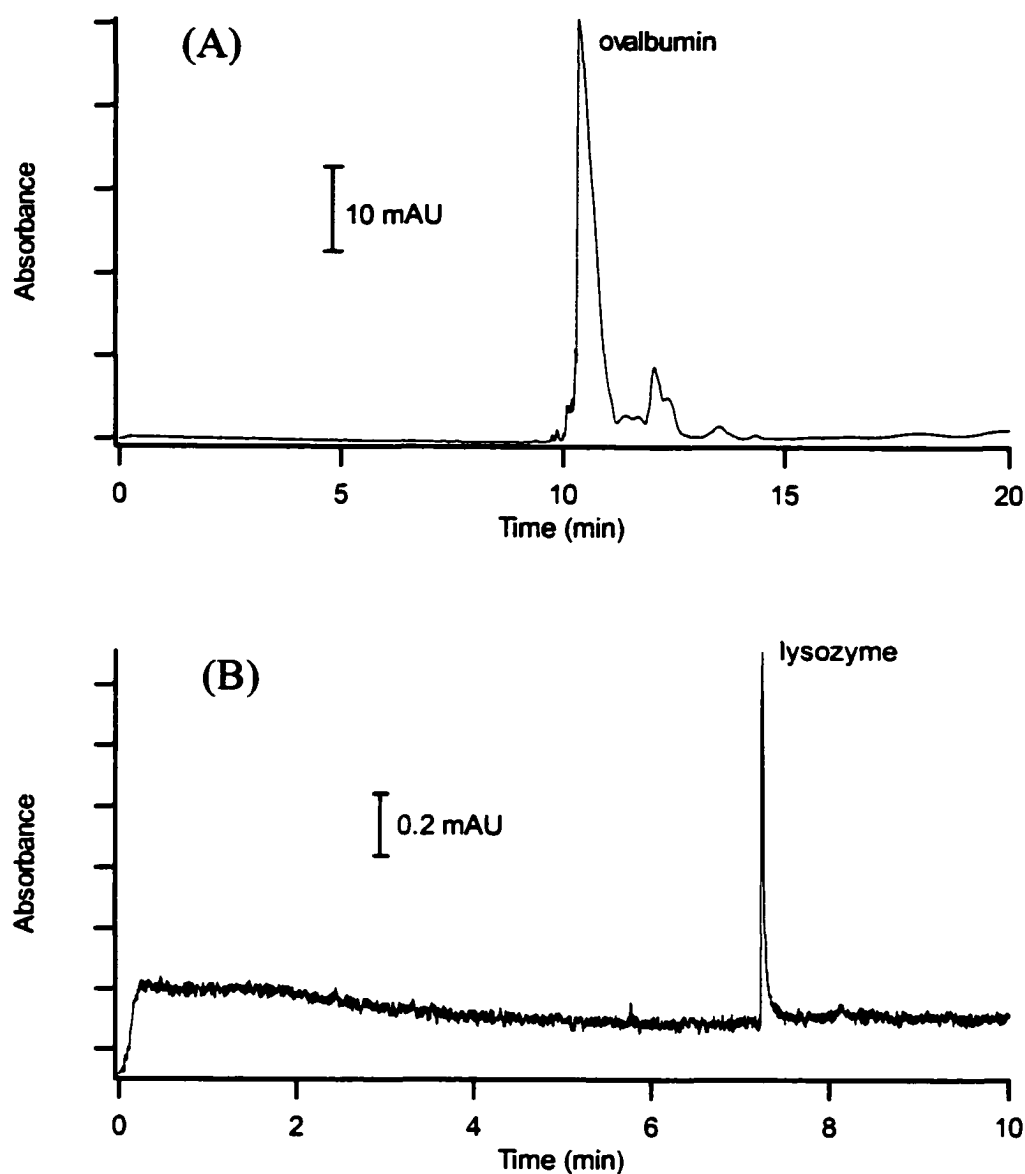
Figure 5-11. (A) Analysis of ovalbumin in an egg white sample. (B) Analysis of lysozyme in an egg white sample. Experimental conditions: 50-cm capillary (40 cm to detector); temperature, 25°C; separation buffer, 20 mM Tris-HCl at pH 7.4; sample, 1:20 diluted egg white in buffer; applied voltage, A)-20 kV, B)+20 kV; direct UV detection at 214 nm. Coating procedure: 20 min rinse with 0.1 mM DLPC in 20 mM Tris-HCl pH 7.4 buffer containing 20 mM CaCl₂ followed by a 1 min rinse with separation buffer to remove excess phospholipid; between runs phospholipid rinse time was shortened to 5 min.

ovalbumin (negative voltage applied) and B) lysozyme (positive voltage applied).

Identities of the proteins were confirmed by injecting standards. The efficiency of the

ovalbumin peak was 15 000 plates/m while the efficiency of the lysozyme peak was 750

000 plates/m. After three runs, the lysozyme peak degraded, indicating adsorption was

occurring onto the wall. This is consistent with the protein recovery data obtained for

lysozyme at pH 7.4 (64% recovery).

5.4.5 DLPC analogs for use as capillary coatings

The C_{10} analog of DLPC, 1,2-didecanoyl-*sn*-phosphatidylcholine (DDPC),

required 5 min to achieve a stable EOF in a pH 7.4 Tris-HCl buffer containing 20 mM

calcium. However, upon rinsing the capillary with 20 mM Tris-HCl pH 7.4 buffer in 1-

minute intervals, the EOF rapidly increased. This demonstrates that the coating desorbs

from the wall after each rinse. Thus, DDPC acts more like a dynamic coating (single-

chained surfactants, *e.g.* CTAB) than a semi-permanent coating (double-chained

surfactants, *e.g.* DDAB (Chapter Four) and DLPC (Section 5.4.1)), as a stable EOF is

achieved only when phospholipid is present in the separation buffer. Since the CVC of a

double-chained surfactant increases by 100-fold with removal of 2 carbon units from

each hydrocarbon chain (from C_{12} to C_{10}), the coating loss is most likely due to an

increase in water solubility. The poor coating that DDPC provides at the capillary wall

was confirmed by attempting a separation of cationic proteins at pH 7.4. The cationic

proteins lysozyme, a-chymotrypsinogen A, cytochrome c, and ribonuclease A completely

adsorbed to the DDPC-coated wall such that no peaks were detected.

The C_{14} analog of DLPC, 1,2-dimyristoyl-*sn*-phosphatidylcholine (DMPC),

performs similarly to its C_{12} counterpart with one difference. DMPC appears to aggregate

in solution more rapidly than DLPC based on the time it takes for a solution to become clear upon sonication. Typically a DLPC solution required 30 min of sonication while a DMPC solution needed only 10 min of sonication to become clear. Aggregation is expected to be more favourable for DMPC as the longer hydrocarbon chain length will promote increased hydrophobic interaction. DLPC can require up to 15 minutes to coat the capillary at pH 7.4 while DMPC never required more than 5 minutes under the same conditions (0.1 mM phospholipid in 20 mM Tris-HCl pH 7.4 buffer containing 20 mM $CaCl_2$). Upon a 1 min high-pressure rinse with 20 mM Tris-HCl pH 7.4 buffer, the EOF was +0.2 x 10^{-4} cm^2/Vs. Rinsing the capillary for an additional 10 minutes only changed the EOF to +0.27 x 10^{-4} cm^2/Vs, indicating the ability to remove excess surfactant from the buffer and still achieve a stable EOF. A DMPC-coated capillary was able to separate lysozyme, cytochrome c, ribonuclease A, and α-chymotrypsinogen A with efficiencies as high as 1.3 million plates/m and migration time RSD less than 1.0% (n=16). Anionic proteins (insulin chain A, trypsin inhibitor, and α-lactalbumin) were separated with efficiencies as high as 300 000 plates/m and migration time RSD values lower than 1.1% (n=16). These separations are shown in Figure 5-12A (cationic proteins) and 5-12B (anionic proteins). Since DMPC displays similar behavior and performance to DLPC at pH 7.4, it is assumed that it will also be an effective and stable coating for enabling the separation of highly adsorbing proteins over a wide range of pH values.

5.4.6 AFM imaging of phospholipid analogs

To confirm the presence or absence of a phospholipid coating on the capillary surface during CE, I employed AFM imaging to study phospholipid adsorption in the electrophoretic buffer used for our separations (Tris-HCl, pH 7.4). Fused silica plates
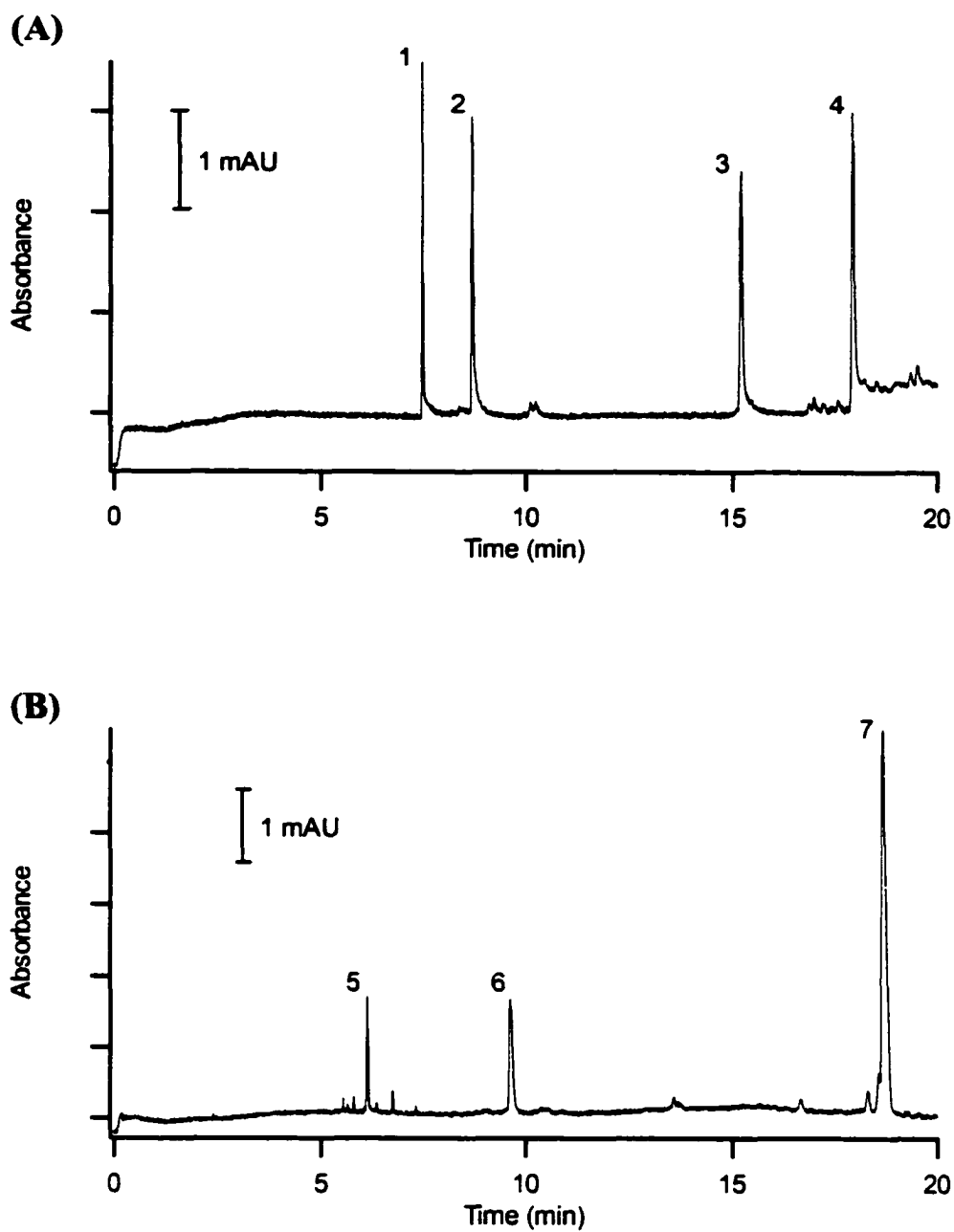
Figure 5-12. Separation of (A) cationic proteins and (B) anionic proteins at pH 7.4 using a DMPC-coated capillary. Peaks, (1) lysozyme, (2) cytochrome c, (3) ribonuclease A, (4) α-chymotrypsinogen A, (5) insulin chain A, (6) trypsin inhibitor, and (7) α-lactalbumin. Experimental conditions as in Figure 5-6 (cationic proteins) and Figure 5-7 (anionic proteins).

were used as the imaging substrate to mimic the inside wall of a capillary. The silica surface was first imaged after phospholipid adsorption. A 1-μm square hole was then scraped in the coating and the surface re-imaged. Figure 5-13 shows the AFM images of (A) 0.1 mM DDPC-, (B) 0.1 mM DLPC-, and (C) 0.1 mM DMPC-coated silica after scraping off a small square with the AFM tip. In Figure 5-13A, a flat surface is observed similar to the image seen for silica imaged in buffer without phospholipid. There is no evidence of a dark square (removed area of coating) indicating that DDPC did not coat the silica surface. This was expected since the EOF data presented in section 5.4.5 showed that DDPC (C_{10} analog) did not form a stable coating at the capillary wall. Figure 5-13B (DLPC, C_{12}) shows a dark square with dimensions of roughly 1 μm x 1 μm. This dark square corresponds to the area of the coating scraped off with the AFM tip. A similar image is observed for DMPC (C_{14}), shown in Figure 5-13C. The measured height of the phospholipid coating is roughly 2 nm for DMPC and DLPC. This does not correspond to the height of a bilayer (~ 4 nm). It is possible that the AFM tip was too weak to penetrate the entire layer and scrape right down to the silica surface. An AFM tip with a greater spring constant was not investigated.

5.5 Conclusions

The phospholipid DLPC (C_{12}; essentially a double-chained, zwitterionic surfactant) forms a stable coating at the capillary wall that effectively suppresses the EOF and prevents the adsorption of both cationic and anionic proteins over the pH range of 3 to 10. The coating is semi-permanent in nature, meaning that excess phospholipid can be removed from the electrophoretic buffer prior to separation. The C_{10} analog of DLPC
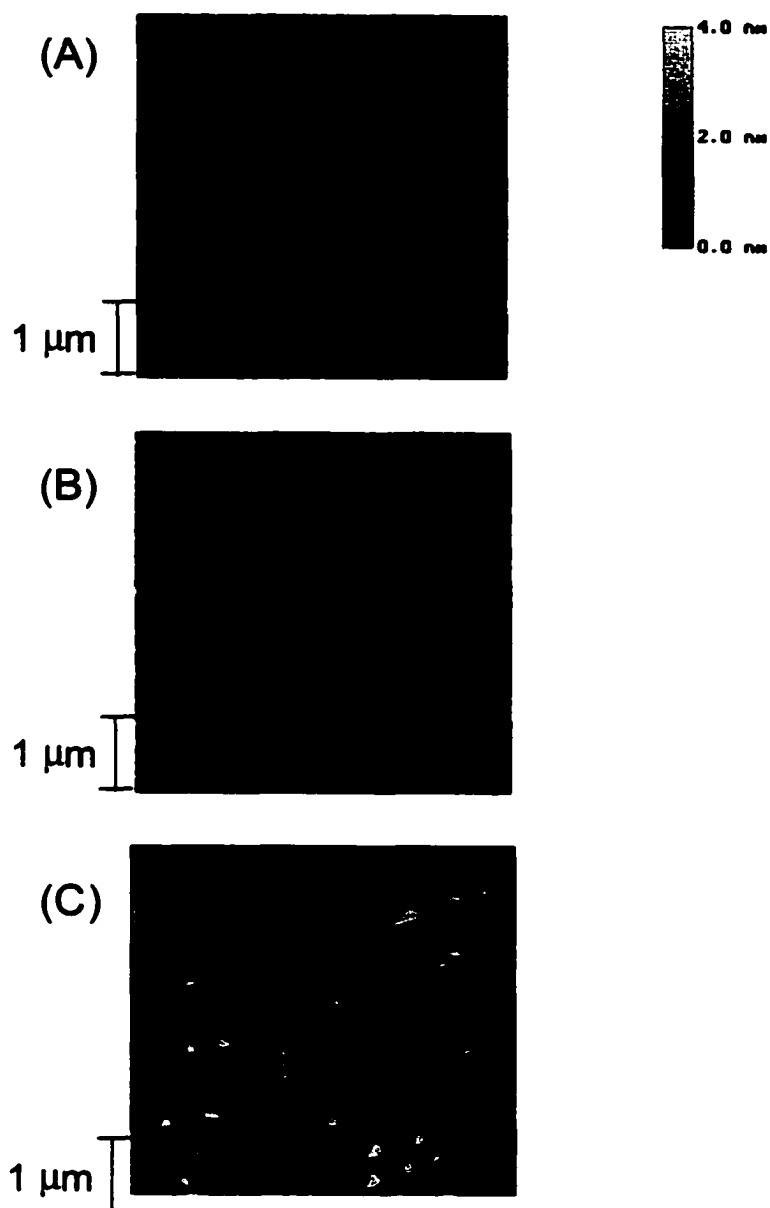
Figure 5-13. AFM images of (A) DDPC, (B) DLPC and (C) DMPC on silica after scraping off a portion of the coating with the AFM tip. See sections 5.3.7 and 5.4.6 for details.

(DDPC) does not form a stable coating at the capillary wall while the C_{14} analog of

DLPC (DMPC) forms a stable coating that prevents protein adsorption to the same extent

as its C_{12} counterpart.

5.6 References

(1)   Holmlin, R. E.; Chen, X.; Chapman, R. G.; Takayama, S.; Whitesides, G. M.

         Langmuir **2001**, *17*, 2841.

(2)   Emmer, A.; Jansson, M.; Roeraade, J. *J. Chromatogr. A* **1994**, *672*, 231.

(3)   Emmer, A.; Roeraade, J. *J. Liq. Chromatogr.* **1994**, *17*, 3831.

(4)   Gong, B. Y.; Ho, J. W. *Electrophoresis* **1997**, *18*, 732.

(5)   Yeung, K. K. C.; Lucy, C. A. *Anal. Chem.* **1997**, *69*, 3435.

(6)   Chapman, D. *Langmuir* **1993**, *9*, 39.

(7)   Malmsten, M. *J. Colloid Interface Sci.* **1995**, *172*, 106.

(8)   Murphy, E. F.; Lu, J. R. *Macromolecules* **2000**, *33*, 4545.

(9)   Ross, E. E.; Bondurant, B.; Spratt, T.; Conboy, J. C.; O'Brien, D. F.; Saavedra, S.

         S. *Langmuir* **2001**, *17*, 2305.

(10)   Pasenkiewicz-Gierula, M.; Takaoka, Y.; Miyagawa, H.; Kitamura, K.; Kusumi,

         A. *Biophys. J.* **1999**, *76*, 1228.

(11)   Watts, T. H.; Brian, A. A.; Kappler, J. W.; Marrack, P.; McConnell, H. *Proc.*

         Natl. Acad. Sci. USA **1984**, *81*, 7564.

(12)   Sackmann, E. *Science* **1996**, *271*, 43.

(13)   www.avantilipids.com .

(14)   Keller, C. A.; Glasmastar, K.; Zhdanov, V. P.; Kasemo, B. *Phys. Rev. Lett.* **2000**,

         84, 5443.

(15)   Leonenko, Z. V.; Carnini, A.; Cramb, D. T. *Biochim. Biophys. Acta* **2000**, *1509*,

         131.

(16)   Tang, Z.; Jing, W.; Wang, E. *Langmuir* **2000**, *16*, 1696.

(17) Muresan, A. S.; Lee, K. Y. C. *J. Phys. Chem. B* **2001**, *105*, 852.

(18) Jass, J.; Tjarnhage, T.; Puu, G. *Biophys. J.* **2000**, *79*, 3153.

(19) Reviakine, I.; Brisson, A. *Langmuir* **2000**, *16*, 1806.

(20) Rapuano, R.; Carmona-Ribeiro, A. *J. Colloid Interface Sci.* **1997**, *193*, 104.

(21) Williams, B. A.; Vigh, G. *Anal. Chem.* **1996**, *68*, 1174.

(22) Towns, J. K.; Regnier, F. E. *Anal. Chem.* **1991**, *63*, 1126.

(23) Cook, H. A.; Hu, W.; Fritz, J. S.; Haddad, P. R. *Anal. Chem.* **2001**, *73*, 3022.

(24) Hu, W.; Haddad, P. R.; Hasebe, K.; Tanaka, K. *Anal. Commun.* **1999**, *36*, 97.

(25) Puu, G.; Gustafson, I. *Biochim. Biophys. Acta* **1997**, *1327*, 149.

(26) Kolb, H.-A.; Enders, O.; Schauer, R. *Appl. Phys. A* **1999**, *68*, 247.

(27) Reviakine, I.; Simon, A.; Brisson, A. *Langmuir* **2000**, *16*, 1473.

(28) Leckband, D. E.; Helm, C. A.; Israelachvili, J. *Biochemistry* **1993**, *32*, 1127.

(29) Lehninger, A. L.; Nelson, D. L.; Cox, M. M. In *Principles of Biochemistry*; Worth Publishers: New York, 1993, pp Chapter 9.

(30) Cordova, E.; Gao, J.; Whitesides, G. M. *Anal. Chem.* **1997**, *69*, 1370.

(31) Schmalzing, D.; Piggee, C. A.; Foret, F.; Carrilho, E.; Karger, B. L. *J. Chromatogr. A* **1993**, *652*, 149.

(32) St'astna, M.; Radko, S. P.; Chrambach, A. *Electrophoresis* **2000**, *21*, 985.

(33) Legaz, M. E.; Pedrosa, M. M. *J. Chromatogr. A* **1993**, *655*, 21.

(34) Ciccone, B. *Am. Lab.* **2001**, *33*, 30.

(35) Astephen, N.; Wheat, T. *FASEB/ASBMB Symposium* **1991**, *poster #4789*.

(36) Chen, F.-T. A.; Tusak, A. *J. Chromatogr. A* **1994**, *685*, 331.

(37)   Besler, M.; Steinhart, H.; Paschke, A. *Food and Agricultural Immunology* **1998,** *10*, 157.

CHAPTER SIX. Semi-permanent Surfactant Coatings for EOF Control in Capillary Electrophoresis[*]

6.1 Introduction

As explained in Chapter One, a CE separation is based on the electrophoretic mobility, which is a function of the charge-to-mass ratio of the ion. Also involved in an electrophoretic separation is the electroosmotic flow (EOF). In a bare silica capillary, anions will naturally migrate towards the anode while the EOF migrates in the opposite direction, toward the cathode. This results in counter-EOF migration, which increases the separation time. As an alternative, the EOF can be reversed so that anions co-migrate with the EOF and thus the separation time is reduced. However, sometimes a reversed EOF moves the anions too quickly to the detector for baseline resolution to be achieved. In this case being able to lower the magnitude of the EOF would be desirable to optimize the separation.

Alternatively zwitterionic coatings such as the phospholipid bilayer coating presented in Chapter Five suppress the EOF to near zero. Such a coating is inappropriate for analysis of low mobility species such as proteins whose pI are near the separation buffer pH. In such a case the proteins would not migrate through the capillary in a reasonable time. Here, the ability to increase the EOF would be useful for achieving an improved separation.

Commonly, dynamic capillary coatings are used in CE to modify the EOF [1]. In dynamic coatings, a buffer additive equilibrates with the capillary surface and alters the

---

effective surface charge, thus altering the magnitude of the EOF. Surfactant additives are

often the method of choice for EOF modification since they are inexpensive and simple

to use. Cationic surfactants such as tetradecyltrimethylammonium bromide (TTAB) can

generate a strongly reversed EOF (Chapter Four), while zwitterionic surfactants such as

CAS U effectively suppress the EOF (Chapter Two). Control of EOF from fully reversed

to near zero has been demonstrated using mixtures of cationic and zwitterionic

surfactants [2]. However, single-chained surfactants such as TTAB and CAS U must be

present in the electrophoretic buffer at relatively high concentrations for the coating to

stay intact and generate a reproducible EOF [3]. This can lead to interactions such as ion-

pairing between analyte anions and buffer micelles [4] that may deteriorate the separation

and/or interfere with the detection scheme. This chapter presents a simple method of

tuning the EOF using surfactants that form semi-permanent coatings at the capillary

surface. The semi-permanent nature of the coatings allows excess surfactant to be

removed from the buffer prior to separation, thereby eliminating these unwanted

interactions. This method will be demonstrated for the separation of analytes ranging

from inorganic anions to protein mixtures.

6.2 Experimental

6.2.1 Apparatus

A Beckman P/ACE 5000 System (Fullerton, CA, USA) with a UV absorbance

detector was used for all experiments. Untreated silica capillaries (Polymicro

Technologies, Phoenix, AZ, USA) with an inner diameter of 50 μm, outer diameter of

365 μm, and total length of 47 cm (40 cm to detector) were used. Capillaries were

thermostated to 25°C. Data acquisition (10 Hz) and control was performed using P/ACE

Station Software for Windows 95 (Beckman) on a Pentium 120 MHz microcomputer.

6.2.2 Reagents

All solutions were prepared in Nanopure 18 MΩ ultrapure water (Barnstead,

Chicago, IL, USA). Buffers were prepared from either Ultra Pure Tris (Schwartz/Mann

Biotech, Cleveland, OH, USA) adjusted to the desired pH with hydrochloric acid

(Anachemia, Montreal, PQ, Canada) or potassium chromate (BDH, Darmstadt, Germany)

adjusted to the desired pH with phosphoric acid (BDH). The surfactants

didodecyldimethylammonium bromide (DDAB, Fig. 4-1A; Aldrich, Milwaukee, WI,

USA) and 1,2-dilauroyl-sn-phosphatidylcholine (DLPC, Fig. 5-1; Sigma, St. Louis, MO,

USA) were used as received. Calcium chloride dihydrate (molecular biology grade,

Sigma) was used as received. Mesityl oxide (Aldrich) was used as a neutral marker for

the EOF measurements. Anion solutions were prepared from sodium nitrite (BDH),

potassium nitrate (BDH), potassium bromide (Fisher Scientific, Fair Lawn, NJ, USA),

sodium fluoride (Fisher Scientific), sodium chloride (BDH), sodium sulfate (Fisher

Scientific), potassium oxalate (Matheson, Norwood, OH, USA), sodium iodide (BDH),

potassium thiocyanate (BDH), and potassium perchlorate (Fisher Scientific) without

further purification. The proteins lysozyme (chicken egg white), cytochrome-c (bovine

heart), ribonuclease-A (bovine pancreas), α-chymotrypsinogen A (bovine pancreas),

myoglobin (horse skeletal muscle) and α-lactalbumin (bovine milk) were used as

received from Sigma.

6.2.3 Preparation of capillary coatings

Solutions containing DDAB and DLPC were prepared as follows. DDAB or DLPC was suspended in the appropriate buffer and stirred for 15 min. The solution was then sonicated for 10 min periods. Between each 10-min period there was a 10 min "rest" interval where the solution was cooled and stirred at room temperature. This sonicate/stir cycle was repeated about 3 times or until the solution was clear. DDAB solutions prepared without sonication (Chapter Four) were just as effective as solutions prepared with sonication (Chapter Six). DLPC solutions, however, always require sonication.

Employing 100% DDAB or 100% DLPC as the wall coating, a 0.1 mM solution in 20 mM Tris-HCl and 20 mM $CaCl_2$, pH 7 buffer was rinsed through the capillary at high pressure (20 psi) for 5 min or 15 min respectively. Excess surfactant and $CaCl_2$ was removed by rinsing (20 psi) for 2 min with 20 mM Tris-HCl, pH 7 buffer.

DLPC-DDAB mixtures were used as wall coatings in an identical fashion (15 min rinse time, 20 psi). The composition of the 0.1 mM surfactant mixtures is expressed as % DLPC and % DDAB where the percentage refers to the mole fraction of the surfactant in the mixture.

6.2.4 EOF measurements

New capillaries were pretreated by rinsing at high pressure (20 psi) with 0.1 M NaOH for 10 min and water for 5 min. Capillaries were initially coated with surfactant and the excess surfactant was rinsed out with separation buffer (see Section 6.2.3). Prior to each run, the capillary was rinsed with the desired surfactant (20 psi, 3 min) and the excess surfactant was rinsed out with separation buffer (20 psi, 2 min).

Two methods were used to calculate the electroosmotic mobility (μ_{EOF}). When μ_{EOF} was above 1.0×10^{-4} cm^2/Vs, a single injection method was used where 1 mM mesityl oxide was directly injected onto the capillary (1.0 s, 0.5 psi) and a constant voltage of -15 kV was applied. Detection was at 254 nm. The value of μ_{EOF} was calculated according to Eqn 1-4. When μ_{EOF} was smaller than 1.0×10^{-4} cm^2/Vs, the electroosmotic flow was measured using the three-injection method introduced in Section 2.2.3. The first mesityl oxide marker was injected using low pressure (0.5 psi) for 1.0 s. This band was pushed through the capillary for 2 min using low pressure. A second mesityl oxide marker was then introduced by an identical low-pressure injection and the two bands were pushed with low pressure for 2 min. A constant voltage of $+15$ kV was applied for 3 min which causes the two markers to move within the capillary. A third marker was then injected and all the bands were eluted by applying low pressure for 12 min. The value of μ_{EOF} measured using this method was calculated as described in Section 2.2.3.

6.2.5 Anion separations

New capillaries were pretreated by rinsing at high pressure (20 psi) with 0.1 M NaOH for 10 min and water for 5 min. Capillaries were initially coated with surfactant as described in Section 6.2.3. Prior to each run, the capillary was rinsed with the appropriate surfactant mixture (20 psi, 3 min) and then the excess surfactant was rinsed out with separation buffer (20 psi, 2 min).

For direct detection of inorganic anions, the capillary was coated with the desired surfactant mixture. Excess surfactant was rinsed from the capillary (20 psi, 2 min) with 20 mM Tris-HCl, pH 7 buffer. A 0.5 mM mixture of KNO_3, $NaNO_2$, NaI, KBr, and

KSCN in water was injected at low pressure (0.5 psi) for 3.0 s. The applied potential was −20 kV and the detector rise time was 0.1 s. The anions were detected using direct UV absorbance detection at 214 nm.

For the indirect detection of nine inorganic anions, the capillary was coated using a 95% DLPC-5% DDAB solution. Excess surfactant was rinsed from the capillary with the separation buffer of 5 mM potassium chromate adjusted to pH 8 with phosphoric acid (20 psi, 2 min). A mixture of 0.5 mM $NaNO_2$, KNO_3, KBr, NaI, KSCN, NaF, NaCl, Na_2SO_4, and $K_2C_2O_4$ in water was injected using low pressure (0.5 psi) for 3.0 s. The applied potential was −20 kV and the detector rise time was set to 0.1 s. The anions were detected using indirect UV absorbance detection at 254 nm. A 0.5 mM solution of $KClO_4$ in water was also injected and detected in the same manner as the anion mixture. All anion separations were performed in triplicate.

6.2.6 Protein separations

New capillaries were pretreated by rinsing at high pressure (20 psi) with 0.1 M NaOH for 10 min and water for 5 min. Capillaries were initially coated with a surfactant mixture as described in Section 6.2.3. Prior to each run, the capillary was rinsed with the surfactant solution (20 psi, 3 min) and then the excess surfactant and calcium was rinsed out with separation buffer (20 psi, 2 min). Protein mixtures (0.1 mg/mL in water) were injected for 3 s (0.5 psi) and separated in 20 mM Tris-HCl pH 7 buffer (void of calcium and surfactant) with an applied voltage of -20 kV. Proteins were detected at 214 nm. Protein separations were performed in triplicate.

6.3 Results and Discussion

6.3.1 Use of DDAB for inorganic anion analysis

The standard method for inorganic anion analysis in capillary electrophoresis involves adding the single-chained surfactant tetradecyltrimethylammonium bromide (TTAB) to the buffer to reverse the EOF [5]. With single-chained surfactants such as TTAB, it is necessary that the surfactant be present in the buffer at a concentration above the CMC to achieve a stable reversed EOF [3]. Invariably, the micelles in solution will interact with the analyte ions [4]. This can be detrimental to the separation of mixtures containing strongly interacting ions. The double-chained surfactant didodecyldimethylammonium bromide (DDAB) also reverses the EOF with the added advantage of forming a stable coating on the capillary wall. As shown in Chapter Four, DDAB has a packing factor of 0.620 which is within the range associated with bilayer formation. As a consequence, DDAB monomers aggregate to form a flat bilayer structure at the capillary wall (Section 4.5.2) that is extremely stable. Consequently, the excess surfactant can be removed from the buffer prior to electrophoretic separation as seen in Chapter Four.

DDAB was previously implemented as a wall coating for the ultra-rapid separation of nitrate and nitrite at low pH [6]. However it has never been used for separation of more complex anion mixtures. Herein, DDAB is employed to reverse the EOF for the separation of five inorganic anions. A 0.1 mM solution of DDAB in 20 mM Tris-HCl pH 7 buffer is used to coat the capillary wall. The excess DDAB is removed by rinsing the capillary with Tris-HCl pH 7 buffer. The separation of five UV-absorbing anions: bromide, nitrite, nitrate, iodide, and thiocyanate is shown in Figure 6-1. DDAB
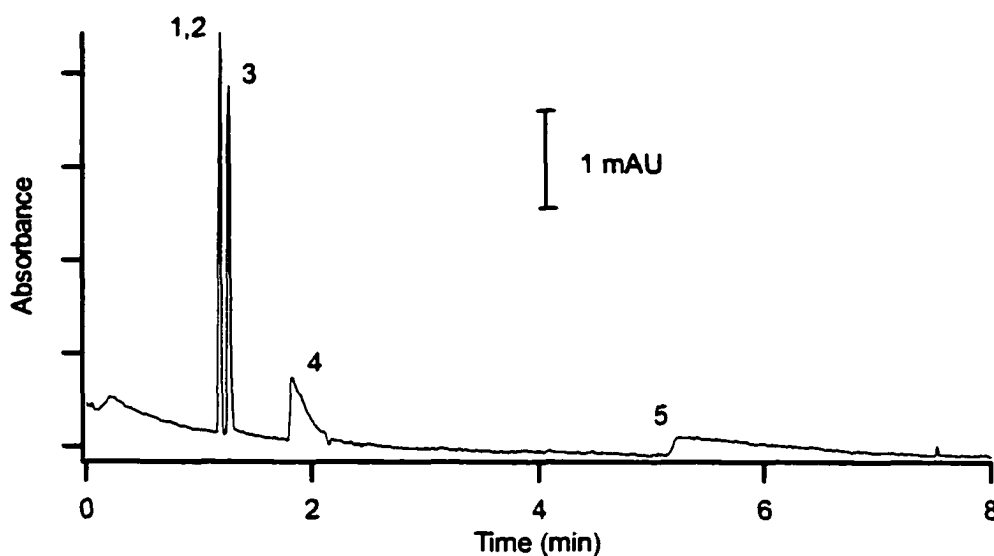
Figure 6-1. Separation of five inorganic anions using a DDAB-coated capillary. Peaks: (1,2) bromide+nitrite, (3) nitrate, (4) iodide, (5) thiocyanate. Experimental conditions: 47-cm capillary (40 cm to detector); temperature, 25°C; separation buffer, 20 mM Tris-HCl at pH 7; sample, 0.5 mM anion mixture in water; -20 kV applied voltage; direct UV detection at 214 nm. Coating procedure: 5 min rinse with 0.1 mM DDAB in buffer followed by a 2 min rinse with separation buffer to remove excess surfactant; between runs DDAB rinse time was shortened to 3 min.

strongly reversed the EOF to a value of -7.0×10^{-4} cm^2/Vs. The rapid EOF does not allow sufficient time for a separation to develop between bromide and nitrite. Further, iodide and thiocyanate strongly interact with the wall coating, leading to poor peak shapes and a long separation time (>7 min). The same behavior has been observed previously in open-tubular ion-exchange CEC of inorganic anions [7]. Breadmore *et al.* found that chaotropic anions such as iodide, thiocyanate and thiosulfate strongly interacted with a quaternary aminated stationary phase.

Although the excess surfactant can be removed from the separation buffer, this system is not ideal for anion analysis. The EOF produced is too fast to obtain baseline resolution of all anions and the interaction between chaotropic anions and the DDAB wall coating is detrimental to peak shape.

6.3.2 EOF control using a mixed surfactant system

The ability to tune the magnitude of the reversed EOF is a necessary tool for the optimization of anion separations and the simultaneous separation of acidic and basic proteins. Previously it has been shown that the reversed EOF can be fine-tuned using mixtures of the zwitterionic surfactant Rewoteric AM CAS U and the cationic surfactant TTAB [2]. The zwitterionic surfactant has a net charge of zero and effectively dilutes the positive charge at the capillary wall when mixed with TTAB. When the two surfactants are mixed, the magnitude of the EOF can be modified from near zero to fully reversed. This ability to control the reversed EOF was used to improve the separation of inorganic anions [2] as well as for ultra-high resolution separations of isotopes [8]. The use of single-chained surfactants for EOF control demands that the surfactants be present in the buffer

to maintain the wall coating (Section 4.5.1). Again, this approach can lead to unwanted interactions between analytes and buffer micelles, thus degrading the separation.

Herein the mixed surfactant approach is investigated using double-chained surfactants that are known to form semi-permanent capillary coatings. As discussed above and in Chapter Four, DDAB forms a stable capillary coating and is used as the cationic surfactant in the mixture. Phosphatidylcholines are zwitterionic, double-chained surfactants that are commonly employed to mimic biological membranes [9-12]. In Chapter Five I showed that phosphatidylcholines are also useful in CE since they form stable, semi-permanent coatings on the capillary wall. The effect of mixing the zwitterionic surfactant 1,2 dilauroyl-sn-phosphatidylcholine (DLPC) with DDAB on the magnitude of the reversed EOF is shown in Figure 6-2. At pH 7, the EOF can be modified from near zero (0.2×10^{-4} cm^2/Vs) to fully reversed (-7.0×10^{-4} cm^2/Vs) where 100% DLPC produces the near zero EOF and 100% DDAB generates the fully reversed EOF.

Measurement of the EOF can be used as an indirect test of the stability of a capillary coating [13]. The stability of each mixed surfactant coating was tested by first coating the capillary with the desired mixture and then measuring the EOF after rinsing out the excess surfactant with Tris-HCl pH 7 buffer. Good stability was observed for each surfactant mixture for over 10 runs (5 min per run). The EOF never decreased by more than 5 % over the 50 min of the stability test. Figure 6-3 shows a representative stability plot for the mixed surfactant capillary coatings. Day-to-day reproducibility of all EOF measurements was less than 5% RSD. However, solutions were kept for no longer than 5 days as migration time reproducibilities were compromised after this time period.
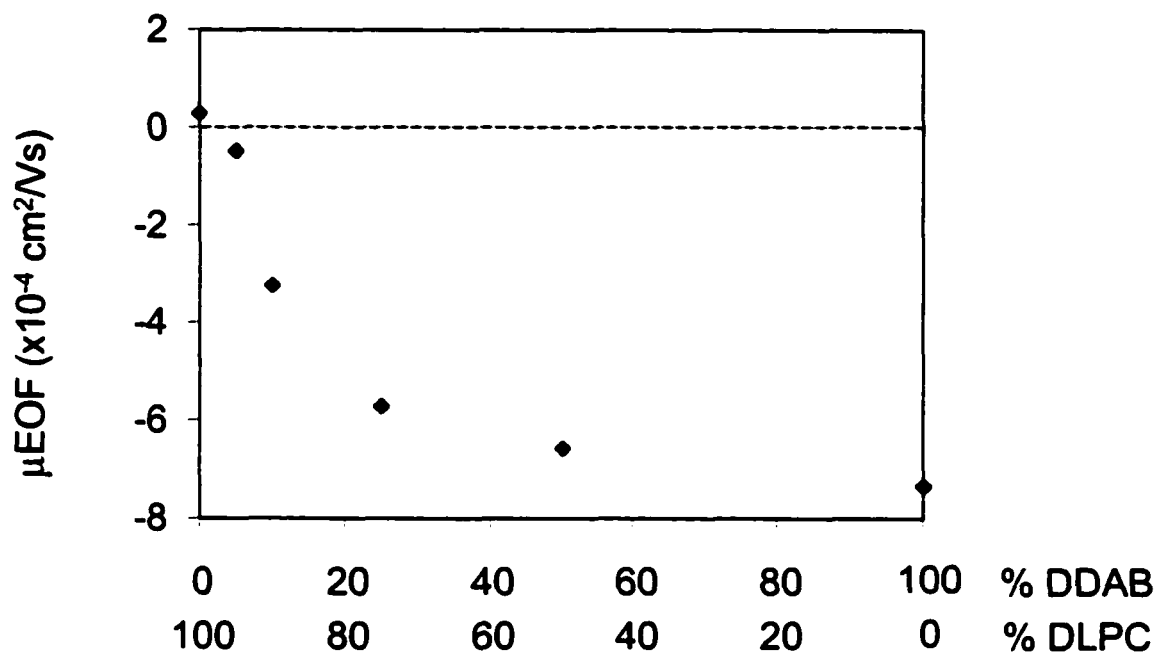
Figure 6-2. Effect of 0.1 mM DLPC-DDAB mixtures on the EOF. Experimental conditions: 47-cm capillary (40 cm to detector); temperature, 25°C; separation buffer, 20 mM Tris-HCl at pH 7; applied voltage, -15 kV (fast reversed EOF) or +15 kV (slow EOF, 3 peak injection method used, see section 6.2.4); direct UV detection at 254 nm.
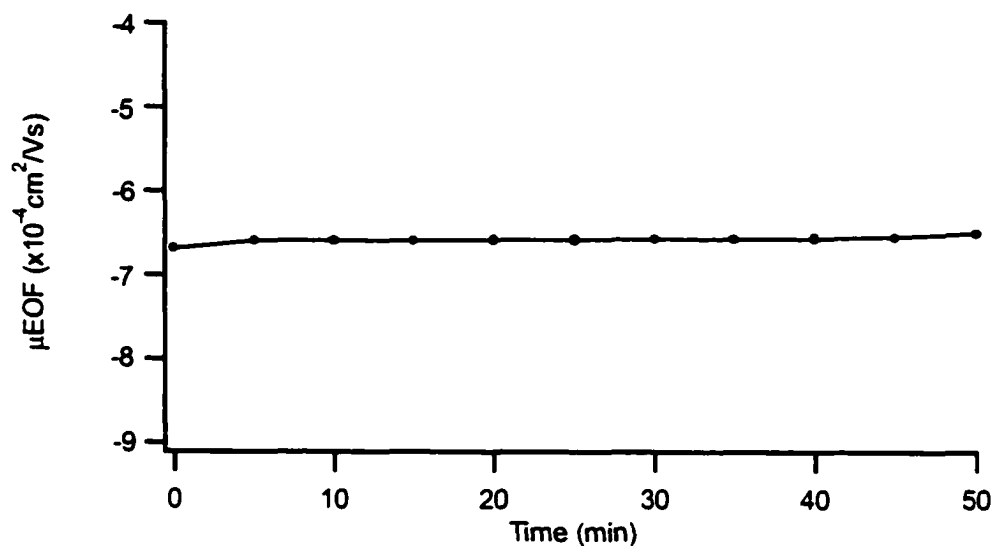
Figure 6-3. Coating stability of 50% DLPC-50% DDAB as reflected by the EOF as a function of time. Successive injections performed after an initial flushing of excess surfactant from the capillary. Capillary rinsed with 20 mMTris-HCl, pH 7 buffer (1 min) between injections. Line through points acts only as a guide to the eye.

6.3.3 Use of a mixed DLPC-DDAB capillary coating for anion analysis

The separation of the same five UV-absorbing anions shown in Figure 6-1 was performed using a mixture of DLPC and DDAB. Figure 6-4 shows the separation of the anions bromide, nitrite, nitrate, iodide, and thiocyanate using a 95% DLPC-5% DDAB mixture as a wall coating. The five anions are baseline resolved in a separation time of under 2.5 min. This mixed surfactant coating produced a relatively low, reversed EOF (-0.5×10^{-4} cm^2/Vs), ideal for obtaining baseline resolution between bromide and iodide and nitrite and nitrate while maintaining a rapid co-EOF separation. Further, the peak shapes of the chaotropic anions (iodide and thiocyanate) are Gaussian (assymmetry factor< 1.5), a huge improvement over the peak shapes observed in Figure 6-1. The anions do not strongly interact with the phosphatidylcholine headgroup as they do with the quaternary amine group of DDAB.

Since only a few anions absorb UV light, indirect detection is commonly used for anion analysis. To determine the compatibility of the DLPC-DDAB coating with a standard indirect UV probe, an inorganic anion separation was performed using 5 mM chromate adjusted to pH 8.0 as the electrophoretic buffer. Chromate is the typical probe ion used in indirect detection [14]. A bare capillary was coated with a 95% DLPC-5% DDAB mixture and the excess surfactant was rinsed out with chromate buffer, as described in Section 6.2.5. Figure 6-5 shows the separation of nine anions using indirect UV detection at 254 nm. The separation was accomplished in less than 2.8 minutes. Baseline resolution is achieved between all anions with the exception of iodide and chloride, which are nearly baseline resolved (R=0.95 according to Eqn. 1-8). As before, the DLPC-DDAB coating did not degrade peak shape.
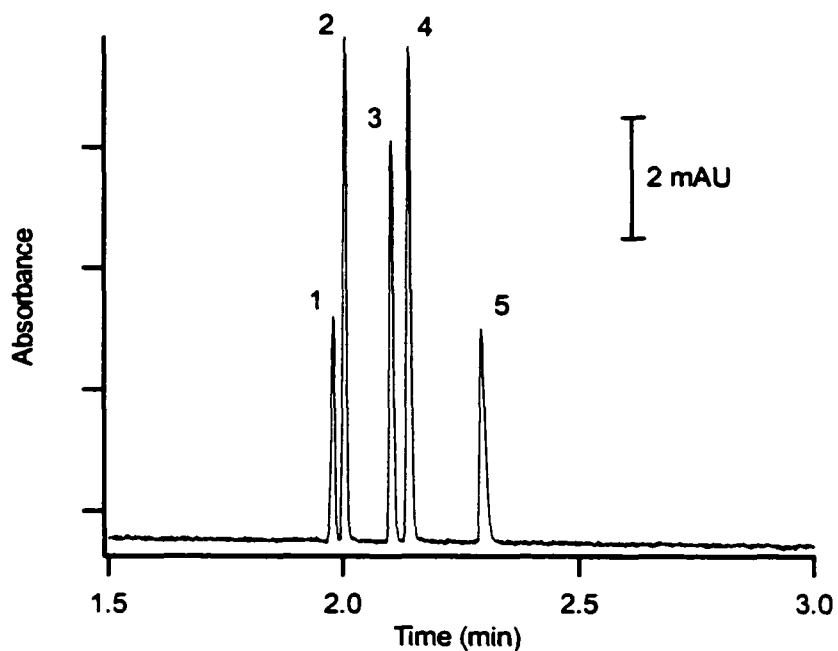
**Figure 6-4.** Separation of five inorganic anions using a capillary coated with a 0.1 mM DLPC-DDAB (95%:5%) surfactant mixture. Peaks: (1) bromide, (2) iodide, (3) nitrite, (4) nitrate, (5) thiocyanate. Experimental conditions: 47-cm capillary (40 cm to detector); temperature, 25°C; separation buffer, 20 mM Tris-HCl at pH 7; sample, 0.5 mM anion mixture in water; -20 kV applied voltage; direct UV detection at 214 nm. Coating procedure: 15 min rinse with a 0.1 mM DLPC-DDAB (95%:5%) mixture in buffer followed by a 2 min rinse with separation buffer to remove excess surfactant; between runs surfactant rinse time was shortened to 3 min.
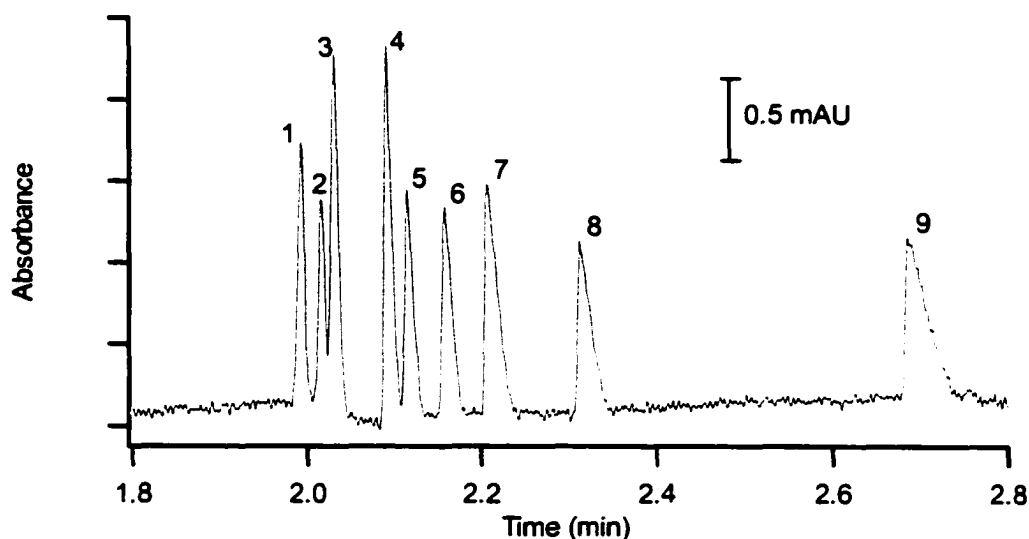
Figure 6-5. Separation of nine inorganic anions using a capillary coated with 0.1 mM DLPC-DDAB (95%:5%) surfactant mixture. Peaks: (1) bromide, (2) iodide, (3) chloride, (4) sulfate, (5) nitrite, (6) nitrate, (7) oxalate, (8) thiocyanate, (9) fluoride. Experimental conditions: 47-cm capillary (40 cm to detector); temperature, 25°C; separation buffer, 5.0 mM chromate adjusted to pH 8.0 with phosphoric acid; sample, 0.5 mM anion mixture in water; -20 kV applied voltage; indirect UV detection at 254 nm. Coating procedure: 15 min rinse with a 0.1 mM DLPC-DDAB (95%:5%) mixture in buffer followed by a 2 min rinse with separation buffer to remove excess surfactant; between runs surfactant rinse time was shortened to 3 min.

A plot of ionic equivalent conductance (conductance at zero ionic strength) as a function of migration time of the singly charged anions separated in Figure 6-5 is shown in Figure 6-6. There is an excellent reciprocal relationship between these two variables for all singly charged anions. Jones and Jandik previously showed that this relationship existed for most anions [5]. However the highly chaotropic anions iodide, thiocyanate, and perchlorate strongly deviated from the plot in Jones and Jandik's work with TTAB [5] as shown in Figure 6-6 (inset). These anions strongly interacted with the TTAB micelles in the buffer (perchlorate interacted the most), which led to extremely long migration times (also seen here for iodide and thiocyanate in Figure 6-1 using DDAB). Although not present in the anion separation shown in Figure 6-5, perchlorate was also injected and indirectly detected using a DLPC-DDAB coated capillary (it partially overlapped with the thiocyanate peak in the mixture). Perchlorate has been added to the plot in Figure 6-6 and follows the reciprocal relationship. Thus, interactions between the chaotropic anions (iodide, thiocyanate, perchlorate) and the DLPC-DDAB wall coating are not present and separations are governed solely by the electrophoretic mobility of the anions.

6.3.4 Use of a mixed DLPC-DDAB capillary coating for protein separations

Separating cationic and anionic proteins in a single run is a challenge in CE because the capillary walls must be coated to prevent adsorption, while a fairly strong EOF is needed to sweep both cations and anions to the detector. However, coating the capillary wall to prevent both cationic and anionic protein adsorption would intuitively necessitate a neutral coating, and a neutral coating will generate an EOF of zero. As shown in Chapter Two, adding a chaotropic anion to a buffer containing the zwitterionic surfactant CAS U produced an EOF that was strong enough for the simultaneous
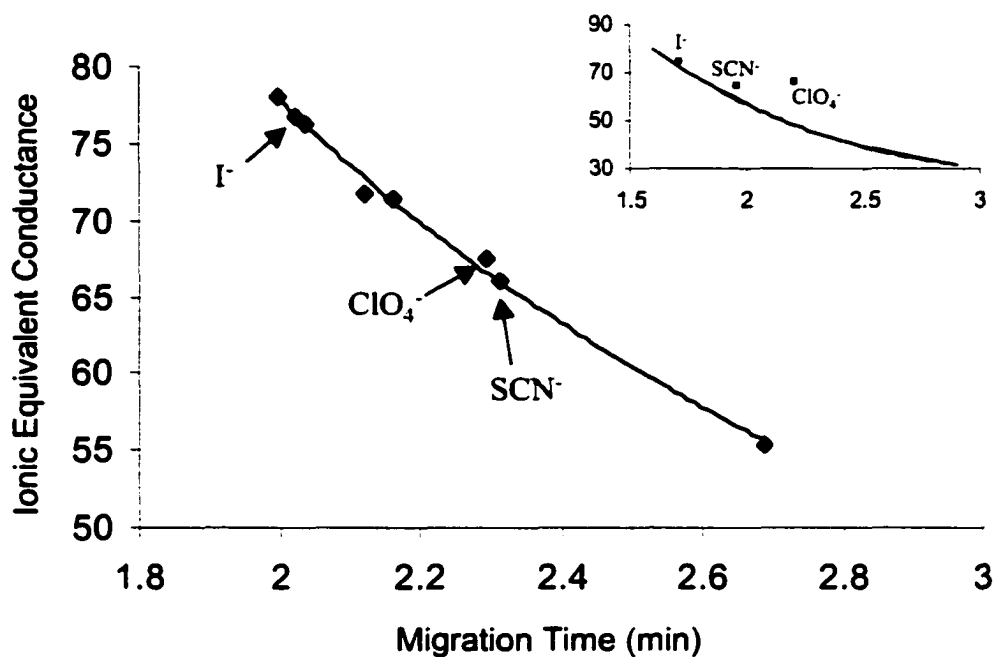
Figure 6-6. Migration times of singly charged anions plotted against ionic equivalent conductance. Note that the chaotropic anions (iodide, thiocyanate, and perchlorate) follow the reciprocal relationship. Line shown is a best fit to a reciprocal function. Inset is the same plot based on data from Jones and Jandik's work[5]. Note that the chaotropic anions (iodide, thiocyanate, and perchlorate) strongly deviate from the reciprocal relationship.

separation of cationic and anionic proteins. The zwitterionic surfactant also coated the capillary wall, which prevented both cationic and anionic protein adsorption. However, the EOF (+1 x 10^{-4} cm^2/Vs) was still not strong enough to allow the detection of some higher mobility anionic proteins.

Figure 6-7 shows a separation of the proteins: α-lactalbumin, myoglobin, ribonuclease A, α-chymotrypsinogen A, cytochrome c, and lysozyme using a 90% DLPC-10% DDAB coated capillary at pH 7. The EOF generated using this coating system was –3.7 x 10^{-4} cm^2/Vs. At this pH, α-lactalbumin is anionic, myoglobin is roughly neutral, and ribonuclease A, α-chymotrypsinogen A, cytochrome c, and lysozyme are cationic. Table 6-1 provides the pIs, molecular weigths, and the corresponding effective electrophoretic mobility (μ_e) of each protein in the 20 mM Tris-HCl pH 7 buffer. All six proteins are efficiently separated (N> 400 000 plates/m) in just over 10 min. The reproducibility of the protein migration times was less than 1.6 % RSD from run-to-run (n=16). This system is an improvement over the separations shown in Chapter Five, since cationic and anionic proteins can be separated in a single run. Further, proteins with a mobility similar to the EOF can be detected in a reasonable time. Using a 100% DLPC coating (Chapter Five) on the capillary generates an EOF of roughly zero (0.2 x10^{-4} cm^2/Vs), which does not allow for a separation of these near-neutral proteins as their migration through the capillary would have taken an impractical amount of time. The simultaneous separation of proteins demonstrated here is also an improvement over the separation shown in Chapter Two, as higher mobility anionic proteins are swept to the detector and the surfactant need not be present in the separation buffer.
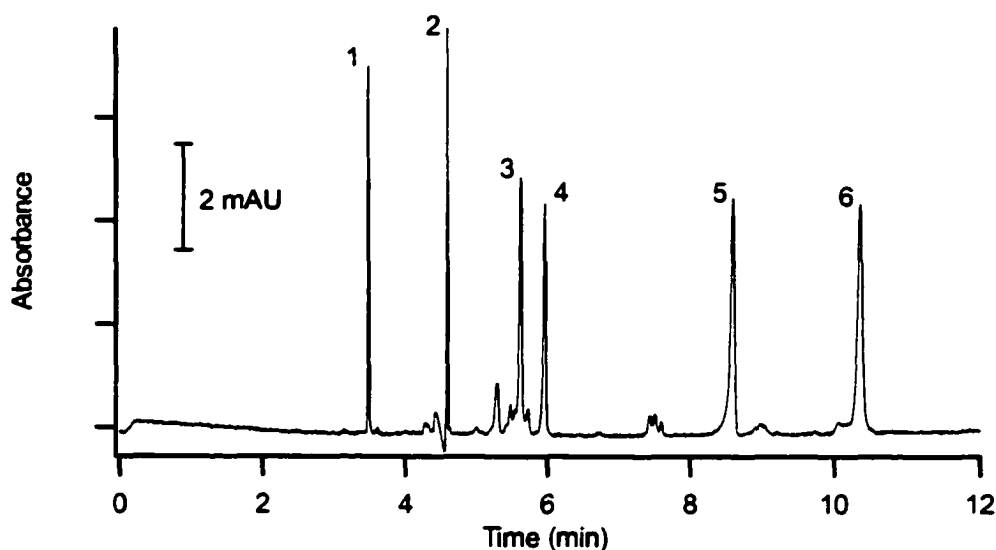
Figure 6-7. Separation of cationic and anionic proteins at pH 7 using a 0.1 mM DLPC-DDAB (90%:10%) surfactant coating. Peaks, (1) α-lactalbumin, (2) myoglobin, (3) α-chymotrypsinogen A, (4) ribonuclease A, (5) cytochrome c, (6) lysozyme. Experimental conditions: 40-cm capillary (47 cm to detector); temperature, 25°C; separation buffer, 20 mM Tris-HCl, pH 7; sample, 0.1 mg/ml protein mixture in water; applied voltage, -20 kV; direct UV detection at 214 nm. Coating procedure: 15 min rinse with 0.1 mM DLPC-DDAB (90%:10%) in 20 mM Tris-HCl pH 7 buffer containing 20 mM CaCl₂ followed by a 2 min rinse with separation buffer to remove excess surfactant; between runs surfactant rinse time was shortened to 3 min.

Table 6-1. Effective electrophoretic mobility, molecular weight, and pI of each protein separated on a 90% DLPC-10% DDAB coated capillary at pH 7 (See Figure 6-7 for separation)

Protein	pI	molecular weight (g/mol)	Effective mobility (μ_e, x 10^{-4} cm^2/Vs)
lysozyme	11	14 300	1.9
cytochrome c	9.5	12 200	1.6
ribonuclease A	9.6	13 700	0.8
α-chymotrypsinogen A	8.7	25 600	0.6
myoglobin	7.0	16 900	0.03
α -lactalbumin	4.8	14 200	-1.1

6.4 Conclusions

Using capillary coatings comprised of mixtures of a double-chained cationic surfactant (DDAB) and a double-chained zwitterionic surfactant (DLPC), the EOF can be controlled from fully reversed to effectively zero. Tuning the EOF in this manner can optimize the separation of inorganic anions or proteins. The coating is semi-permanent in nature, and therefore excess surfactant can be flushed from the capillary prior to the electrophoretic separation. Separations can then be performed in a simple buffer system (no surfactant) where interactions between analyte anions and the surfactant additive have been eliminated.

6.5 References

(1)   Melanson, J. E.; Baryla, N. E.; Lucy, C. A. *Trends Anal. Chem.* **2001**, *20*, 365.

(2)   Yeung, K. K.-C.; Lucy, C. A. *J. Chromatogr. A* **1998**, *804*, 319.

(3)   Lucy, C. A.; Underhill, R. S. *Anal. Chem.* **1996**, *68*, 300.

(4)   Kaneta, T.; Tanaka, S.; Taga, M.; Yoshida, H. *Anal. Chem.* **1992**, *64*, 798.

(5)   Jones, W. R.; Jandik, P. *J Chromatogr.* **1991**, *546*, 445.

(6)   Melanson, J. E.; Lucy, C. A. *J. Chromatogr. A* **2000**, *884*, 311.

(7)   Breadmore, M. C.; Boyce, M.; Macka, M.; Avadlovic, N.; Haddad, P. R. *J. Chromatogr. A* **2000**, *892*, 303.

(8)   Yeung, K. K.-C.; Lucy, C. A. *Electrophoresis* **1999**, *20*, 2554.

(9)   Tang, Z.; Jing, W.; Wang, E. *Langmuir* **2000**, *16*, 1696.

(10)   Reviakine, I.; Brisson, A. *Langmuir* **2000**, *16*, 1806.

(11)   Kumar, S.; Hoh, J. H. *Langmuir* **2000**, *16*, 9936.

(12)   Jass, J.; Tjarnhage, T.; Puu, G. *Biophys. J.* **2000**, *79*, 3153.

(13)   Cordova, E.; Gao, J.; Whitesides, G. M. *Anal. Chem.* **1997**, *69*, 1370.

(14)   Doble, P.; Haddad, P. R. *J. Chromatogr. A* **1999**, *834*, 189.

CHAPTER SEVEN. Summary and Future Work

7.1 Summary

This thesis has demonstrated the necessity and utility of surfactant-based capillary wall coatings for capillary electrophoresis (CE) separations of proteins (Chapters Two, Five, Six). Further, the control of the electroosmotic flow that was gained by manipulating these wall coatings was the basis for a novel on-line sample preconcentration technique (Chapter Three) as well as improved separations of small inorganic anions (Chapter Six).

Surfactants were used for forming the capillary wall coatings. I found that a zwitterionic surface (generated using a zwitterionic surfactant) allowed for the separation of both acidic and basic proteins (Chapters Two and Five). Further, with a zwitterionic surface, the concept of electrostatic ion chromatography could be exploited to change the EOF while still preventing protein adsorption. Chaotropic ions added into the buffer can alter the charge at the capillary surface and hence alter the EOF.

It was also found that the structure of the surfactant dictated the degree of coverage the coating provided (Chapter Four). If a surfactant has a packing factor (P) that is between $1/3$ and $1/2$, spherical micelles form above the CMC. Generally, single-chained surfactants possess a P-value in this range. If a surfactant has a P-value between $1/2$ and 1, vesicles are favoured and are formed above the CVC. These P-values are common for double-chained surfactants. I discovered that single-chained surfactants form an incomplete coating at the capillary wall (unstable, dynamic) while double-chained surfactants form a coating that completely covers the surface (stable, semi-permanent). The increased coverage that the double-chained surfactant aggregates

provide over single-chained surfactant aggregates (micelles) is responsible for improved

protein separations with minimal protein adsorption to the capillary wall. It also explains

why the double-chained surfactant could be removed from the buffer prior to separation.

In summary, an ideal wall coating for the separation of proteins by capillary

electrophoresis can be formed using a double-chained surfactant with a zwitterionic

headgroup such as DLPC. This coating allows for the separation of both acidic and basic

proteins and is semi-permanent, thus separations can be performed in surfactant-free

buffer. Alternatively, if low pH conditions are used, the double-chained cationic

surfactant, DDAB, could be employed since most proteins will have a net positive charge

at this pH. DDAB also forms a stable, semi-permanent coating at the wall such that

excess surfactant can be removed from the buffer prior to separation.

The following sections provide details on a few projects that would be interesting

to study in the future.

7.2 Future Work

7.2.1 Permanent cross-linked surfactant coatings

As shown in Chapters Four and Five, double-chained surfactants form semi-

permanent coatings at the capillary wall. The excess surfactant could therefore be

removed from the electrophoretic buffer prior to separation. The electroosmotic flow

was used as an indirect test of the coating stability. The coatings were termed semi-

permanent because the electroosmotic flow declined slightly over the course of a 75 min

run (~3%) indicating that there was some desorption from the wall. An interesting area

of research would be to convert the semi-permanent coating into a permanent coating by

cross-linking the bilayer in place. This idea is based on the use of polymerized micelles

for micellar electrokinetic chromatography (MEKC) [1]. MEKC uses surfactant micelle

solutions as a pseudostationary phase for chromatographic separation. In Palmer and

Terabe's work [1], a cross-linkable analog of sodium dodecylsulfate (with a terminal

double bond) was used to form micelles in solution. A UV-radiation or free-radical

initiator was used to chemically cross-link the double bonds and polymeric micelles

resulted.

Recently it was demonstrated that stable lipid bilayers can be formed on a silicon

dioxide surface by cross-linking a polymerizable phospholipid (phospholipid containing

double bonds) [2]. This methodology could be extended to capillary coatings by forming a

bilayer at the wall with the commercially available phospholipid 1,2-dimyristelaidoyl-*sn*-

glycero-3-phosphocholine (Figure 7-1; Avanti Polar Lipids Inc., Alabaster, AL, USA) in

an analogous manner to DLPC (Chapter Five). The bilayer could then be cross-linked in

place using $K_2S_2O_8/NaHSO_3$. The stability of the wall coating would be determined as

described in Sections 4.5.1 and 5.4.1.

7.2.2   On-line CE-ESI-MS using semi-permanent surfactant wall coatings

A common problem with dynamic surfactant-based capillary wall coatings

(single-chained surfactants) is their incompatibility with electrospray inonization mass

spectrometry (ESI-MS) detection. ESI-MS is an increasingly popular and powerful

method for protein identification [3,4]. Further, there are already commercial interfaces

available for coupling a CE instrument with (ESI-MS) detection allowing for fast on-line

separation and detection. This is desirable for proteomics since there are millions of

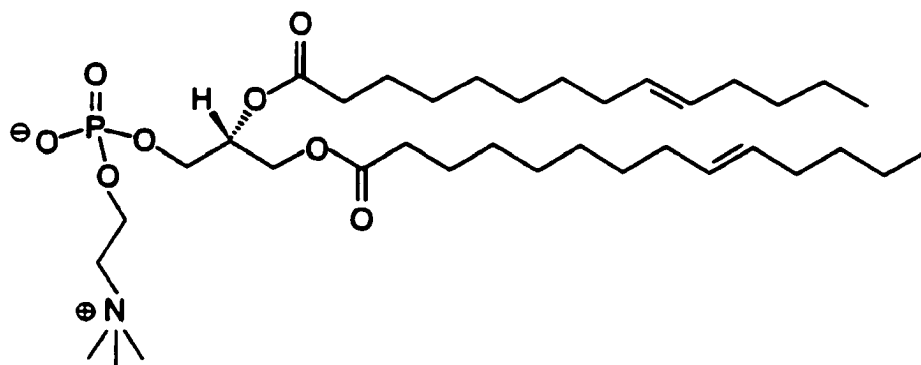proteins to characterize. When dynamic capillary coatings are used, the surfactant

Figure 7-1. Structure of 1,2-dimyristelaidoyl-*sn*-glycero-3-phosphocholine.

monomers must be present in the buffer to keep the coating intact. This gives rise to a

suppressed MS signal and poor sensitivity. The major portion of the total electrospray

ion current is carried by the surfactant thereby suppressing the protonated protein signal.

Also, adsorption of the surfactant monomers onto the counter-electrode (nozzle)

diminishes sensitivity over time, necessitating frequent cleaning [3].

Therefore, the semi-permanent capillary wall coatings comprised of DDAB

(Chapter Four) and DLPC (Chapter Five) should be tested for their compatibility with

ESI-MS detection. As stated in Section 4.7, Yeung et al. have already demonstrated the

compatibility of the DDAB coating with off-line matrix-assisted laser desorption

ionization mass spectrometry (MALDI-MS) [5]. These coatings would be ideal for CE-

ESI-MS since surfactant does not have to be present in the buffer, and they are cheap,

easy, and quick to apply to the capillary wall.

7.2.3   Second-generation protein recovery studies

It is apparent from my research and that of others [6,7] that peak efficiency by itself

is not an adequate measurement of coating quality. Protein recovery, discussed in Chapter

Two and applied throughout the chapters of this thesis, is a better measure of coating

effectiveness. However, the current method is incompletely characterized. That is, no

studies have been performed to determine the dependence on factors such as the relative

capillary lengths. More importantly, the current methods of monitoring protein recovery

have only been performed at high protein concentrations (0.1 mg/mL) due to the limited

sensitivity of UV detection. These concentrations are not representative of the trace

protein levels that are common in proteomic studies. Thus, a new methodology for

determining protein recovery should be developed. Righetti et al. have tried to develop a

176

new method to measure protein recovery [7], however their procedure is difficult to follow and is not very versatile. Briefly, they labeled the protein myoglobin with a fluorescent probe and coated a capillary with this protein. They then removed the adsorbed protein by using SDS that was electrophoretically driven into the capillary. The desorbed protein was collected in the outlet vial and a plug of this sample re-injected along with a fluorescent internal standard. A second desorption with SDS was performed and the protein was detected using argon-ion laser induced fluorescence and the internal standard detected with helium-neon laser induced fluorescence. The method was restricted to pH 5 and necessitates a CE system with dual-laser induced fluorescence detection capability. Further, accurate quantification would have been impossible judging by the peaks shown in their electropherograms [8].

The proposed idea for a new method is based on the method of Righetti described above [7]. My proposed method involves initially determining a number that represents 100% adsorption to the capillary wall. For this, a bare capillary would be rinsed with a solution containing the protein of interest for a length of time that allows the protein to completely adsorb to the wall. Excess unbound protein would then be rinsed out of the capillary with buffer. Finally, the adsorbed protein could be desorbed from the wall by rinsing the capillary with a solution containing SDS, as documented in the literature [7]. I have demonstrated the ability of SDS to desorb protein from the wall by achieving the same EOF measured prior to introducing protein and after desorption with a SDS solution. The desorbed protein would be detected using UV absorbance detection. The area of the protein peak represents 100% adsorption to the capillary wall. To determine the amount of protein adsorbed to the wall of a coated capillary, the coated capillary

would be treated in an identical fashion to the bare capillary. A protein solution would be rinsed through the coated capillary, the excess protein rinsed out, and the protein desorbed using a SDS solution. The area of this protein peak would then be compared to the area of the protein peak found for a bare capillary. The ratio of the two areas would represent the amount of protein adsorbed to the coated capillary. Note that when the SDS front passes the detector window there is a large change in refractive index that obscures the protein peaks. Therefore blanks must be run on the bare capillary and coated capillary prior to introducing the protein solution.

Instead of coating the entire capillary with protein it would be desirable to extend the above methodology to a "normal" CE separation, meaning inject a protein into the capillary, apply a separation voltage, and then determine how much of the protein initially injected adsorbed to the wall. Intuitively, the above methodology would translate easily by just desorbing any adsorbed protein with a SDS solution following the voltage separation. However, the small amount of protein desorbed would be undetectable using UV absorbance. Therefore a more sensitive detection scheme would be needed.

Employing laser-induced fluorescence (LIF) detection is an attractive alternative to the poor sensitivity UV absorbance provides. Indeed LIF has commonly achieved detection limits in the low pM range [9]. However, labeling of proteins with fluorescent tags results in multiple products [10], which would complicate the study of protein adsorption. A class of proteins known as the heme proteins (e.g. myoglobin, cytochrome c) contains an intrinsic fluorophore, which is excitable at 400 nm. This native fluorescence could be exploited by using the violet (400 nm) diode laser for laser-induced

fluorescence detection in CE [11]. This detection scheme would be useful in combination

with the second-generation protein recovery study for detecting the trace amounts of

protein that adhere to the capillary wall.

7.3 References

(1)   Palmer, C. P.; Terabe, S. *Anal. Chem.* **1997,** *69*, 1852.

(2)   Ross, E. E.; Bondurant, B.; Spratt, T.; Conboy, J. C.; O'Brien, D. F.; Saavedra, S.

       S. *Langmuir* **2001,** *17*, 2305.

(3)   Varghese, J.; Cole, R. B. *J. Chromatogr. A* **1993,** *652*, 369.

(4)   Severs, J. C.; Smith, R. D. In *Handbook of Capillary Electrophoresis*; Landers, J.

       P., Ed.; CRC Press: Boca Raton, FL, 1997, pp 806.

(5)   Yeung, K. K.-C.; Kiceniuk, A. G.; Li, L. *J. Chromatogr. A* **2001,** *931*, 153.

(6)   Towns, J. K.; Regnier, F. E. *Anal. Chem.* **1992,** *64*, 2473.

(7)   Verzola, B.; Gelfi, C.; Righetti, P. G. *J. Chromatogr. A* **2000,** *874*, 293.

(8)   Verzola, B.; Gelfi, C.; Righetti, P. G. *J. Chromatogr. A* **2000,** *868*, 85.

(9)   Pentoney, S. L.; Sweedler, J. V. In *Hanbook of Capillary Electrophoresis*;

       Landers, J. P., Ed.; CRC Press: Boca Raton, FL, 1994, pp 162.

(10)   Craig, D. B.; Dovichi, N. J. *Anal. Chem.* **1998,** *70*, 2493.

(11)   Melanson, J. E.; Lucy, C. A. *Analyst* **2000,** *125*, 1049.

APPENDIX ONE. Curriculum Vitae

Personal Information

Date of Birth: April 21, 1976
Place of Birth: Winnipeg, Manitoba, CANADA

Academic history

07/1999-04/2002	The University of Alberta Edmonton, Alberta, CANADA Ph.D. GPA 8.67/9.0
09/1998-06/1999*	The University of Calgary Calgary, Alberta, CANADA M.Sc. program GPA 4.0/4.0

*supervisor then moved to The University of Alberta

09/1994-05/1998	The University of Manitoba Winnipeg, Manitoba, CANADA B.Sc. (Hons) GPA 4.27/4.5 Dean's Honour List 1995, 1996, 1997, 1998

Awards and honours

• Analytical Chemistry Division Graduate Student Award in Honour of Douglas E. Ryan ($750), University of Alberta 06/02

• ACS Division of Analytical Chemistry Academic Year Graduate Fellowship sponsored by Eli Lilly & Co. ($15,000 US per 9 months), University of Alberta 09/01-05/02

• International Symposium on Microscale Separations and Analysis (HPCE 2002) Travel Scholarship (SEK 4 500), Stockholm, Sweden 04/02

• Walter H. Johns Graduate Fellowship ($3,992), University of Alberta 09/01-05/02

• NSERC Post-Graduate Scholarship B ($19,100 per annum), University of Alberta 09/00-02/02

• Mary Louise Imrie Graduate Student Award for travel to High Performance Capillary Electrophoresis (HPCE 2001) conference ($800), Boston, MA 01/01

- High Performance Capillary Electrophoresis (HPCE 2001) Travel Scholarship ($400 US), Boston, MA 01/01

- Walter H. Johns Graduate Fellowship ($3,888), University of Alberta 09/00-05/01

- Best Student Oral Paper Presentation, 46th International Conference on Analytical Sciences and Spectroscopy ($100), Winnipeg, MB 08/00

- First Prize in Poster Competition at High Performance Liquid Chromatography (HPLC 2000) conference ($2,500 US), Seattle, WA 06/00

- High Performance Liquid Chromatography (HPLC 2000) Travel Award ($400 US), Seattle, WA 06/00

- Walter H. Johns Graduate Fellowship ($3,718), University of Alberta 09/99-05/00

- Faculty of Science Scholarship ($2,000), University of Alberta 09/99

- NSERC Post-Graduate Scholarship A ($ 17,400 per annum), University of Calgary/University of Alberta 09/98 - 09/00

- Fee Scholarship ($3,000), University of Calgary 09/98

- ACS Undergraduate Award in Analytical Chemistry, University of Manitoba 09/98-04/99

- Dr. N. Demchuck Award ($250), University of Manitoba 09/98-04/99

- Canadian Society for Chemistry Medal (medal), University of Manitoba 09/97-05/98

- David Renfrew Petrie Memorial Medal (medal, $50), University of Manitoba 09/97-05/98

- Reverend Joseph Hogg Scholarship ($1,800), University of Manitoba 09/97-05/98

- A.N. Campbell Scholarship ($150), University of Manitoba 09/97-05/98

- Chemical Institute of Canada Student Award ($125), University of Manitoba 09/97-05/98

- Glaxo Wellcome Scholarship in the Biological Sciences ($1,000), University of Manitoba 09/97-05/98

- UMSU Scholarship ($475), University of Manitoba 09/97-05/98

- Faculty of Science Undergraduate Student Research Award ($2,500), University of Manitoba 05/97-08/97

- Merck Frosst Award ($1,000), University of Manitoba 09/96-05/97

- A.N. Campbell Scholarship ($150), University of Manitoba 09/96-05/97

- Reverend Joseph Hogg Scholarship ($650), University of Manitoba 09/96-05/97

- A.N. Campbell Scholarship ($90), University of Manitoba 09/95-05/96

- NSERC Targeted Undergraduate Research Award ($3,600), University of Manitoba 05/95-08/95

- Canada Scholarship ($10,000), University of Manitoba 09/94-05/98

- Chown Centennial Scholarship ($500), University of Manitoba 09/94-05/95

Refereed publications

7. Nicole E. Baryla and Charles A. Lucy. "Semi-Permanent Surfactant Coatings for Inorganic Anion Analysis in Capillary Electrophoresis", *Journal of Chromatography A*, in press.

6. Jennifer M. Cunliffe, Nicole E. Baryla, and Charles A. Lucy. "Phospholipid Bilayer Coatings for the Separation of Proteins in Capillary Electrophoresis", *Analytical Chemistry*, 2002, *74*, 776-783.

5. Nicole E. Baryla, Jeremy E. Melanson, Mark T. McDermott, and Charles A. Lucy. "Characterization of Surfactant Wall Coatings in Capillary Electrophoresis by Atomic Force Microscopy", *Analytical Chemistry*, 2001, *73*, 4558-4565.

4. Jeremy E. Melanson, Nicole E. Baryla, and Charles A. Lucy. "Dynamic Capillary Coatings for Electroosmotic Flow Control in Capillary Electrophoresis", *TRAC Trends in Analytical Chemistry*, 2001, *20*, 365-374. (invited)

3. Nicole E. Baryla and Charles A. Lucy. "pH Independent Large Volume Sample Stacking of Positive or Negative Analytes in Capillary Electrophoresis", *Electrophoresis*, 2001, *22*, 52-58.

2. Jeremy E. Melanson, Nicole E. Baryla, and Charles A. Lucy. "Double-Chained Surfactants for Semi-Permanent Wall Coatings in Capillary Electrophoresis", *Analytical Chemistry*, 2000, *72*, 4110-4114.

1. Nicole E. Baryla and Charles A. Lucy. "Simultaneous Separation of Cationic and Anionic Proteins Using Zwitterionic Surfactants in Capillary Electrophoresis", *Analytical Chemistry*, 2000, *72*, 2280-2284.

Presentations

20. Nicole E. Baryla and Charles A. Lucy, "Semi-permanent Wall Coatings for Protein Separations and EOF Control in Capillary Electrophoresis", *Canadian Society for Chemistry National Meeting & Exhibition* (CSC 2002), Vancouver, B.C., June 1-5, 2002. (oral, **DOUGLAS RYAN GRADUATE STUDENT AWARD LECTURE**)

19. Nicole E. Baryla, Jennifer M. Cunliffe, and Charles A. Lucy, "Protein Separations in Capillary Electrophoresis Using Phospholipid Bilayer Coatings", *High Performance Capillary Electrophoresis* (HPCE 2002), Stockholm, Sweden, April 13-18, 2002. (poster)

18. Charles A. Lucy, Nicole E. Baryla, and Jeremy E. Melanson, "Methods for Quantifying Protein Recovery in Capillary Electrophoresis", *Pittcon 2002*, New Orleans, LA, March 17-22, 2002. (oral)

17. Nicole E. Baryla, "Capillary Coatings for Protein Separations in Capillary Electrophoresis", Eli Lilly & Co., Indianapolis, Indiana, February 2002. (invited oral)

16. Nicole E. Baryla, "Capillary Wall Coatings for Protein Separations in Capillary Electrophoresis", Eli Lilly Canada, Toronto, Ontario, November 2001. (invited oral)

15. Nicole E. Baryla, Jennifer M. Cunliffe, and Charles A. Lucy, "Control of the Reversed Electroosmotic Flow in Capillary Electrophoresis Using Semi-Permanent Surfactant Coatings", *International Ion Chromatography Symposium* (IICS 2001), Chicago, IL, September 9-12, 2001. (oral)

14. Charles A. Lucy and Nicole E. Baryla, "Surfactant Additives for Prevention of Protein Adsorption in Capillary Zone Electrophoresis", *Canadian Society for Chemistry National Meeting & Exhibition* (CSC 2001), Montreal, Quebec, May 26-30, 2001. (oral)

13. Jennifer M. Cunliffe, Nicole E. Baryla, and Charles A. Lucy, "Phospholipid Bilayer Coatings for the Separation of Proteins in Capillary Electrophoresis", *15th Annual Western Canadian Undergraduate Chemistry Conference* (WCUCC 2001), Burnaby, B.C., May 3-5, 2001. (oral)

12. Nicole E. Baryla and Charles A. Lucy, "Imaging of Surfactant Wall Coatings in Capillary Electrophoresis Using Atomic Force Microscopy", *High Performance Capillary Electrophoresis* (HPCE 2001), Boston, MA, January 13-18, 2001. (poster)

11. <u>Charles A. Lucy</u> and Nicole E. Baryla, "pH Independent Large Volume Sample Stacking of Positive or Negative Analytes in Capillary Electrophoresis", *High Performance Capillary Electrophoresis* (HPCE 2001), Boston, MA, January 13-18, 2001. (oral)

10. <u>Nicole E. Baryla</u>, "Modification of the Capillary Wall for Prevention of Protein Adsorption in Capillary Electrophoresis", Department of Chemistry, University of Manitoba, December 2000. (invited oral)

9. <u>Charles A. Lucy</u>, Jeremy E. Melanson, and Nicole E. Baryla "Surfactant Coatings for Electroosmotic Flow Control in Capillary Zone Electrophoresis", *International Ion Chromatography Symposium* (IICS 2000), Nice, France, September 11-14, 2000. (oral)

8. <u>Nicole E. Baryla</u>, Jeremy E. Melanson, and Charles A. Lucy, "Atomic Force Microscopy Studies of Surfactant Wall Coatings in Capillary Electrophoresis", *International Conference on Analytical Sciences and Spectroscopy* (ICASS 2000), Winnipeg, Manitoba, August 13-16, 2000. (oral, **BEST ORAL PAPER PRESENTATION**)

7. <u>Nicole E. Baryla</u> and Charles A. Lucy, "A Universal Method for Large Volume Sample Stacking of Positive or Negative Analytes in Capillary Electrophoresis", *High Performance Liquid Chromatography* (HPLC 2000), Seattle, Washington, June 24-30, 2000. (poster)

6. <u>Charles A. Lucy</u>, Nicole E. Baryla, Jeremy E. Melanson and Ken K.-C. Yeung, "Surfactant Additives as Dynamic Coatings in Capillary Zone Electrophoresis", *High Performance Liquid Chromatography* (HPLC 2000), Seattle, Washington, June 24-30, 2000. (oral)

5. <u>Nicole E. Baryla</u> and Charles A. Lucy, "The Link Between Electrostatic Ion Chromatography and the Separation of Proteins in Capillary Electrophoresis", *High Performance Liquid Chromatography* (HPLC 2000), Seattle, Washington, June 24-30, 2000. (poster, **BEST POSTER AWARD**)

4. <u>Jeremy E. Melanson</u>, Nicole E. Baryla, and Charles A. Lucy, "Semi-Permanent Wall Coatings in Capillary Electrophoresis Formed Using Double-Chained Cationic Surfactants", *Canadian Society for Chemistry National Meeting & Exhibition* (CSC 2000), Calgary, Alberta, May 28-31, 2000 (oral)

3. <u>Nicole E. Baryla</u> and Charles A. Lucy, "Use of Zwitterionic Surfactants for the Simultaneous Separation of Cationic and Anionic Proteins", *Canadian Society for Chemistry National Meeting & Exhibition* (CSC 2000), Calgary, Alberta, May 28-31, 2000. (oral)

2. <u>Nicole E. Baryla</u> and Charles A. Lucy, "Intriguing Behavior of the Electroosmotic Flow in Capillary Electrophoresis in the Presence of Zwitterionic Surfactants", *Federation of Analytical Chemistry and Spectroscopy Societies*, (FACSS 1999), Vancouver, B.C., October 1999. (poster)

1. <u>Nicole E. Baryla</u> and Charles A. Lucy, "Efficient Simultaneous Separation of Cationic and Anionic Proteins Using Zwitterionic Surfactants in Capillary Electrophoresis." Northern Lights Laser Lab Group Symposium, Edmonton, Alberta, August 1999. (poster)